THE JOURNAL
OF
CHEMICAL PHYSICS

VOLUME 9 FEBRUARY, 1941 NUMBER 2

# Dissociation Treatment of Condensing Systems—IV

C. CH'ENG, T. P. TSENG, S. K. FENG AND W. BAND
*Physics Department, Yenching University, Peiping, China*

(Received May 9, 1940)

The more exact dissociation theory of Part II, is applied to eighteen different gases and vapors, ranging in molecular weight from $H_2$ to Xe. Interaction energies per molecule in clusters formed during condensation of the saturated vapors are found as functions of temperature. From the differences between surface energy and measured surface tension, which remain finite at $T_c$, estimates are made of the numbers of heavy clusters maintained in the saturated vapor over the liquid surface, also as functions of temperature. In the case of eight vapors, the theory predicts measurable differences between the two critical points, $T_c$ at which the meniscus blurs, and $T_\gamma$ at which the densities equalize; the largest differences being for water, 6.5°K; methyl alcohol, 5.1°K; and nitrous oxide, 4.1°K. True critical volumes at $T_\gamma$ are calculated.

## INTRODUCTION

IN Part III,[1] the simple theory of Part I has been applied to the vapors of $H_2O$, $CO_2$, $NH_3$ and $CH_3Cl$. The theoretical formula for $PV/NkT$ of the saturated vapors was assumed to agree approximately with the facts, even up to the critical temperature, and from this assumed agreement, curves were obtained for the surface energies against temperature. As was to be expected, these curves agreed well with surface tension data only for temperatures sufficiently below $T_c$. Actually, however, the range of temperatures showing agreement should have been higher and the discrepancies appearing between $0.5T_c$ and about $0.9T_c$ required special interpretation. It was there suggested that the clusters involved in the liquid vapor equilibrium were actually small clusters, and that, therefore, the surface energy computed by the theory referred rather to these small clusters than to the true surface tension of the liquid phase. A very rough estimate was given of the size of the clusters required to account for the observed discrepancies from this point of view. In the light of later work to be reported in the present paper, a much better explanation has been developed, and it now seems clear that the improved theory of Part II is sufficiently accurate to give true surface energy terms right up to the critical point without any such special assumption.

In the simple theory of the saturation conditions of a vapor, Part I, the internal energy $\bar{W}_s$ of a cluster of type $s$ was expressed in the form, I(10)

$$\bar{W}_s=(s-1)W+\chi(s, T) \qquad (1)$$

because the part of $\bar{W}_s$ linear in $(s-1)$ controlled the convergence of the series of terms which gave the concentrations of the several types of cluster, see I(13). The sum of the series at saturation then depended only on the nonlinear part

[1] Previous papers in this series, hereafter referred to as Part I, Part II, and Part III, respectively: W. Band, J. Chem. Phys. **7**, 324–326 (1939); W. Band, J. Chem. Phys. **7**, 927–931 (1939); T. P. Tseng, S. K. Feng, C. Ch'eng and W. Band, J. Chem. Phys. **8**, 20–23 (1940).

$\chi(s, T)$, written briefly as $\chi$ in I(16); finally the linear part, $W$, was eliminated from the theoretical expression for $PV/NkT$ at the saturated state, I(17).

In the second approximation which includes cluster sizes, Part II, it remains necessary to separate $\bar{W}_s$ in the above manner, and for the same reasons; but the term $W$ is no longer eliminated exactly from the expression for $P(V-V_1)/NkT$ at saturation, see II(23) and II(9).

On the other hand, no such separation of $\bar{W}_s$ is required for the equations of an imperfect gas, see II(38) and II(39), where $W+\chi_2=\bar{W}_2$.

The separation of $\bar{W}_s$ is essentially a mathematical device required for the handling of a purely mathematical problem arising in the study of saturated conditions of a vapor; but it has an obvious physical significance. In Part III, (6) it was found convenient to write

$$\chi(s, T)=\alpha A(T)(s^{\frac{1}{3}}-1), \tag{2}$$

and the quantity $\alpha A(T)$ was evidently the surface tension per molecule of the liquid as ordinarily defined for large clusters. For small clusters there is no definition of surface tension, and formula (2) is to be regarded simply as a definition of $\chi_s$ in terms of the surface tension per molecule, $\alpha A(T)$ of large clusters. It may be regarded as an acceptable definition of the surface energy of small clusters, but, in fact, this idea will not be used here.

Now it is physically reasonable that the interaction energy $\bar{W}_2$ between pairs should not be separated in the above treatment of an imperfect gas, where there is no liquid phase; and equally reasonable that the surface term should play a distinct part, as it is found to do, in the behavior of the saturated vapor where a surface must exist.

Now the critical point conditions can be approached either from the equations of the saturated vapor or from those of the imperfect gas, and since the surface energy occurs in the one approach, and not in the other, a comparison of the two at once leads, as will be shown below, to conditions on $\chi(s, T)$, or rather on $\chi_2\equiv\chi(2, T_c)$ at the critical temperature.

TABLE I. *Molecular interaction energy at critical point. $\bar{W}_2(a)$ from Eq. (5); (b) from Eq. (6); (c) from Eq. (7) and (16), (d) from Eq. (29); units are $10^{-14}$ erg.*

| GAS | $T_c$ °K | $P_c$ ATMOS. | $V_c$ | $-\bar{W}_2$ (a) | (b) | (c) | (d) |
|---|---|---|---|---|---|---|---|
| $H_2$ | 33.2 | 12.80 | 64.92 | 0.88 | 0.94 | — | — |
| He | 5.2 | 2.26 | 58.13 | 0.01 | 0.02 | — | — |
| $NH_3$ | 406.0 | 115.0 | 72.94 | 77.1 | 52.0 | 78. | 58. |
| $H_2O$ | 653.5 | 217.7 | 51.6 | 87. | 84. | 119. | 106. |
| Ne | 44.4 | 26.9 | 42.2 | 3.3 | 3.4 | 2.4 | 2.9 |
| $N_2$ | 126. | 33.5 | 91.0 | 14.3 | 14.3 | 8.7 | 14. |
| $O_2$ | 154. | 49.7 | 75.0 | 18.1 | 18.3 | 25 | 15. |
| $CH_3OH$ | 513.1 | 79.7 | 117.7 | 99. | 77. | 101. | 166. |
| A | 155.6 | 48.0 | 75.8 | 18.4 | 18.5 | — | — |
| $N_2O$ | 309.6 | 77.5 | 96.9 | 44.0 | 44.3 | 58. | 62.8 |
| $CO_2$ | 304.2 | 73.0 | 94.8 | 43.0 | 43.4 | 57. | 10.6 |
| $C_2H_5OH$ | 516.2 | 62.7 | 167.0 | 86.6 | 83.7 | 107. | 123. |
| $CH_3Cl$ | 416.3 | 66.7 | 138.0 | 91.6 | 65.4 | 83.7 | 35. |
| $CH_3COOH$ | 594.7 | 58.0 | 171.2 | 142. | 102. | 131. | 196. |
| $C_3H_7OH$ | 264.0 | 50.6 | 219.7 | 56.0 | 41.6 | 69. | 90. |
| $2(C_2H_5)O$ | 194.0 | 36.0 | 282.3 | 40.8 | 30.8 | 80. | 55. |
| Hg | 1500.? | 203.? | 50.? | 390.? | 300.? | — | 230.? |
| Xe | 287.8 | 57.2 | 113.6 | 48.1 | 48.2 | — | — |

## MOLECULAR INTERACTION ENERGY AND SURFACE ENERGY AT $T_c$

In Part II (38), (39) the equation of an imperfect gas was obtained approximately in the form of Dieterici:

$$\left.\begin{aligned} &P(V-B)=NkT\exp(-A/NkTV),\\ \text{where}\quad &A=N^2h^3(\pi m)^{-\frac{3}{2}}(kT)^{-\frac{1}{2}}e^{-\bar{W}_2/kT}, \end{aligned}\right\} \tag{3}$$

and $B$ is a function of $T$ not given very precisely by the theory. If $B$ and $AT^{\frac{1}{2}}$ are approximately constant near the critical point, the latter is given by the usual equations:

$$V_c=2B,\quad P_c=A/4e^2B^2,\quad T_c=A/4NkB. \tag{4}$$

The function $B$ can be eliminated:

$$P_c(kT_c)^{-5/2}=2^{\frac{1}{2}}h^{-3}(2\pi m)^{\frac{3}{2}}e^{-2}\exp(\bar{W}_2/kT_c), \tag{5}$$

$$V_c(kT_c)^{\frac{3}{2}}=\tfrac{1}{2}Nh^3(\pi m)^{-\frac{3}{2}}\exp(-\bar{W}_2/kT_c). \tag{6}$$

Values of $\bar{W}_2$ obtained from (5) and (6) using the experimental values of $P_c$, $V_c$ and $T_c$ are shown in Table I.

Since the equations of the saturated vapor are extended up to $T_c$ only formally, they lead to no perfectly clear and definite condition for that point. Three different ways of applying the formal relations will be given leading to results which do not differ too badly from each other.

Elimination of $(V-V_1)$ from between II(21) and II(23) for the saturated vapor leads to

$$P=(2\pi m)^{\frac{3}{2}}(kT)^{5/2}h^{-3}e^{W/kT}(1+\phi_0). \tag{7}$$

Comparison with (5) shows that

$$\exp(\chi_2/kT_c)=(e^2/2)(1+\phi_{0c}), \tag{8}$$

which determines both $\chi_2/kT_c$ and $\phi_{0c}$:

$$\chi_2/kT_c=2.075, \quad \phi_{0c}=0.429. \tag{9}$$

On the other hand II(23) can itself give a critical point at which $V=V_1$, namely

$$\beta_0\phi=N(2\pi mkT)^{-\frac{1}{2}}h^3e^{-W/kT}, \tag{10}$$

which is consistent with (6) only if

$$2^{\frac{1}{2}}\beta_0\phi=V_c\exp(\chi_2/kT_c).$$

But Eq. II(16) gives $V_c=\beta_0\phi/(1+\phi_{3c})$ and hence

$$\exp(\chi_2/kT_c)=2^{\frac{1}{2}}(1+\phi_{3c}). \tag{11}$$

Again this determines both $\chi_2/kT_c$ and $\phi_{3c}$:

$$\chi_2/kT_c=1.666, \quad \phi_{3c}=2.754. \tag{12}$$

Finally (9) and (11) lead to the relation

$$(1+\phi_3)=(e^2/\sqrt{2})(1+\phi_c),$$

which determines both sums:

$$\phi_{0c}=4.1, \quad \phi_{3c}=16.2, \quad \chi_2/kT_c=3.2. \tag{13}$$

The general inference would be that at the critical temperature the term $\chi_2/kT_c$ should be roughly the same for every substance, somewhere between, say, about 1.5 and 3.5. Any attempt to make a zero value satisfy the various equations results in violent disagreements. The circumstance that the theory demands a positive value of $\chi_2$ at $T_c$ indicates, through (2), that $\alpha A(T)$ and, therefore, the surface energy of large clusters does not vanish at $T_c$.

## Curves of Interaction Energy *vs.* Temperature

From Eq. (8) it is possible to find $W$ as a function of $T$ right up to $T_c$ if $\phi_0$ can first be found throughout this range. This is done by means of the data on $P(V-V_1)/NkT$ and the Eq. II(23). From Part II, Eqs. (16) and (22) we have:

$$V_c=N\rho/(1+\phi_{3c})$$

and

$$V_c=(V_c/V_1)(\beta_0\phi)/(1+\phi_3),$$

so that

$$\beta_0\phi/N\rho=(V_1/V_c)(1+\phi_3)/(1+\phi_{3c}),$$

and II(23) simplifies to

$$P(V-V_1)/NkT=(1+\phi_0)/(1+\phi_3)-(V_1/V_c)(1+\phi_0)/(1+\phi_{3c}). \tag{15}$$

This relation is at once amenable to computation, leading from the data on $P(V-V_1)/NkT$ and $(V_1/V_c)$ to the temperature dependence of $\phi_0$ and $\phi_3$. The critical point occurs in (15) formally as the point at which $(V_1/V_c)$ is actually unity, and the whole expression zero. In view of the known discrepancy at $T_c$, and the existence of $T_\gamma$ above $T_c$, the critical point in (15) will be interpreted as $T_\gamma$ rather than $T_c$, so that the equation will be written as:

$$P(V-V_1)/NkT=(1+\phi_0)/(1+\phi_3)-(V_1/V_\gamma)(1+\phi_0)/(1+\phi_{3\gamma}). \tag{16}$$

Table II. *Revised values of* $\phi_0$, $\phi_3$, $(1+\phi_0)/(1+\phi_3)$ *in terms of* $w$.*

| $w$ | $\phi_0$ | $\phi_3$ | $\frac{(1+\phi_0)}{(1+\phi_3)}$ | $w$ | $\phi_0$ | $\phi_3$ | $\frac{(1+\phi_0)}{(1+\phi_3)}$ |
|---|---|---|---|---|---|---|---|
| 0.5 | 145.2 | 3311. | 0.044 | 5 | 0.1783 | 0.3913 | 0.847 |
| 1.0 | 16.21 | 141.2 | 0.121 | 6 | 0.09231 | 0.1947 | 0.914 |
| 1.5 | 5.391 | 27.17 | 0.227 | 7 | 0.04924 | 0.1016 | 0.953 |
| 2.0 | 2.482 | 9.247 | 0.340 | 8 | 0.02671 | 0.05443 | 0.974 |
| 2.5 | 1.368 | 4.215 | 0.454 | 9 | 0.01463 | 0.02959 | 0.986 |
| 3.0 | 0.8337 | 2.269 | 0.561 | 10 | 0.008058 | 0.01623 | 0.992 |
| 3.5 | 0.5401 | 1.3510 | 0.655 | 11 | 0.004456 | 0.008949 | 0.996 |
| 4.0 | 0.3644 | 0.8588 | 0.734 | — | — | — | — |

* $w=\alpha A(T)/kT$.

The direct summation of $\phi_0$ and $\phi_3$ for smaller values of $\alpha A(T)$ has been carried out, and Table I of Part III improved. These results are shown in Table II. Tables were next constructed showing the quantities on the right side of (16) as functions of $\alpha A(T)$ and $(V_1/V_\gamma)$ for several choices of $\phi_{3\gamma}$. These tables then directly gave $\alpha A(T)$ at all temperatures at which data were available both on $P(V-V_1)/NkT$ and $(V_1/V_\gamma)$, for any choice of $\phi_{3\gamma}$. Actually $V_\gamma$ is unknown in most cases, but then never differs much from $V_c$, which was, therefore, used instead of $V_\gamma$ as a first approximation.

The actual choice of $\phi_{3\gamma}$ is somewhat arbitrary, and was made in the following manner. In most cases the data on $P(V-V_1)/NkT$ and $(V_1/V_c)$ show sudden drops to zero and unity, respectively, at $T_c$, and, in the light of Callendar's work on $H_2O$,[2] this discontinuity is probably spurious. Therefore, the two quantities were determined at $T_c$ by a very slight extrapolation which ignored this discontinuity in both curves, adjusting the projected curves so that they would both arrive

[2] Callendar, Proc. Roy. Soc. **A120**, 460 (1928).

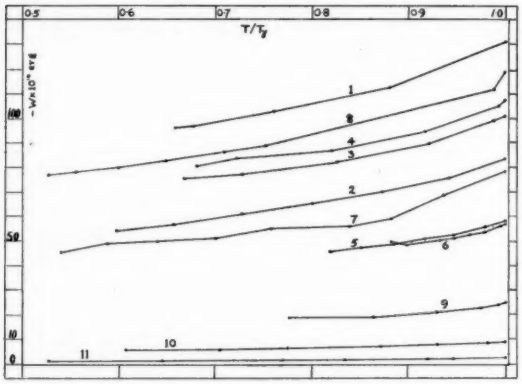


FIG. 1. *Mean molecular interaction energies in clusters formed in saturated vapors.* 1.—$CH_3COOH$; 2.—$CH_3Cl$; 3.—$CH_3OH$; 4.—$C_2H_5OH$; 5.—$N_2O$; 6.—$CO_2$; 7.—$NH_3$; 8.—$H_2O$; 9.—$O_2$; 10.—$N_2$; 11.—Ne. Abscissae, $T/T_\gamma$; ordinates, $-W\cdot 10^{14}$ erg.

at their respective zero and unit values at the same temperature. If this extrapolation gives $P(V-V_1)/NkT=J$, and $(V_1/V_c)=K$ at $T_c$, these values are inserted in (16). The values of $\phi_0$ and $\phi_3$ at $T_c$ are arbitrarily assumed to be those given by (13) for all substances without attempting to adjust them to individual cases. This then gives

$$(1+\phi_{3\gamma})=4.74K/(0.276-J). \tag{17}$$

This determines $\phi_{3\gamma}$ which, in turn fixes the, whole curve of Eq. (16) as applied to the determination of $\alpha A(T)$. The best way to find $T_\gamma$ then appears to be an extrapolation of the curve of $\alpha A(T)$ to its value corresponding to $\phi_{3\gamma}$. As a check, the previous extrapolations of $P(V-V_1)/NkT$ and $(V_1/V_c)$ are available. It must be admitted that this process has been very arbitrary, but it is quite definite, and any other reasonable way of applying the formal relation (16) would lead to substantially the same results. Having thus secured $\phi_0$ as a function of $T$, $W$ at once follows from (17) as mentioned above. The value of $\chi_2$ having already been fixed at $3.2kT_c$, this results in an estimate of $\overline{W}_2=W+\chi_2$, at $T_c$. These estimates are included in Table I. They compare fairly satisfactorily with those found from the imperfect gas equations. The actual discrepancies might be reduced by a more careful choice of $\phi_{3c}$ and hence of $\phi_{3\gamma}$ for individual cases.

Figure 1 shows curves of $W$ against $T/T_\gamma$, for some of the substances appearing in Table I. At first sight it is surprising that the energy increases in magnitude with increasing temperature, but this is due to the increasing density of the saturated vapor towards $T_c$. There is most decidedly no tendency for $W$ to vanish either at $T_c$ or even at $T_\gamma$.

## Redeterminations at the Critical Points

In a few cases, the discrepancy between $T_c$ and $T_\gamma$ leads to significant changes in accepted critical point data. In these cases let $V_c$ continue to represent the mean volume at $T_c$, as computed by the law of rectilinear diameters:

$$1/V+1/V_1=2/V_c. \tag{18}$$

Also let $J$ be the extrapolated value at $T_c$ of

$$P_c(V-V_1)/NkT_c=J. \tag{19}$$

From (18) and (19) both true volumes $V$ and $V_1$ at $T_c$ can be found. The true critical volume $V_\gamma$ at $T_\gamma$ can then be found by extending the rectilinear diameter to $T_\gamma$:

$$2/V_\gamma=a+bT, \tag{20}$$

where $a$ and $b$ are found from the data on $V$ and $V_1$ expressed in the form, near $T_c$,

$$1/V+1/V_1=a+bT.$$

The actual results of these calculations are shown in Table III. In this table the extrapolated value $J$ is given, and the corresponding value of $\phi_{3\gamma}$. $V_{1c}$ is the true liquid volume at $T_c$, and $V_c$ is the ordinarily accepted mean volume at $T_c$, in $cm^3$/mole.

## Application of Nernst's Heat Theorem

Either by using the theoretical expression, obtained below, for the latent heat $L$, or simply by assuming Clapeyron's relation, $L$ can be found in terms of the temperature derivative of

TABLE III. *Critical point values at $T_c$ and $T_\gamma$.*

| GAS | $\phi_{3\gamma}$ | $J$ | $T_c$ °K | $T_\gamma$ °K | $V_c$ | $V_{1c}$ | $V_\gamma$ |
|---|---|---|---|---|---|---|---|
| $H_2O$ | 24. | 0.114 | 647.0 | 653.5 | 51.6 | 42.1 | 47.8 |
| Ne | 170. | 0.252 | 44.4 | 46.9 | 41.8 | 30.7 | 44.2 |
| $N_2$ | 35. | 0.172 | 126.0 | 128.5 | 90.2 | 70.8 | 91.3 |
| $CH_3OH$ | 60.7 | 0.213 | 513.1 | 518.0 | 117.7 | 60.7 | 119.4 |
| $N_2O$ | 37.1 | 0.181 | 309.6 | 313.7 | 96.9 | 65.5 | 98.7 |
| $CO_2$ | 26.9 | 0.133 | 304.2 | 304.6 | 94.8 | 72.1 | 94.9 |
| $C_2H_5OH$ | 24.4 | 0.114 | 516.2 | 518.0 | 166.6 | 128.9 | 167.9 |
| $CH_3COOH$ | 22.3 | 0.114 | 594.7 | 598.0 | 171.2 | 122.6 | 172.2 |

$(W/kT)$. Then assuming Nernst's heat theorem this equation can be integrated to give $W$ without the arbitrary factor of $T$, in terms of the data on $L$. This process is by no means precise, if only because the function can hardly be assumed continuous down to 0°K, through the various phase changes, but it can be regarded as a rough check on the other methods of finding $W$.

Thus, the total energy of the vapor assembly is

$$E=N\sum_{s=1}\mu_s kT^2(\partial/\partial T)\ln f_s(T), \qquad (21)$$

and if we use the expression (2) of Part II for $f_s(T)$ this reduces to

$$E=N\sum_{s=1}\mu_s kT^2(\partial/\partial T)\ln(1-\beta_s) + 3kT/2+\bar{W}_s-\partial\bar{W}_s/\partial T. \qquad (22)$$

Neglecting the temperature variation of $\beta_s$, and the contribution of the surface energies of the clusters in the vapor, this becomes

$$E=(\tfrac{3}{2})NkT\sum_{s=1}\mu_s + N\sum_{s=1}(s-1)\mu_s(W-T\partial W/\partial T). \qquad (23)$$

In the liquid phase, again neglecting the surface energy, the total energy, to the same approximation, is

$$E_1=N(W-T\partial W/\partial T) \qquad (24)$$

so that the total latent heat is approximately

$$L=E-E_1+P(V-V_1) =[P(V-V_1)/NkT][5NkT/2 -N(W-T\partial W/\partial T)]. \qquad (25)$$

The procedure now is to take experimental values of $L$ and of $P(V-V_1)/NkT$ and to write

$$W-T\partial W/\partial T=5NkT/2 -(L/N)[NkT/P(V-V_1)] =F(T), \text{ say.} \qquad (26)$$

Then $F(T)$ is expanded in the form $C+DT^2+\cdots$ and, using Nernst's theorem, integrated at once to give

$$W=C-DT^2-\cdots. \qquad (27)$$

The coefficients $C$ and $D$ for several substances were found in this way and are shown in Table IV. The values of $\bar{W}_2=W+\chi_2$ at $T_c$ found from these values appear in Table I. Agreement is not very precise, but is much better in those cases where $T_c$ is low.

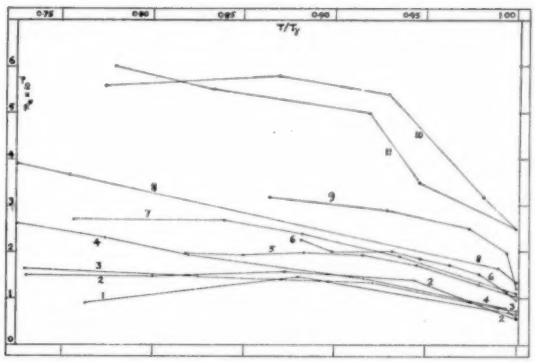

FIG. 2. *Mean numbers per cm² of heavy clusters maintained over liquid surfaces in saturated vapors.* Numbers identical with those in Fig. 1. The ordinate scale for Ne has been reduced by one-half. Abscissae, $T/T_\gamma$; ordinates, $n_k\cdot 10^{-6}$.

### SURFACE ENERGY AND SURFACE TENSION

As described above, $\phi_0$ was found as a function of $T$. From Table II this means that by using (7) and (8) of Part III, the surface energy function $\alpha A(T)$ is known. As in (21) of Part III the true surface tension should be given by

$$E(T)=(1/4.837)\nu_v^{\frac{1}{3}}\alpha A(T), \qquad (28)$$

where $\nu_v$ is the number of molecules per cm³ in the liquid. Actually $E(T)$, as given by (28), is always greater than the measured surface tension, remaining finite at $T_c$. This has already been explained as due to the gravitational settling down of the larger clusters over the liquid surface. Thus suppose the mean size of these clusters is $k$ molecules, and their mean number per cm² over the liquid is $n_k$. Then the surface tension actually measurable will be

$$S(T)=E(T)+n_k\{kW+\alpha A(T)k^{\frac{1}{3}}\}. \qquad (29)$$

TABLE IV. *Application of Nernst's theorem to* $W=C-DT^2$. *C in ergs, D in ergs/(°K)².*

| GAS | $-C\cdot10^{13}$ | $D\cdot10^{19}$ | GAS | $-C\cdot10^{13}$ | $D\cdot10^{19}$ |
|---|---|---|---|---|---|
| $NH_3$ | 3.9 | 1.2 | $CH_3OH$ | 6.3 | 39.2 |
| $H_2O$ | 7.30 | 7.81 | $C_2H_5OH$ | 8.0 | 16.4 |
| Ne | 0.23 | 0.30 | $CH_3Cl$ | 2.75 | 4.75 |
| $N_2$ | 0.90 | 33.0 | $CH_3COOH$ | 6.8 | 36.3 |
| $O_2$ | 1.0 | 0.21 | $C_3H_7OH$ | 8.5 | 17.0 |
| $CO_2$ | 0.17 | 9.6 | $2(C_2H_5)O$ | 4.0 | 6.9 |

It is certain that $k$ must be at least of the order $10^7$, so the term in $k^{\frac{1}{3}}$ will be negligible. Then the product $n_k k$ can be found from the relation:

$$-n_k k W = E(T) - S(T). \tag{30}$$

The interaction energy $-W$ having already been determined, either as in Fig. 1 or in Table IV, this equation at once gives $n_k k$ as a function of temperature. Assuming the mean value of $k = 10^7$, and $W$ from Fig. 1, the results are shown in Fig. 2.

It is specially remarkable that the numbers $n_k$ tend to increase with decreasing temperature, and that they are generally larger for those substances showing marked difference between $T_c$ and $T_\gamma$. To fully appreciate these results it is necessary to abandon naive conceptions of a static interface between liquid and vapor, and, with Adam[3] realize that, from a microscopic point of view, the surface is in violent motion and almost never really "flat." The present results very strongly suggest that the exchange across the boundary does not consist only of single molecules, but that the motion is so violent that whole clusters of molecules are also being torn from the surface in sufficient numbers to maintain, against gravitational sedimentation, a permanent layer over the surface of the liquid.

## Precision of the Theory

The theory lacks precision at two points. First in the arbitrary choice of $\phi_{3c}$. To check this, the data on $CO_2$ were analyzed, using values of $\phi_{3c}$ ranging from 2.3 to 5000; the values of $kn_k$ changed by a factor of five, while those of $W$ by about 40 percent. This might thus be used to get a better agreement between the different parts of the theory, although too large a value of $\phi_{3c}$ would be forbidden by Eqs. (9), (12) and (13).

The other point is more fundamental and has already been emphasized by Mayer.[4] The cluster is here defined in terms of interaction energy between pairs, and it is necessary to fix arbitrarily a limiting interaction distance beyond which the energy shall be neglected and a pair not counted as a cluster. Regions of less than normal density are not accounted for at all. Above $T_\gamma$, this objection must always be valid, there being no actual demarcation between clustered and unclustered phases. But below $T_c$ the situation is surely improved by the existence of a definite distinction between the two phases. For clusters sufficiently large, the intrinsic pressure will operate and render unstable clusters of density intermediate between liquid and vapor. The limiting interaction distance thus ceases to be arbitrary. However, for small clusters this definite distinction between phases can still not be claimed; in fact, our present results on $\bar{W}_2$ for the saturated vapor, shown in Fig. 1, definitely indicate that the clusters formed in the saturated vapor have densities which increase towards $T_c$, and which must, therefore, be intermediate between liquid and vapor densities. In spite of these failings, the method has proved very convenient, and productive of interesting results, which do not appear to be without significance.

[3] N. K. Adam, *The Physics and Chemistry of Surfaces* (Oxford, second edition, 1938), pp. 6, 7.

[4] J. E. Mayer and S. F. Streeter, J. Chem. Phys. 7, 1019–1025 (1939).

# Raman Spectra of Some Ethers Containing One or More Phenyl Groups

M. J. MURRAY, *Department of Chemistry*
AND
FORREST F. CLEVELAND, *Department of Physics*
*Illinois Institute of Technology, Chicago, Illinois*
(Received October 23, 1940)

Raman frequencies, estimated intensities and depolarization factors are listed for *n*-propylphenyl, *n*-butylphenyl, ethylbenzyl, *n*-butylbenzyl and dibenzyl ethers. Intense frequencies characteristic of monosubstituted benzenes whose values were constant in the five ethers are 618(5)0.8, 1001(10)0.1, 1029(7)0.3, 1156(4)0.8, 1176(4)0.8, 1588 and 1604 (6)0.7, 3058(9)0.3. Frequencies characteristic of the C−O−C bond may be those near 440, 900 and 1125 $cm^{-1}$.

## INTRODUCTION

IN a recent study of the simultaneous catalytic dehydration and dehydrogenation of benzyl alcohol,[1] it was desired to obtain information in regard to the composition of an intermediate fraction by use of Raman spectra. In this connection it was found necessary to determine the Raman spectrum of dibenzyl ether since no data for this compound were found in the literature. Since that time, depolarization factors for this ether and displacements, estimated intensities and depolarization factors for ethylbenzyl, *n*-butylbenzyl, *n*-propylphenyl and *n*-butylphenyl ethers have been obtained. The five ethers are related in that each contains at least one phenyl group and may thus be regarded as a monosubstituted benzene.

## EXPERIMENTAL

The experimental technique and the apparatus employed were essentially the same as described in a previous paper.[2] The spectra were obtained in the liquid state, the liquids being carefully purified by distillation in a 30-cm, continuous spiral packed, heated column. The slit width was 0.08 mm for the regular exposure and 0.12 mm for the polarization exposures. Previous data apparently have been obtained only for dibenzyl ether.[1] Details regarding the samples (all Eastman products) are as follows:

*n-propylphenyl ether.* b.p. 77° at 17 mm; exposure 1.0 hr.; polarization exposures 2.5 hr. each
*n-butylphenyl ether.* b.p. 95° at 17 mm; exposure 1.3 hr.; polarization exposures 2.0 hr. each
*ethylbenzyl ether.* b.p. 70° at 15 mm; exposure 3.0 hr.; polarization exposures 2.0 hr. each
*n-butylbenzyl ether.* b.p. 88° at 6–7 mm; exposure 1.8 hr.; polarization exposures, 2.8 hr. each
*dibenzyl ether.* b.p. 176° at 20 mm; exposure 1.0 hr.; polarization exposures, 1.0 hr. each.

## RESULTS

The Raman displacements $\Delta\nu$ in $cm^{-1}$, estimated intensities $I$ and depolarization factors $\rho$ are given in Table I. Certain lines that are unusually sharp or broad are designated by the letters *s* and *b*, respectively. Data in regard to which there is some uncertainty are enclosed by parentheses. The frequencies joined with a brace represent cases in which the corresponding lines were unresolved on the polarization spectrogram and the depolarization factor given in such cases is the value read for the unresolved line. In a few instances it was not possible to list a numerical value for the depolarization factor but only to designate it as polarized (*P*).

## DISCUSSION

### Phenyl group frequencies

The molecules concerned in the present study are of interest not only as ethers but also as monosubstituted benzenes.[3] Kahovec and Reitz[4]

[1] Douglas Meigs, Thesis, Armour Institute of Technology, 1940.
[2] Forrest F. Cleveland, M. J. Murray, Herschel H. Haney and Julia Shackelford, J. Chem. Phys. **8**, 153 (1940).
[3] For a review of the Raman spectra of benzene and its derivitives, see K. W. F. Kohlrausch, Physik. Zeits. **37**, 58–79 (1936).
[4] L. Kahovec and A. W. Reitz, Akad. Wiss. Wien, Ber. **145**, IIb, 1033 (1936).

TABLE I. *Raman spectra of ethers containing one or more phenyl groups.*

| *n*-PROPYLPHENYL | | | *n*-BUTYLPHENYL | | | ETHYLBENZYL | | | *n*-BUTYLBENZYL | | | DIBENZYL | | | DESIGNATION |
|---|---|---|---|---|---|---|---|---|---|---|---|---|---|---|---|
| $\Delta\nu$ | $I$ | $\rho$ | $\Delta\nu$ | $I$ | $\rho$ | $\Delta\nu$ | $I$ | $\rho$ | $\Delta\nu$ | $I$ | $\rho$ | $\Delta\nu$ | $I$ | $\rho$ | |
| | | | 185 | 1 | — | 171 | 1 | 0.9 | 190 | 1 | — | | | | |
| **248** | 4 | 0.8 | **245** | 4 | 0.7 | **227** | 3*b* | 0.9 | 225 | 2 | — | **200** | 3 | 0.9 | $\gamma$ |
| **319** | 3 | 0.6 | **291** | 3 | 0.8 | **323** | 4 | 0.7 | 285 | 2 | — | **226** | 2*b* | 0.8 | $\omega_{10}$ |
| | | | | | | 353 | 1 | — | | | | | | | |
| 413 | 4 | 0.7 | | | | | | | | | | | | | |
| | | | 427 | 2 | 0.7 | | | | | | | | | | |
| 450 | ½ | — | | | | 454 | 1 | — | | | | | | | |
| 512 | 1 | — | 510 | 1 | 0.9 | | | | | | | | | | |
| **592** | 2*b* | (0.4) | **591** | 1 | — | **504** | 1 | — | 1468 | ½ | — | **479** | 2*b* | 0.9 | $\omega_1$ |
| | | | | | | 600 | 1 | — | | | | | | | |
| **614** | 5*s* | 0.7 | **615** | 5*s* | 0.7 | **619** | 6*s* | 0.8 | **620** | 5*s* | 0.9 | **620** | 5*s* | 0.7 | $\omega_2$ |
| | | | | | | | | | 734 | 1 | 0.8 | | | | |
| **753** | 4 | 0.7 | **754** | 3 | 0.9 | **743** | 2 | — | 749 | 1 | | **740** | 2*b* | 0.8 | $\gamma$(CH)? |
| | | | 775 | 1 | — | | | | | | | | | | |
| **817** | 5 | 0.4 | **797** | 3 | 0.5 | **803** | 4 | 0.4 | **804** | 3 | 0.5 | **801** | 4 | 0.7 | $\omega_4$ |
| **832** | 3 | | **812** | 3 | | | | | 819 | 4 | | **816** | 4 | | $\gamma$(CH) |
| | | | **827** | 1 | <0.8 | **822** | 5 | 0.4 | | | | | | | |
| | | | 843 | 1 | | 849 | 3 | *P* | 852 | 2 | — | 844 | 4 | 0.6 | |
| | | | 878 | 2 | <0.8 | | | | 878 | 1 | — | | | | |
| 886 | 1 | 0.6 | 908 | 1 | <0.8 | 887 | 3*b* | *P* | 902 | 1 | — | 903 | 3 | 0.6 | |
| | | | | | | | | | | | | 947 | 2 | 0.8 | |
| 975 | 4 | <0.7 | 974 | 1 | — | | | | | | | | | | |
| **999** | 10 | 0.1 | **999** | 10 | 0.1 | **1003** | 10 | 0.1 | **1002** | 10 | 0.1 | **1001** | 10 | 0.1 | $\omega^3$ |
| **1029** | 6 | 0.2 | **1029** | 8 | 0.2 | **1030** | 7 | 0.3 | **1029** | 7 | 0.3 | **1028** | 7 | 0.4 | $\omega_{11}$ |
| | | | 1068 | 1 | — | 1068 | ½ | — | | | | | | | |
| | | | | | | 1098 | 1 | — | | | | | | | |

have listed eighteen frequencies which "more or less unambiguously" correspond to characteristic vibrations of monosubstituted benzenes ($C_6H_5-X$). The frequencies in Table I which correspond to these are set in boldface type and the designations of the frequencies as given by Kahovec and Reitz are written in the column at the right. While some of the selections are rather arbitrary, the frequencies agree, on the whole, quite well with those listed by Kahovec and Reitz. Depolarization factors for some of these phenyl group lines, are listed by Kohlrausch[3] for $X=NH_2$, $CH_3$, Cl and Br. The mean of the numerical values of the depolarization factors listed by Kohlrausch for the various frequencies of the four compounds and the mean of the corresponding values obtained here for the ethers are compared in Table II. Excluding

TABLE I.—*Continued.*

| *n*-PROPYLPHENYL | | | *n*-BUTYLPHENYL | | | ETHYLBENZYL | | | *n*-BUTYLBENZYL | | | DIBENZYL | | | DESIGNATION |
|---|---|---|---|---|---|---|---|---|---|---|---|---|---|---|---|
| $\Delta\nu$ | $I$ | $\rho$ | $\Delta\nu$ | $I$ | $\rho$ | $\Delta\nu$ | $I$ | $\rho$ | $\Delta\nu$ | $I$ | $\rho$ | $\Delta\nu$ | $I$ | $\rho$ | |
| 1131 | 1 | — | 1122 | 1 | 0.6 | 1124 | 4 | 0.6 | 1125 | 1 | — | | | | |
| **1155** | 3 | 0.9 | **1152** | 4 | 0.8 | **1159** | 4 | 0.8 | **1155** | 4 | 0.8 | **1158** | 4 | 0.9 | $\delta$(CH) |
| **1174** | 4 | 0.6 | **1173** | 5 | 0.8 | **1179** | 4 | 0.8 | **1176** | 4 | 0.8 | **1180** | 4 | 0.9 | $\delta$(CH) |
| 1227 | 1 | 0.9 | 1222 | 1 | 0.7 | | | | | | | | | | |
| **1245** | 5 | 0.4 | **1246** | 6 | 0.4 | **1210** | 7 | 0.2 | **1210** | 7 | 0.4 | **1210** | 6*b* | 0.3 | $\omega_6$ |
| 1281 | 2 | — | 1298 | 5*b* | 0.6 | 1273 | 1 | 0.8 | 1296 | 4*b* | 0.8 | | | | |
| 1299 | 4 | 0.6 | | | | | | | | | | | | | |
| 1340 | ½ | — | 1333 | 1 | 0.7 | | | | 1361 | 1 | — | | | | |
| 1393 | ½ | — | 1390 | 1 | 0.9 | | | | | | | 1385 | 1 | — | |
| **1438** | 2 | — | **1433** | 3 | 0.8 | | | | **1436** | 4 | 0.8 | | | | $\delta$(CH) |
| 1456 | 4 | 0.7 | 1450 | 4 | | 1452 | 5*b* | 0.7 | 1454 | 5 | | 1455 | 4 | 0.7 | |
| | | | 1467 | 1 | — | | | | | | | | | | |
| **1500** | 1 | — | **1497** | ½ | — | **1485** | 1 | 0.7 | **1481** | 4 | 0.9 | **1476** | 3 | | $\omega_5$? |
| **1587** | 4 | 0.7 | **1590** | 4 | 0.7 | **1588** | 3 | 0.6 | 1588 | 3 | 0.7 | **1586** | 4 | 0.8 | $\omega_{7,8,9}$ |
| **1600** | 5 | | **1600** | 6 | | **1607** | 7 | | 1607 | 8 | 0.7 | **1607** | 8 | 0.7 | |
| 2872 | 5 | 0.2 | 2870 | 7 | 0.1 | 2847 | 4 | 0.2 | 2863 | 8*b* | 0.2 | 2856 | 5*b* | 0.3 | |
| | | | | | | 2867 | 6 | | | | | | | | |
| 2912 | 4 | 0.7 | 2911 | 6 | 0.6 | | | | 2911 | 8 | 0.6 | | | | |
| 2937 | 6 | 0.3 | 2937 | 5 | 0.2 | 2931 | 8 | 0.1 | 2937 | 8 | 0.3 | 2932 | 3*b* | 0.4 | |
| 2973 | 2 | 0.9 | 2963 | 2 | 0.8 | 2980 | 4 | 0.7 | 2960 | 3 | 0.9 | 2976 | 1 | — | |
| **3015** | ½ | — | | | | **3008** | 1 | — | **3008** | 1 | — | **3004** | 1 | — | $\nu$(CH) |
| | | | | | | **3040** | 4 | — | **3045** | 4 | 0.3 | **3040** | 3 | 0.3 | $\nu$(CH) |
| **3066** | 9*b* | 0.3 | **3068** | 8 | 0.3 | **3062** | 9 | 0.3 | **3064** | 9 | | **3061** | 9 | | |
| | | | | | | **3165** | ½ | — | **3166** | ¼ | — | **3162** | ½ | — | $\nu$(CH) |
| | | | | | | 3206 | ¼*b* | — | 3202 | ¼*b* | — | 3204 | ¼*b* | — | |

the uncertain values for $\omega_1$, $\omega_4$ and $\gamma$(CH), the agreement is quite good, the average deviation being 0.08.

The phenyl group frequencies corresponding to seven of the more intense lines are remarkably constant in a wide variety of monosubstituted benzenes. The mean values of these constant frequencies obtained from the list of Kahovec and Reitz (for X=$NH_2$, OH, F, $CH_3$, Cl, SH, Br and I) are compared with the corresponding mean values for the present ethers in Table III. Mean intensities and (for the ethers) mean depolarization factors are included.

### Frequencies near 3000 cm$^{-1}$

The investigations of Ingold and associates[5] and of Langseth and Lord[6] indicate that the

[5] Angus, Bailey, Hale, Ingold, Leckie, Raisin, Thompson and Wilson, J. Chem. Soc. 971 (1936).

[6] A. Langseth and R. C. Lord, Jr., Kgl. Danske Vid. Sels. Math.-fys. Medd. **16**, 1–85 (1938).

frequency 3062 should be assigned to the C−H valence frequency of the phenyl group and that the less intense frequencies at 3009 and 3164 are overtones. The 3062 line is resolved into two components in the benzyl ethers.

The weak line near 3204 may be the first overtone of the 1600 frequency. It was observed only for the benzyl ethers. A strong line at 2911 appeared for the three ethers containing propyl or butyl groups but was not observed for the other two. This frequency does not in general appear for methyl compounds and is weak in ethyl compounds, but is strong in all normal alkyl hydrocarbons containing chains of three or more carbon atoms. It thus appears to be more characteristic of the chain than of the $CH_3$ group, to which Fox and Martin[7] have assigned the weak infra-red band at 2912. It may be that the frequency sometimes observed in the ethyl compounds is an overtone of the 1450 frequency.

The polarized frequency near 2860 ($\nu_{||}$) and the depolarized frequency near 2945 ($\nu_{\perp}$) have been attributed to the $-CH_2-$ group.[2,8] The polarized frequency is higher in the two phenyl ethers than in the three benzyl ethers. In ethylbenzyl ether it is resolved into two components. As would be expected, it is strongest in the butyl ethers which contain the greatest number of $-CH_2-$ groups. The depolarized frequency has a value considerably higher than the value 2945 assigned to the "normal methylene group."[8a] It is highest in the ether containing the ethyl group, lower in propylphenyl and dibenzyl ethers, and lowest in the two ethers containing the butyl group. This slight variation in frequency may be caused by the presence of different atoms or groups adjacent to the $-CH_2-$ group, to a neighboring unresolved methyl group frequency, or to shifts involving some resonance interaction. Fox and Martin have concluded from infra-red studies[5] that the symmetrical and unsymmetrical frequencies of the $-CH_2-$ group are 2853 and 2926, respectively. The latter is more intense than the former in the infra-red spectra.

TABLE II. *Mean depolarization factors of phenyl group lines.*

| Frequency | Kohlrausch | Ethers | Frequency | Kohlrausch | Ethers |
|---|---|---|---|---|---|
| $\gamma$ | 0.86 | 0.83 | $\omega_3$ | 0.07 | 0.10 |
| $\omega_{10}$ | 0.78 | 0.73 | $\omega_{11}$ | 0.18 | 0.28 |
| $\omega_1$ | 0.29 | (0.65) | 1155, $\delta$(CH) | 0.88 | 0.84 |
| $\omega_2$ | 0.86 | 0.76 | $\omega_6$ | 0.21 | 0.34 |
| $\omega_4$ | 0.12 | (0.50) | $\omega_{7,8,9}$ | 0.85 | 0.68 |
| $\gamma$(CH) | *dp* | (0.50) | | | |

TABLE III. *Constant frequencies of the phenyl group.*

| Frequency | Kahovec and Reitz | | Ethers | | |
|---|---|---|---|---|---|
| | $\Delta\nu$ | $I$ | $\Delta\nu$ | $I$ | $\rho$ |
| $\omega_2$ | 615 | 4 | 618 | 5 | 0.8 |
| $\omega_3$ | 1001 | 11 | 1001 | 10 | 0.1 |
| $\omega_{11}$ | 1024 | 6 | 1029 | 7 | 0.3 |
| $\delta$(CH) | 1157 | 4 | 1156 | 4 | 0.8 |
| $\delta$(CH) | 1178 | 3 | 1176 | 4 | 0.8 |
| $\omega_{7,8,9}$ | 1590 | 6 | 1588<br>1604 | 6 | 0.7 |
| $\nu$(CH) | 3062 | 10 | 3058 | 9 | 0.3 |

## Frequencies of the ether group, R−O−R′

Pai,[9] using 1102, 921 and 416 as fundamentals for dimethyl ether, calculated a value of 102° for the C−O−C valence angle. This is in the neighborhood of the value 111±4° found by Sutton and Brockway[10] from an electron diffraction investigation. Recently Crawford and Joyce[11] have assigned the frequencies 1122 and 940 in dimethyl ether to vibrations involving a stretching of the C−O bond and the frequency 412 to a C−O−C deformation vibration. Frequencies observed for the present ethers which may correspond to these are the ones near 900, 440 (observed in only three cases) and 1125.

[7] J. J. Fox and A. E. Martin, Proc. Roy. Soc. **A175**, 208 (1940).

[8] (a) K. W. F. Kohlrausch, *Der Smekal-Raman Effekt*, p. 190; (b) Forrest F. Cleveland and M. J. Murray, J. Am. Chem. Soc. **62**, 3185 (1940).

[9] Gopala Pai, Current Sci. **2**, 386 (1934).

[10] L. E. Sutton and L. O. Brockway, J. Am. Chem. Soc. **57**, 473 (1935).

[11] B. L. Crawford, Jr. and L. Joyce, J. Chem. Phys. **7**, 307 (1939).

# Absorption Spectra of the Chrome Alums at Low Temperatures

D. L. KRAUS AND G. C. NUTTING
*Department of Chemistry, University of California, Berkeley, California*
(Received July 11, 1940)

Line absorption spectra of thirteen sulfate and selenate chrome alums have been measured at 15–20°K. Pronounced differences in the spectra are attributed to structural differences in the crystals and are related to the size of the anions and the univalent cations. Anomalous behavior on change of temperature is shown by potassium sulfate and ammonium sulfate and selenate alums. Transitions disrupting the lattice and significantly altering the spectrum occur in ammonium chromium sulfate at 81±1°K and in ammonium chromium selenate at 106±5°. Combination of electronic frequencies of $Cr^{+++}$ with internal oscillations of anions are weak. Combination of lattice vibrations with both upper and lower electronic states of $Cr^{+++}$ are found. Bands are observed in all the alums shifted about 330, 570 and 800 $cm^{-1}$ to higher frequencies than the electronic absorption lines. These are thought due to photo-excitation of a nonhomopolar complex, probably $Cr(H_2O)_6^{+++}$. Repetition of the electronic multiplet and associated vibrational structure at some of these higher frequencies is found in several of the alum spectra.

## INTRODUCTION

DISCONTINUOUS absorption spectra of a large number of coordination compounds of trivalent chromium at liquid-air temperature have been recorded.[1-3] Sauer, especially, has studied the effect of isomorphous replacement in a group of eleven sulfate and selenate chrome alums at −190°C, and in a smaller number of these alums at −78° and +18° also. The discrete absorption is in general found within a range of a few hundred wave numbers in the red and orange and merges into a strong continuum with maxima at approximately 5700 and 4000A. With lowering temperature the continuum narrows, revealing additional lines and bands. The latter also become narrower and less diffuse and often resolve into finer structures.

An investigation in this laboratory[4] of potassium chromium sulfate alum was carried out in the temperature range −190° to −259°. The qualitative effects of changing temperature measured by Sauer are found in heightened degree in the lower range. The bands of continuous absorption are so narrowed at the temperature of liquid hydrogen that a series of sharp lines is revealed in the blue which seems to show a relationship to the violet continuum similar to that of the red-orange discrete spectrum to the yellow-green continuum. In addition a gradual change in the relative intensity and structure of the strong "characteristic doublet" and its associated weaker lines near 6700A is noted which suggests the presence of a multiple lower state. Magnetic behavior of potassium chrome alum at temperatures down to about 1°K makes it seem unlikely that the lower electronic state of $Cr^{+++}$ is multiple. Alternatively, characteristic oscillation frequencies of the crystal lattice or of some ion or complex composing it might conceivably combine with the single electronic state of $Cr^{+++}$ to give an ensemble of states showing the observed temperature behavior.

The spectra of other alums, notably the selenates, are richer in lines than potassium chromium sulfate, and the lines are superior in sharpness at the temperature of liquid air. With the increased definition and precision of measurement made possible at liquid hydrogen temperature it was hoped that constant frequency differences, repetition of line groups, or frequencies equal to infra-red or Raman frequencies might be found in the absorption spectra which would give a clue to the origin of the numerous absorption lines of these alums. In addition, further information on the effect of temperature on the structure of the characteristic doublets was desired. Accordingly, an investigation was made of the visible absorption spectra of as many different chrome alums as could be prepared. The spectra of single crystals of the following thirteen chrome alums have been

[1] Schnetzler, Ann. d. Physik **10**, 373 (1931).
[2] Snow and Rawlins, Proc. Camb. Phil. Soc. **28**, 522 (1932).
[3] Sauer, Ann. d. Physik **87**, 197 (1928).
[4] Spedding and Nutting, J. Chem. Phys. **2**, 421 (1934).

TABLE I. *Absorption lines of the chrome alums. Intensities with respect to the background (I) have been estimated roughly on the scale 1–10. The letter s indicates a line or band whose edges are sharp and well-defined; d a line or band whose edges are diffuse and less precisely measurable. The total width (w) of most of the lines has been measured and is reported in cm⁻¹.*

(a) $CsCr(SeO_4)_2 \cdot 12H_2O$ 20°

| $cm^{-1}$ | $I$ | $w$ | $cm^{-1}$ | $I$ | $w$ |
|---|---|---|---|---|---|
| 14,931 | 1*s* | | 15,178.5 | 2*d* | 11 |
| 937.5 | 10*s* | 1.5 | 205 | 1*d* | 10 |
| 941.5 | 10*s* | 1.1 | 255 | 3*d* | 12 |
| 944.0 | 3*s* | | 270 | 3*d* | 12 |
| 946.1 | 3*s* | | 292.5 | 1*d* | 13 |
| 978.5 | 1*d* | 11 | 373 | 1*d* | 17 |
| 15,004 | 1*d* | 12 | 431 | 1*d* | 14 |
| 028 | 1*d* | 8 | 465 | 1*d* | 10 |
| 048.3 | 4*s* | 1.6 | 501.8 | 8*s* | 5 |
| 052.2 | 4*s* | 1.2 | 510.5 | 3*d* | 5 |
| 057 | 1*s* | | 549 | 2*d* | 4 |
| 065 | 1*d* | 8 | 553 | 2*d* | 4 |
| 079 | 2*d* | 6 | 574 | 1*d* | 8 |
| 087 | 2*s* | | 675 | 1*d* | 9 |
| 093.5 | 3*s* | 1 | 682.5 | 2*d* | 7 |
| 098 | 2*s* | | 709 | 5*d* | 20 |
| 103 | 1*s* | | 731 | 4*d* | 11 |
| 106.5 | 4*s* | | 755 | 5*d* | 13 |
| 111 | 2*s* | | 781 | 1*d* | 8 |
| 113 | 1*s* | | 800 | 1*d* | 5 |
| 118 | 1*d* | 8 | 835 | 1*d* | 9 |
| 123 | 1*d* | | 849 | 2*d* | 11 |
| 128 | 1*d* | 4 | 875 | 3*d* | 17 |
| 134.5 | 1*s* | 1 | 923 | 2*d* | 12 |
| 142 | 1*s* | | 979 | 2*d* | 19 |
| 146 | 1*s* | | 16,042 | 1*d* | 34 |
| 162.5 | 1*d* | 5 | | | |

(b) $RbCr(SeO_4)_2 \cdot 12H_2O$ 20°

| $cm^{-1}$ | $I$ | $w$ | $cm^{-1}$ | $I$ | $w$ |
|---|---|---|---|---|---|
| 14,923.1 | 10*s* | 1.9 | 15,134.7 | 3*s* | 3 |
| 928.0 | 10*s* | 1.4 | 147 | 1*d* | 8 |
| 930.4 | 3*s* | | 163 | 3*d* | 13 |
| 942 | 1*d* | | 187 | 2*s* | 2 |
| 952 | 1*d* | | 192 | 2*s* | 3 |
| 990 | 1*d* | | 228 | 1*d* | 7 |
| 995 | 1*d* | | 234.6 | 2*s* | 3 |
| 15,003 | 1*d* | | 239.8 | 2*s* | 4 |
| 007 | 1*d* | | 260 | 3*d* | 16 |
| 011 | 1*d* | | 282 | 1*d* | 13 |
| 017 | 1*d* | | 359 | 1*d* | 24 |
| 022 | 1*d* | | 364 | 2*s* | |
| 033.2 | 4*s* | 2.2 | 419 | 2*d* | 9 |
| 038.3 | 4*s* | 2.3 | 455 | 3*d* | 9 |
| 044 | 1*s* | | 489.5 | 7*s* | 7 |
| 052 | 1*d* | 8 | 497.2 | 5*s* | 7 |
| 064.7 | 3*s* | 3 | 534.9 | 3*s* | 4 |
| 070.9 | 4*s* | 2 | 540.7 | 3*s* | 3 |
| 076.0 | 3*s* | 3 | 555 | 2*d* | 5 |
| 081.7 | 3*s* | 3 | 646 | 2*d* | 27 |
| 087.3 | 3*s* | 3 | 672 | 1*d* | 6 |
| 092 | 1*s* | | 697 | 3*d* | 22 |
| 094.5 | 3*s* | 2 | 719 | 2*d* | 8 |
| 100.2 | 3*s* | 2 | 742 | 3*d* | 14 |
| 108.2 | 3*s* | 2 | 764 | 1*d* | 7 |
| 114.0 | 5*s* | 3 | 783 | 1*d* | 7 |
| 119.5 | 4*s* | 2 | 823 | 1*d* | 20 |
| 124.2 | 2*s* | 3 | 862 | 1*d* | 30 |
| 128.2 | 3*s* | 3 | | | |

(c) $TlCr(SeO_4)_2 \cdot 12H_2O$ 20°

| $cm^{-1}$ | $I$ | $w$ | $cm^{-1}$ | $I$ | $w$ |
|---|---|---|---|---|---|
| 14,898 | 1*s* | | 15,240 | 4*s* | |
| 906 | 1*s* | | 246 | 2*d* | |
| 922.1 | 10*s* | 1.7 | 252 | 3*d* | |
| 927.9 | 10*s* | 1.3 | 259 | 2*d* | |
| 980 | 1*s* | 17 | 279 | 1*d* | 24 |
| 15,005 | 1*s* | | 353 | 1*d* | 27 |
| 013 | 2*s* | | 420 | 1*d* | 20 |
| 020 | 1*s* | | 454 | 2*d* | 12 |
| 031 | 4*s* | | 486 | 8*s* | 8 |
| 037 | 4*s* | | 497 | 5*s* | 7 |
| 042 | 1*s* | | 533 | 2*d* | 8 |
| 049 | 1*s* | 5 | 555 | 1*d* | |
| 061 | 3*s* | | 638 | 1*d* | 25 |
| 068 | 5*s* | | 660 | 1*d* | 19 |
| 074 | 3*s* | | 697 | 4*d* | 22 |
| 080 | 4*s* | | 721 | 1*d* | 9 |
| 086 | 4*s* | | 741 | 4*d* | 14 |
| 092 | 4*s* | | 760 | 2*d* | 8 |
| 098 | 4*s* | | 777 | 1*d* | 14 |
| 104 | 2*d* | | 822 | 1*d* | 28 |
| 113 | 4*s* | | 863 | 1*d* | 21 |
| 121 | 3*s* | | 910 | 1*d* | 23 |
| 128 | 3*s* | | 959 | 1*d* | 42 |
| 135 | 2*s* | | 16,052 | 1*d* | 78 |
| 164 | 4*d* | 14 | 240 | 1*d* | 16 |
| 180 | 1*s* | | 279 | 1*d* | 34 |
| 186 | 1*s* | | | | |
| 194 | 1*s* | | | | |
| 233 | 2*s* | | | | |

(d) $KCr(SeO_4)_2 \cdot 12H_2O$ 15°

| $cm^{-1}$ | $I$ | $w$ | $cm^{-1}$ | $I$ | $w$ |
|---|---|---|---|---|---|
| 14,901.7 | 10*s* | 2.2 | 15,092 | 4*s* | |
| 906.6 | 10*s* | 1.9 | 096 | 1*s* | |
| 908.8 | 3*s* | | 105 | 1*d* | 6 |
| 926 | 1*s* | | 112 | 1*d* | |
| 934 | 1*s* | | 122 | 1*d* | 6 |
| 940 | 1*s* | | 135 | 1*d* | 7 |
| 953 | 1*s* | | 140 | 2*d* | 3 |
| 959 | 1*s* | | 163 | 1*d* | |
| 964 | 1*s* | | 168 | 1*d* | |
| 971 | 1*s* | | 203 | 1*d* | |
| 976 | 1*s* | | 205 | 1*d* | |
| 981 | 1*s* | | 213 | 3*s* | |
| 986 | 1*s* | | 218 | 4*d* | |
| 994 | 1*d* | 4 | 237 | 4*d* | 10 |
| 15,004 | 1*d* | | 260 | 1*d* | 15 |
| 012 | 2*d* | | 335 | 1*d* | 17 |
| 018 | 3*s* | | 394 | 1*d* | 10 |
| 043 | 2*d* | | 433 | 1*d* | 12 |
| 050 | 3*s* | | 469 | 4*d* | 10 |
| 054 | 1*s* | | 479 | 4*d* | 10 |
| 061 | 1*s* | | 516 | 2*d* | |
| 068 | 3*s* | | 521 | 2*d* | |
| 073 | 2*d* | | 532 | 2*d* | |
| 077 | 1*s* | | 537 | 2*d* | |
| 083 | 5*s* | | 623 | 1*d* | 19 |
| 087 | 3*s* | | 675 | 1*d* | 18 |

TABLE I.—*Continued.*

| $cm^{-1}$ | $I$ | $w$ | $cm^{-1}$ | $I$ | $w$ |
|---|---|---|---|---|---|
| (e) $NH_4Cr(SeO_4)_2 \cdot 12H_2O$ 110° *Clear crystal* | | | | | |
| 14,851 | 1*d* | 20 | 15,152 | 2*d* | 35 |
| 903.5 | 10*s* | 6 | 227 | 3*d* | 32 |
| 913.8 | 10*s* | 6 | 327 | 1*d* | 44 |
| 955 | 1*d* | 26 | 392 | 1*d* | 25 |
| 15,008 | 1*d* | 30 | 434 | 2*d* | 17 |
| 056 | 1*d* | 33 | 472 | 4*d* | 30 |
| 097 | 3*d* | 32 | 530 | 2*d* | 33 |
| (f) $NH_4Cr(SeO_4)_2 \cdot 12H_2O$ 20° *Shattered crystal* | | | | | |
| 14,846.0 | 9*s* | 2.2 | 15,164 | 1*d* | 14 |
| 878.9 | 10*s* | 2.6 | 187 | 1*d* | 7 |
| 903 | 5*d* | 6 | 202 | 1*d* | 10 |
| 915.4 | 5*s* | 1.3 | 231 | 2*d* | 7 |
| 917.6 | 5*s* | 1.4 | 245 | 3*d* | 9 |
| 921.5 | 10*s* | 2.3 | 255 | 1*d* | 11 |
| 925.0 | 10*s* | 1.8 | 277 | 1*d* | 10 |
| 979 | 1*s* | | 378 | 1*d* | 10 |
| 987 | 1*s* | | 401 | 3*d* | 10 |
| 15,015 | 1*s* | 9 | 432 | 5*s* | 7 |
| 075 | 1*d* | 14 | 452 | 3*d* | 6 |
| 093 | 1*d* | 6 | 487 | 4*d* | 15 |
| 103 | 4*s* | 3 | 590 | 1*d* | 12 |
| 120 | 1*d* | 11 | 609 | 1*d* | 10 |
| 128 | 1*d* | 6 | 648 | 1*d* | 10 |
| 146.5 | 1*d* | 5 | 692 | 1*d* | 22 |
| (g) $NH_4Cr(SO_4)_2 \cdot 12H_2O$ 85° *Clear crystal* | | | | | |
| 14,917 | 5*d* | 9 | 15,399 | 1*d* | 63 |
| 927 | 10*s* | 3 | 455 | 1*d* | 21 |
| 935 | 10*s* | 4 | 484 | 4*d* | 12 |
| 940 | 10*s* | 5 | 501 | 4*d* | 10 |
| 15,124 | 2*d* | 21 | 532 | 1*d* | 15 |
| 185 | 1*d* | 48 | 568 | 1*d* | 20 |
| 259 | 4*d* | 37 | | | |
| (h) $NH_4Cr(SO_4)_2 \cdot 12H_2O$ 75° *Shattered crystal* | | | | | |
| 14,866.2 | 9*s* | 2.4 | 15,134 | 2*d* | 24 |
| 902.3 | 10*s* | 2.3 | 187 | 1*d* | 37 |
| 928.7 | 9*s* | 1.5 | 233 | 1*d* | 15 |
| 932.3 | 10*s* | 2.1 | 265 | 3*d* | 24 |
| 938.4 | 9*s* | 3.2 | 422 | 2*d* | 13 |
| 941.6 | 9*s* | 2.9 | 462 | 477 | 30 |
| 15,069 | 1*d* | 28 | 493 | 2*d* | 18 |
| 101 | 1*d* | 20 | 512 | 1*d* | 7 |
| (i) $NH_4Cr(SO_4)_2 \cdot 12H_2O$ 20° *Shattered crystal* | | | | | |
| 14,868.0 | 10*s* | 1.1 | 15,196 | 3*d* | 19 |
| 885 | 1*d* | 5 | 212 | 1*d* | |
| 904.9 | 10*s* | 1.2 | 235 | 2*d* | 15 |
| 919 | 2*s* | 7 | 250 | 1*d* | |
| 928 | 2*s* | 4 | 264 | 5*d* | 9 |

| $cm^{-1}$ | $I$ | $w$ | $cm^{-1}$ | $I$ | $w$ |
|---|---|---|---|---|---|
| (i) $NH_4Cr(SO_4)_2 \cdot 12H_2O$—*Continued* 20° *Shattered crystal* | | | | | |
| 14,931.8 | 10*s* | 1.1 | 15,276 | 5*d* | 15 |
| 935.9 | 10*s* | 2.2 | 366 | 1*d* | 15 |
| 941.6 | 10*s* | 1.4 | 401 | 1*d* | 11 |
| 944.5 | 10*s* | 1.2 | 422 | 4*d* | 10 |
| 947.5 | 4*s* | 2 | 454 | 4*s* | |
| 955.5 | 2*s* | 3 | 465 | 3*d* | 7 |
| 15,007.5 | 3*s* | 7 | 479 | 3*d* | 7 |
| 025 | 2*s* | | 493 | 3*d* | 14 |
| 042.5 | 3*s* | 9 | 513 | 3*d* | 6 |
| 066 | 1*s* | | 531 | 1*d* | 10 |
| 082 | 2*s* | | 621 | 1*d* | 20 |
| 101 | 2*s* | | 679 | 1*d* | 14 |
| 114 | 2*s* | | 710 | 1*d* | 15 |
| 122 | 1*s* | | 724 | 1*d* | 13 |
| 130 | 5*s* | 8 | 763 | 1*d* | 39 |
| 140 | 3*s* | | 817 | 1*d* | 17 |
| 148.5 | 4*s* | 5 | 853 | 1*d* | 21 |
| 180 | 1*d* | 12 | | | |
| (j) $NH_4Cr(SO_4)_2 \cdot 12H_2O$ 15° *Clear crystal* | | | | | |
| 14,916 | 2*s* | | 15,239 | 4*s* | 6 |
| 923 | 2*s* | | 248 | 2*d* | |
| 925 | 2*s* | | 255 | 5*d* | |
| 929.8 | 10*s* | 1.3 | 263 | 5*d* | |
| 933 | 2*s* | | 273 | 5*d* | |
| 938.0 | 10*s* | 1.4 | 282 | 3*d* | |
| 943 | 2*s* | | 376 | 1*d* | |
| 949 | 1*d* | | 385 | 2*d* | |
| 957 | 1*d* | | 411 | 1*d* | |
| 971 | 1*d* | | 419 | 3*d* | |
| 978 | 1*d* | | 429 | 2*d* | |
| 987 | 1*d* | | 454 | 3*d* | |
| 994 | 1*d* | | 462 | 3*d* | |
| 15,000 | 1*d* | | 488.5 | 8*s* | 3 |
| 009 | 1*s* | | 492 | 8*s* | 4 |
| 021 | 1*d* | 13 | 500.5 | 6*d* | 3 |
| 033 | 1*s* | | 503 | 6*d* | 2 |
| 038 | 1*s* | | 520 | 1*s* | |
| 045 | 1*s* | 6 | 529 | 2*s* | |
| 053 | 1*s* | | 541 | 1*s* | |
| 057 | 1*s* | | 572 | 1*d* | 20 |
| 063 | 2*s* | 5 | 648 | 1*d* | 8 |
| 067 | 2*s* | 4 | 667 | 1*d* | 11 |
| 075 | 3*s* | 4 | 694 | 2*s* | 9 |
| 083 | 2*s* | 4 | 706 | 1*d* | |
| 094 | 1*d* | | 715.5 | 4*s* | 7 |
| 101 | 3*s* | | 734 | 1*s* | 5 |
| 107 | 2*d* | | 746 | 3*s* | 7 |
| 115 | 2*d* | | 753 | 3*s* | 8 |
| 123 | 5*s* | 6 | 770 | 3*d* | 9 |
| 128 | 5*s* | 4 | 795 | 1*d* | 9 |
| 137 | 5*s* | | 814 | 1*d* | 9 |
| 142 | 3*s* | | 843 | 2*d* | 31 |
| 145 | 1*d* | | 882 | 1*d* | 18 |
| 152 | 2*d* | | 926 | 1*d* | 29 |
| 159 | 2*d* | 6 | 977 | 1*d* | 36 |
| 170 | 3*d* | 9 | | | |
| 177.5 | 3*d* | 7 | | | |
| 187 | 3*d* | | | | |
| 197.5 | 3*d* | 5 | | | |
| 205 | 3*d* | 6 | | | |
| 231 | 1*d* | | | | |

TABLE I.—*Continued.*

| cm$^{-1}$ | $I$ | $w$ | cm$^{-1}$ | $I$ | $w$ |
|---|---|---|---|---|---|
| (k) $TlCr(SO_4)_2 \cdot 12H_2O$ 85° | | | | | |
| 14,745.5 | 1*d* | 7 | 15,135 | 7*s* | 7 |
| 796 | 1*d* | 4 | 147 | 5*d* | 6 |
| 822.5 | 1*d* | 7 | 153 | 4*d* | 5 |
| 876 | 1*d* | 8 | 183 | 5*d* | 8 |
| 891 | 1*d* | 4 | 209 | 4*d* | 11 |
| 913 | 3*s* | 4 | 274 | 8*d* | 20 |
| 920.5 | 1*s* | 3 | 390 | 4*d* | 8 |
| 938.5 | 10*s* | 1.8 | 432 | 4*d* | 7 |
| 941.6 | 10*s* | 2.0 | 466 | 4*d* | 14 |
| 948 | 2*s* | | 499 | 9*d* | 4 |
| 953 | 2*s* | | 505 | 4*d* | 7 |
| 961 | 2*s* | 4 | 533 | 4*d* | 8 |
| 969.5 | 2*s* | 5 | 575 | 3*d* | 21 |
| 987 | 2*s* | 7 | 639 | 1*d* | 11 |
| 15,001 | 3*d* | 7 | 672 | 1*d* | 13 |
| 011 | 2*d* | 5 | 709 | 6*d* | 19 |
| 021 | 1*d* | 2 | 734 | 1*d* | 7 |
| 036 | 1*d* | 10 | 757 | 7*d* | 11 |
| 058 | 5*s* | 8 | 804 | 1*d* | 20 |
| 069 | 2*d* | 2 | 838 | 3*d* | 8 |
| 083 | 5*d* | 6 | 869 | 3*d* | 21 |
| 089 | 4*d* | 6 | 921 | 1*d* | 12 |
| 102 | 4*s* | 3 | 981 | 1*d* | 15 |
| 114 | 5*s* | 4 | | | |
| (l) $TlCr(SO_4)_2 \cdot 12H_2O$ 20° | | | | | |
| 14,911 | 1*s* | | 15,259 | 1*d* | 2 |
| 921 | 3*s* | | 271 | 8*d* | 11 |
| 924.5 | 2*s* | 3 | 279 | 8*d* | 6 |
| 934 | 1*s* | | 285 | 8*d* | 6 |
| 939 | 4*s* | | 394 | 6*d* | 10 |
| 942.2 | 10*s* | 1.9 | 433 | 5*d* | 7 |
| 944.8 | 10*s* | 2.0 | 439 | 6*d* | 5 |
| 950 | 1*s* | 2 | 469 | 5*d* | 6 |
| 956 | 1*s* | | 475 | 6*d* | 5 |
| 962.4 | 4*s* | | 503 | 9*s* | 4 |
| 974 | 3*s* | 4 | 508 | 6*d* | 5 |
| 983.5 | 1*d* | 5 | 537 | 7*d* | 12 |
| 994 | 3*s* | 5 | 556 | 2*d* | 8 |
| 15,009.1 | 4*s* | 4 | 583 | 3*d* | 19 |
| 015.4 | 3*s* | 4.2 | 624 | 1*d* | 29 |
| 025 | 2*d* | 4 | 649 | 1*d* | 18 |
| 042 | 3*d* | 8 | 679 | 1*d* | 31 |
| 050 | 1*d* | 4 | 713 | 6*d* | 19 |
| 060.5 | 7*s* | 3.9 | 733 | 5*d* | 9 |
| 064.4 | 7*s* | 3.9 | 761 | 7*d* | 7 |
| 072.5 | 5*s* | 5.6 | 776 | 1*d* | 10 |
| 085.6 | 7*s* | 4.0 | 804 | 1*d* | 13 |
| 093.6 | 5*s* | 2.4 | 816 | 1*d* | 11 |
| 099 | 1*s* | | 841 | 3*d* | 21 |
| 105.2 | 8*s* | 3.1 | 872 | 3*d* | 20 |
| 111 | 1*s* | 4 | 922 | 1*d* | 18 |
| 117.7 | 8*s* | 4.2 | 937 | 1*d* | |
| 124.5 | 2*d* | 3 | 981 | 1*d* | 22 |
| 132 | 1*d* | 2 | 16,030 | 1*d* | 19 |
| 139 | 8*d* | 6 | 063 | 1*d* | 28 |
| 150 | 6*d* | 8 | 104 | 1*d* | 24 |
| 156.5 | 6*d* | 5 | 164 | 1*d* | 26 |
| 176 | 1*d* | | 202 | 1*d* | 14 |
| 187 | 7*d* | 11 | 247 | 1*d* | 30 |
| 198 | 3*s* | 4 | 290 | 1*d* | 25 |
| 212 | 6*d* | 9 | | | |
| (m) $RbCr(SO_4)_2 \cdot 12H_2O$ 20° | | | | | |
| 14,814 | 1*s* | | 15,158.5 | 7*d* | 5 |
| 913 | 1*s* | | 164 | 1*s* | |
| 922 | 1*s* | | 177 | 1*d* | 6 |
| 930 | 1*s* | | 191 | 5*d* | 11 |
| 942 | 1*s* | | 200 | 2*d* | |
| 945.5 | 10*s* | 1.4 | 214 | 4*d* | 9 |
| 947.4 | 10*s* | 1.2 | 262 | 1*d* | |
| 950.7 | 2*s* | | 275 | 8*d* | 8 |
| 954.0 | 3*s* | | 281 | 4*d* | 4 |
| 970 | 3*s* | 3 | 288 | 4*d* | 4 |
| 997.5 | 1*d* | 7 | 398 | 1*d* | 10 |
| 15,012 | 3*s* | 4 | 433 | 2*d* | |
| 020.5 | 1*d* | 9 | 443 | 2*d* | |
| 031 | 1*d* | 8 | 467.5 | 1*d* | 7 |
| 039 | 1*d* | 8 | 476 | 3*d* | 6 |
| 048.5 | 2*d* | 7 | 507.5 | 8*d* | 7 |
| 055.5 | 1*d* | 7 | 513 | 1*d* | 4 |
| 062.5 | 6*d* | 5 | 541 | 4*d* | 9 |
| 067.5 | 6*d* | 5 | 553 | 1*d* | |
| 078.5 | 3*d* | 7 | 562 | 1*d* | |
| 089.9 | 7*s* | 4.2 | 581 | 1*d* | 15 |
| 096.3 | 7*s* | 2.2 | 627 | 1*d* | 23 |
| 102 | 4*s* | | 655 | 1*d* | 21 |
| 107.1 | 7*s* | 2.6 | 686 | 1*d* | 23 |
| 114 | 3*s* | | 716 | 3*d* | 16 |
| 121.7 | 7*s* | 2.1 | 737 | 3*d* | 6 |
| 129 | 3*d* | 2 | 764 | 4*d* | 10 |
| 136 | 3*d* | 3 | 781 | 1*d* | 14 |
| 142.5 | 9*d* | 5 | 846 | 2*d* | 16 |
| 151.5 | 7*d* | 7 | 879 | 2*d* | 22 |
| (n) $NH_3OHCr(SO_4)_2 \cdot 12H_2O$ 20° | | | | | |
| 14,875 | 1*s* | | 15,109 | 4*s* | |
| 884 | 1*s* | | 117 | 1*s* | |
| 889 | 1*s* | | 124 | 1*s* | |
| 895.4 | 10*s* | 1.4 | 134 | 2*s* | 8 |
| 907 | 1*s* | | 148 | 1*s* | |
| 918.9 | 10*s* | 1.5 | 157 | 1*s* | |
| 925 | 1*s* | | 168.5 | 2*s* | 7 |
| 929 | 1*s* | | 192 | 1*s* | 8 |
| 939 | 1*s* | | 216 | 1*d* | |
| 944 | 1*s* | | 223 | 1*d* | |
| 949 | 1*s* | | 229 | 1*d* | |
| 956 | 1*s* | | 240.5 | 4*d* | 5 |
| 963 | 1*s* | | 264.5 | 2*d* | 7 |
| 970 | 1*s* | | 347 | 2*d* | 9 |
| 979 | 1*s* | | 382 | 3*s* | 6 |
| 987 | 1*s* | | 402 | 2*s* | 11 |
| 999 | 1*s* | | 419.5 | 3*s* | 5 |
| 15,007.5 | 1*s* | 3 | 437 | 3*s* | 6 |
| 010 | 1*s* | 2 | 449 | 2*d* | 4 |
| 017.5 | 1*s* | 5 | 460 | 5*s* | 4 |
| 027 | 2*s* | 6 | 471 | 4*s* | |
| 034 | 2*s* | | 486.5 | 3*s* | 7 |
| 047 | 2*s* | | 510.5 | 2*s* | 9 |
| 052 | 2*s* | | 530 | 1*d* | |
| 058 | 2*s* | 4 | 553 | 1*d* | 12 |
| 061.5 | 2*s* | 3 | 617 | 1*d* | 15 |
| 070 | 3*s* | | 643 | 1*d* | 21 |
| 077 | 2*s* | | 669 | 2*d* | 20 |
| 083 | 1*d* | | 714 | 2*d* | 42 |
| 088 | 2*d* | | 757 | 1*d* | 12 |
| 093 | 1*d* | | 819 | 1*d* | 22 |
| 098 | 1*d* | | 850 | 1*d* | 13 |

TABLE I.—*Continued.*

| $cm^{-1}$ | $I$ | $w$ | $cm^{-1}$ | $I$ | $w$ |
|---|---|---|---|---|---|
| (o) $CH_3NH_3Cr(SeO_4)_2 \cdot 12H_2O$ 20° | | | | | |
| 14,573.9 | 10$s$ | 1.6 | 14,946 | 1$d$ | 30 |
| 587 | 1$s$ | | 15,000 | 1$d$ | 30 |
| 621.5 | 1$d$ | 9 | 047 | 1$d$ | 16 |
| 629 | 3$s$ | | 084 | 2$d$ | 20 |
| 653.5 | 1$d$ | 9 | 127 | 4$s$ | 7 |
| 684.5 | 1$d$ | 7 | 145 | 1$s$ | 8 |
| 692.5 | 4$s$ | 5 | 155 | 1$s$ | |
| 701 | 1$s$ | | 163.5 | 2$s$ | 3 |
| 730.5 | 2$s$ | 7 | 176 | 1$s$ | 9 |
| 738 | 3$s$ | | 187 | 3$s$ | 4 |
| 741 | 1$s$ | | 214 | 2$s$ | 7 |
| 756 | 1$s$ | 8 | 240 | 1$d$ | 16 |
| 765 | 1$s$ | 7 | 269 | 1$d$ | 21 |
| 789 | 1$d$ | | 292 | 1$d$ | 3 |
| 797.5 | 4$s$ | 3 | 302 | 1$d$ | 4 |
| 804.5 | 1$s$ | 3 | 321 | 1$d$ | 13 |
| 816 | 1$d$ | 11 | 351 | 1$d$ | 17 |
| 832 | 1$d$ | 7 | 459 | 1$d$ | 6 |
| 876 | 1$d$ | 11 | 508 | 1$d$ | 48 |
| 898 | 1$d$ | 15 | 583 | 1$d$ | 20 |
| 910 | 1$d$ | | | | |
| (p) $CH_3NH_3Cr(SO_4)_2 \cdot 12H_2O$ 20° | | | | | |
| 14,501.2 | 10$s$ | 1.5 | 14,830 | 1$d$ | 11 |
| 507 | 1$s$ | | 946 | 1$d$ | 8 |
| 517 | 1$s$ | | 955 | 1$d$ | 9 |
| 549.5 | 1$s$ | 5 | 974 | 1$d$ | 9 |
| 557 | 1$s$ | 6 | 15,000 | 1$d$ | |
| 566.5 | 1$d$ | 5 | 011 | 3$d$ | 7 |
| 580 | 1$d$ | 11 | 042 | 1$d$ | |
| 593 | 1$d$ | 12 | 046 | 1$d$ | |
| 617 | 1$s$ | | 053 | 2$s$ | |
| 625.5 | 3$s$ | 7 | 060 | 1$d$ | |
| 634 | 1$s$ | | 072 | 1$d$ | |
| 646.5 | 2$s$ | 5 | 083 | 2$s$ | |
| 660 | 2$d$ | 9 | 099 | 1$d$ | 11 |
| 669 | 2$s$ | | 132 | 1$d$ | 29 |
| 677 | 1$s$ | | 241 | 1$d$ | 12 |
| 689.5 | 1$d$ | 5 | 268 | 1$d$ | 18 |
| 719.5 | 1$d$ | 5 | 393 | 1$d$ | 11 |
| 730.5 | 3$s$ | 7 | 416 | 1$d$ | 7 |
| 745 | 1$d$ | 4 | 437 | 1$d$ | 24 |
| 752 | 1$d$ | | 513 | 1$d$ | 12 |

| $cm^{-1}$ | $I$ | $w$ | $cm^{-1}$ | $I$ | $w$ |
|---|---|---|---|---|---|
| (q) $CsCr(SO_4)_2 \cdot 12H_2O$ 20° | | | | | |
| 14,479.3 | 10$s$ | 2.2 | 14,776 | 1$d$ | |
| 517 | 1$s$ | | 787 | 1$d$ | |
| 523.5 | 5$s$ | 2.1 | 810 | 2$d$ | |
| 528 | 1$s$ | | 817 | 3$s$ | |
| 535 | 1$s$ | | 827 | 1$d$ | 10 |
| 537 | 1$s$ | | 841 | 1$d$ | |
| 540.5 | 2$s$ | 5 | 861 | 1$d$ | 10 |
| 549 | 1$s$ | | 927 | 3$s$ | 8 |
| 553 | 3$s$ | 2 | 947 | 1$d$ | 5 |
| 555.5 | 3$s$ | 3 | 960 | 3$s$ | 8 |
| 565 | 1$s$ | | 975 | 1$d$ | 8 |
| 571.7 | 4$s$ | | 995.1 | 9$s$ | 4 |
| 575.1 | 4$s$ | | 15,034.2 | 9$s$ | 4 |
| 578 | 4$s$ | | 040.1 | 10$s$ | 2.4 |
| 582.5 | 4$s$ | | 052.5 | 8$s$ | 4.6 |
| 586.0 | 4$s$ | | 059 | 4$s$ | |
| 600.7 | 9$s$ | 1.7 | 065 | 5$s$ | 6 |
| 612.3 | 5$s$ | 3 | 086 | 1$d$ | 8 |
| 618 | 1$s$ | | 096 | 3$d$ | |
| 626.5 | 4$s$ | 5 | 112 | 1$d$ | 23 |
| 632 | 5$s$ | | 136 | 1$d$ | |
| 635.5 | 4$s$ | 5 | 147 | 1$d$ | |
| 643 | 1$s$ | | 154 | 5$d$ | 8 |
| 650 | 1$s$ | | 161 | 4$d$ | 6 |
| 655.5 | 3$d$ | 7 | 176 | 2$d$ | 9 |
| 663 | 1$d$ | | 184 | 2$d$ | 8 |
| 668 | 1$d$ | | 212 | 3$d$ | 27 |
| 675 | 2$d$ | | 260 | 1$d$ | 12 |
| 679 | 2$d$ | | 276 | 1$d$ | 8 |
| 683 | 2$s$ | | 298 | 1$d$ | 11 |
| 693 | 4$d$ | | 332 | 2$d$ | 25 |
| 696 | 4$d$ | | 371 | 2$d$ | 7 |
| 699 | 4$d$ | | 417 | 3$d$ | 30 |
| 708.1 | 8$s$ | 3.4 | 469 | 1$s$ | |
| 713 | 2$s$ | | 514 | 1$d$ | 12 |
| 719 | 4$s$ | | 544 | 1$d$ | |
| 727 | 1$d$ | | 579 | 1$d$ | 7 |
| 736 | 1$d$ | | 622 | 1$d$ | 36 |
| 742 | 1$d$ | | | | |
| 755 | 2$s$ | 6 | | | |

photographed at 85° and 20° or 15°K: both the sulfate and selenate alums of potassium, rubidium, cesium and thallium, ammonia and methylamine, and the sulfate alum of hydroxylamine.

## EXPERIMENTAL PART

Large single crystals of most of the alums were obtained by evaporation at 6°C of solutions containing equivalent amounts of the sulfates or selenates of chromium and the various univalent cations. Rubidium and cesium chrome alums were obtained as large crystals only after adding concentrated nitric acid to increase the otherwise slight solubility of these salts. The crystals gave no test for nitrate and their spectra were identical with the spectra of the small crystals separating from solutions in water alone.

A guanidine sulfate alum has been reported.[5] The spectrum of the guanidine chromium sulfate which we prepared was widely different from that of any of the chrome alums. Crystallo-

[5] Canneri, Gazz. Chim. Ital. **55**, 611 (1925).

graphic examination of the guanidine compound showed that it has hexagonal symmetry and thus that it is not an alum.

Preparation of alums of many other substituted amines was attempted unsuccessfully. Among them were both the sulfate and selenate alums of ethylamine, dimethylamine, propylamine, and isopropylamine; and sulfate alums of triethylamine, tetramethylamine, aniline, methyl guanidine and dimethyl guanidine. The univalent cations of these organic substances are evidently too large to be included in an alum lattice. The few cubic crystals sometimes obtained were attributable to ammonia or methylamine impurities in the amines employed.[6]

Hydrazine sulfate chrome alum and sodium sulfate and selenate chrome alums[7–9] have been described. We were able to prepare neither these alums nor silver sulfate nor hydroxylamine selenate chrome alum.

The spectra were photographed at the temperature of liquid air and liquid hydrogen, employing apparatus and technique described previously.[4] The thickness of the single crystals used was from 3 to 7 mm. No investigation was made of the polarization of the absorption lines or of the directional dependence of their intensity.

## Description of the Spectra

The position of the centers of the absorption lines, the width and character and the relative intensity are given in Table I for all the alums at hydrogen temperatures, with the exception of $KCr(SO_4)_2 \cdot 12H_2O$, whose spectrum has been reported in detail from this Laboratory. Data at higher temperatures on $TlCr(SO_4)_2 \cdot 12H_2O$ are included because they indicate several excited levels in the lower state not found by Sauer, and data on the ammonium alums because of unusual temperature behavior. The positions reported for the strong, sharp lines in the region of the characteristic doublet are probably correct within a fraction of a $cm^{-1}$ while for the faint, diffuse, multiple lines and bands the error may well be one or more $cm^{-1}$. The spectra are represented graphically in Fig. 1 and by photographs in Figs. 2, 3 and 4.

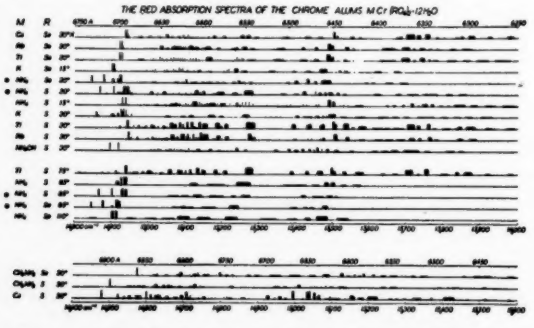

Fig. 1. Graphical representation of the alum spectra. The solid circles at the extreme left indicate that the corresponding crystals were shattered.

At the long wave-length end of the spectrum of all the alums is a line or group of lines of singular sharpness and intensity, originating probably in pure electronic jumps within the $3d$ shell of the $Cr^{+++}$ ion. Extending to perhaps 700 to 1300 $cm^{-1}$ on the violet side of the strong group is a series of weaker lines whose sharpness and resolution decrease very greatly with their separation from the strong group. The discrete absorption ultimately is masked beneath a continuous absorption band. The most striking changes on isomorphous replacement of univalent cations and of anions appear in the electronic spectrum. Three classes may be distinguished. The first class, which comprises most of the alums, has a strong doublet accompanied by a variable number of much fainter lines or satellites grouped close to 6700A. The spectrum of alums of the second class is shifted in its entirety about 400 $cm^{-1}$ toward the red and in place of a characteristic electronic doublet there is a single strong, sharp line near 6900A. The third class shows about six strong lines near 6700A.

To the first class belong the four alums of rubidium and thallium, the selenate alums of cesium and potassium, the sulfate alum of hydroxylamine and the form of all the ammonium alums that is stable at higher temperatures. The position and the separation of the components of the doublet is variable. On lowering the temperature below 85°K the doublets sharpen perceptibly, their satellites become much more pronounced, and many of the diffuse bands narrow and resolve into a number of weak,

[6] Wendekamm, Zeits. f. Krist. **85**, 35 (1933).
[7] Sommer and Weise, Zeits. f. anorg. allgem. Chemie **94**, 51 (1916).
[8] Orlov, Ukrainskii Khem. Zhurnal **3**, 115 (1928).
[9] Sarkar and Bhattacharya, J. Ind. Chem. Soc. **7**, 765 (1930).

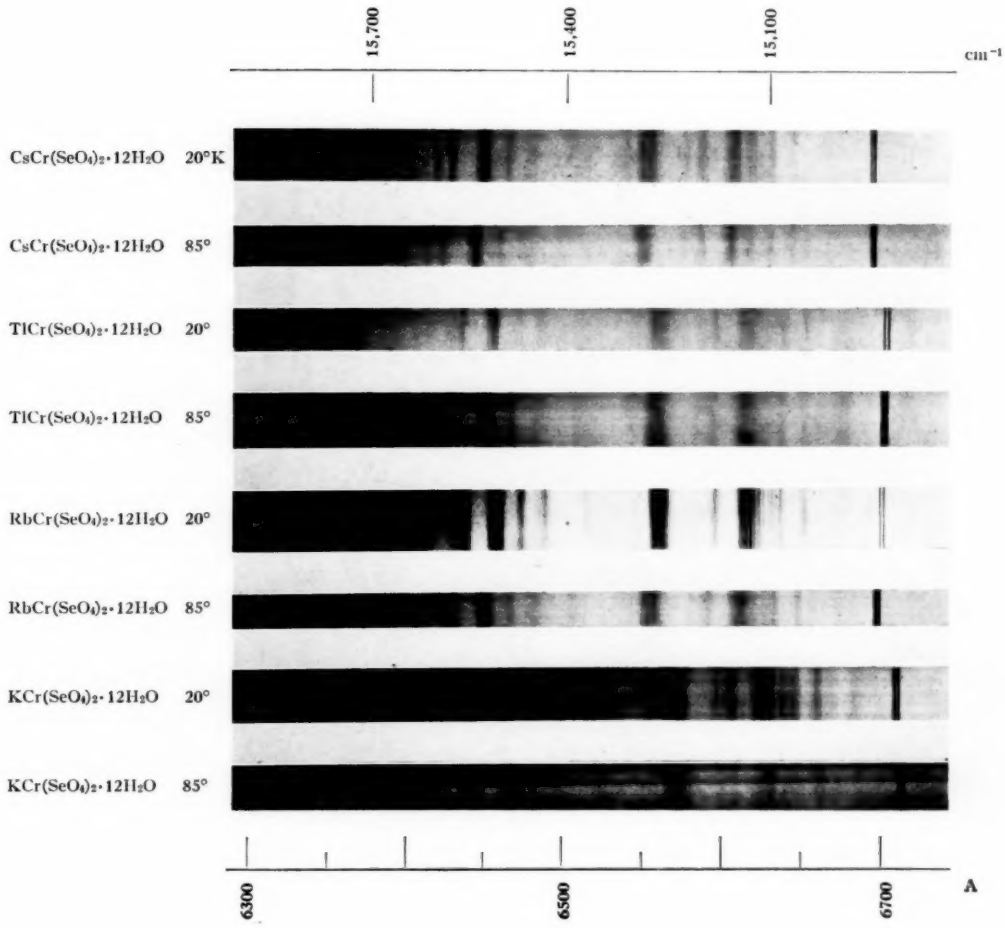


FIG. 2.

sharp, closely spaced lines (about 5 $cm^{-1}$) around 15,100 $cm^{-1}$. (See especially $RbCr(SeO_4)_2 \cdot 12H_2O$ in Fig. 2.) The selenates of this class show remarkable similarity. Their spectra correspond practically line for line in respect to their relative position and intensity. In the sequence potassium, thallium, rubidium and cesium there is a displacement of the entire spectrum to the violet with each succeeding member. The amount of the displacement depends largely on the size of the cation and not upon its mass as the following compilation shows. $\Delta\nu$ is the shift of the mean frequency of the characteristic doublet. Replacing sulfate by selenate in thallous alums induces a red shift of the center of the doublet of 19 $cm^{-1}$; in rubidium alums, 20 $cm^{-1}$. Comparison of sulfate and selenate alums of this class produces little evidence of differences in their spectra which can be associated with characteristic oscillation frequencies of these anions.

| | $K^+$ | $Tl^+$ | $Rb^+$ | $Cs^+$ |
|---|---|---|---|---|
| at wt. | 39 | 204 | 85 | 133 |
| radius | 1.33 | 1.48 | 1.48 | 1.69A |
| $\Delta\nu$ | 0 | 21.0 | 21.5 | 35 $cm^{-1}$ |

The two alums of methylamine and the sulfate alum of cesium constitute the second class. The spectra are characterized by their diffuseness at 85°K. The weak absorption bands of the methylamine alums are, indeed, scarcely visible. At 20° they are, however, quite sharp. The attempt was made to resolve the isolated strong line of this class into a "characteristic doublet." The spectrum of the cesium alum was photographed at 20° in the second order of the grating (dispersion 1.8A per mm) but no indication of resolution was discovered.

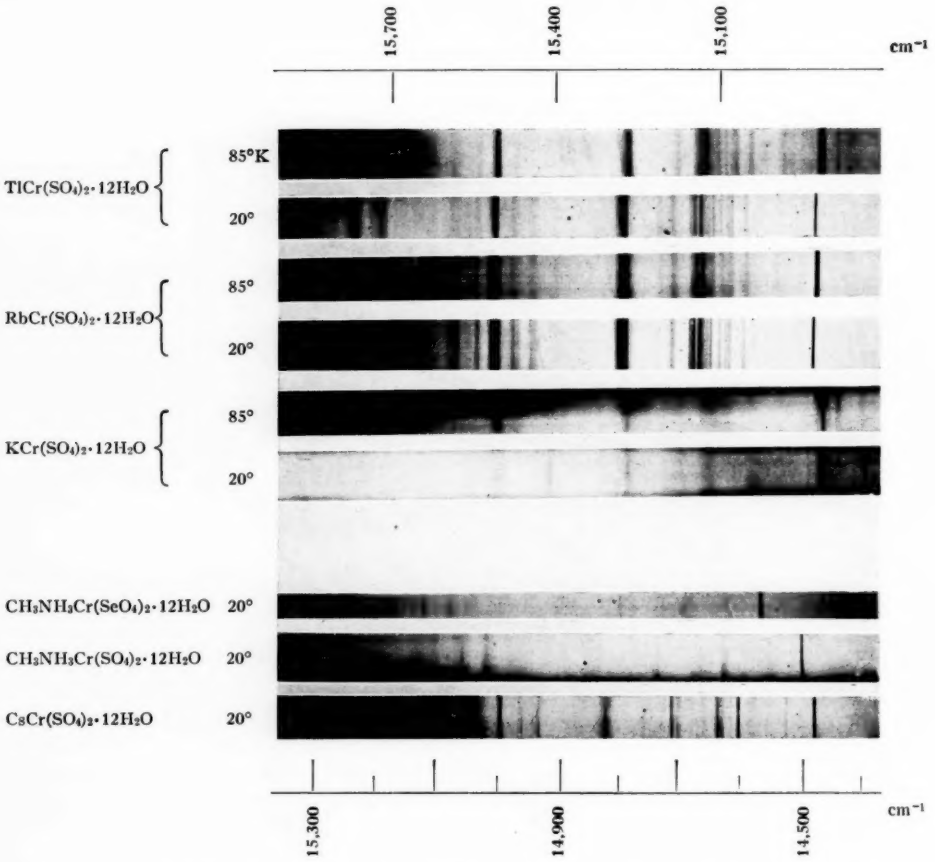


FIG. 3.

Potassium sulfate alum and the low temperature form of the two ammonium alums make up the third class. Characteristic of this group is the large number (six or more) of strong sharp lines which appear near 6700A. In their change with temperature the ammonium alum spectra are as anomalous as the potassium chrome sulfate spectrum, but in a different way. The potassium alum has notably different spectra at 85° and at 14°K, and at intermediate temperatures both spectra appear with prominence which varies with the temperature. The whole behavior is such as to suggest the presence of a close multiplet structure in the lower state. The ammonium alums also have "high" and "low" temperature spectra, but they do not coexist. It is often possible to keep an ammonium sulfate alum crystal indefinitely in liquid nitrogen or liquid hydrogen in its original perfect, highly transparent condition. In this case the spectra at the higher and lower temperatures differ only in the line breadths. On other occasions an apparently perfect crystal retains its transparency for a few minutes after being placed in the cooling liquid and then almost instantaneously becomes practically opaque, as though broken into an infinite number of tiny crystals by the disruption of the lattice. It is these nearly opaque crystals which will be called "shattered crystals" in what follows. Exposure times for the shattered crystals are of the order of one hundred times as long as for the perfect crystals and a thickness of 1 mm is ample. The spectra are quite unlike (Fig. 4). The high temperature form has two strong lines near 6700A, the low temperature form has six lines much more widely spaced.

The influence of temperature upon the ammonium alums was investigated carefully. In liquid oxygen (90°) the sulfate alum gave the spectrum of the high temperature form (Table I (g)). The crystal was gradually cooled further by reducing the pressure on the oxygen until at $81\pm1°$ the crystal suddenly became opaque, and

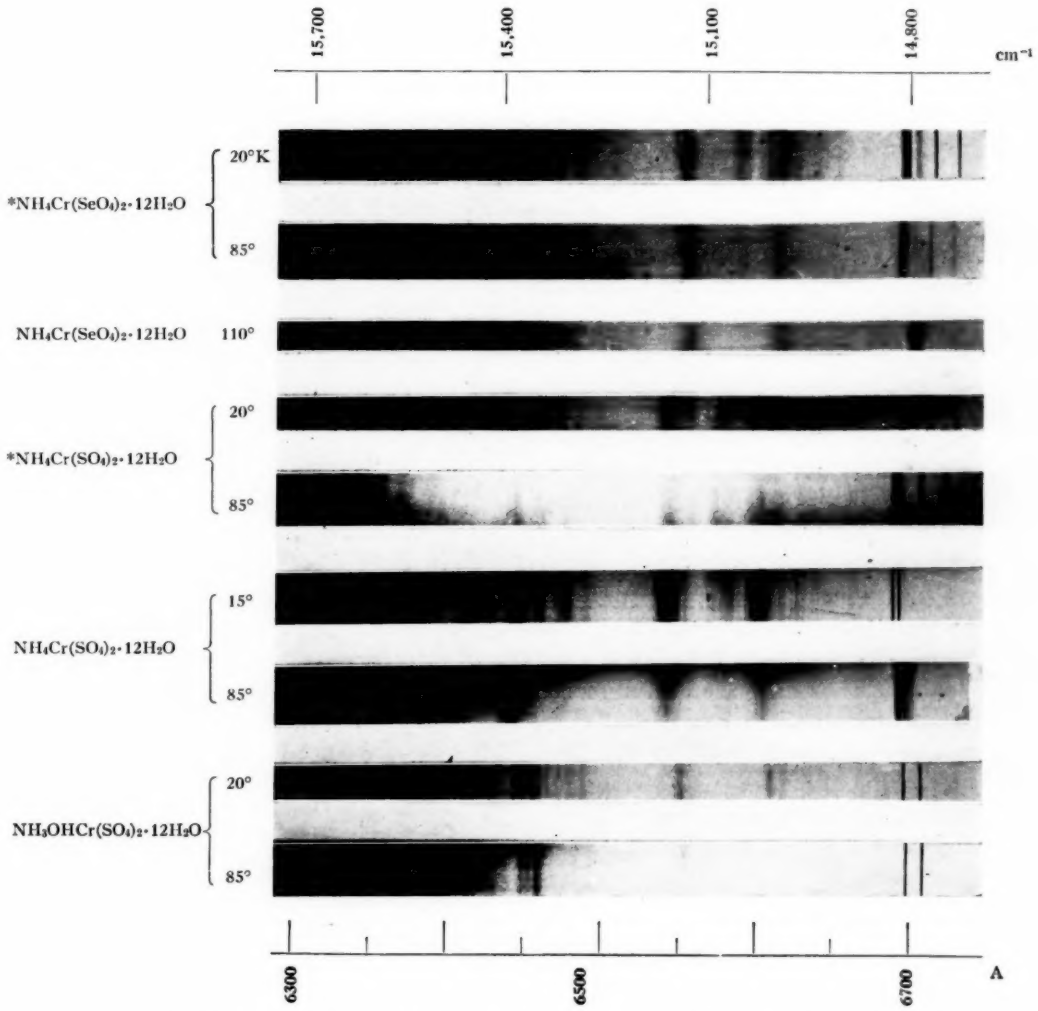


FIG. 4. Spectra of ammonium and hydroxylamine alums. * Indicates shattered crystals.

its spectrum was now that of the low temperature form (Table I (h)). The crystal was warmed to room temperature and re-immersed in liquid oxygen at one atmosphere. It again gave the spectrum of the high temperature form. The selenate alum was treated similarly, using liquefied natural gas (about 90 percent methane) as cooling liquid. In the methane at one atmosphere pressure the crystal gave the high temperature spectrum (Table I (e)). On lowering the temperature the crystal became opaque at $106\pm5°$ as determined roughly by a thermocouple. Its spectrum was now that of the low temperature form (Table I (f)). After standing in the cooling bath until the temperature had risen to about 140° the crystal gave the high temperature spectrum. These experiments clearly indicate the existence of transitions in the crystal lattice of the ammonium alums at low temperatures. It has been possible to supercool the high temperature form of the sulfate alum to 15°K, but in no case was it possible to supercool the selenate alum. Shattered crystals often regain most of their original transparency on warming to room temperature. The density of perfect and of shattered crystals is practically identical.

Discrete absorption bands in the blue have been found at 20° in the following alums: the sulfates and selenates of rubidium, thallium, cesium and methylamine, the sulfate of potas-

sium and the high temperature form of the sulfate of ammonium. The bands are diffuse and very weak. They could be photographed only when thick, perfect crystals were available. The bands extend into the regions of continuous absorption on either side.

## Discussion

The large difference in the spectra of alums of classes I and II is doubtless consequent upon small differences in the lattice structure. Lipson and Beevers[10] have found two distinct structures among the aluminum sulfate alums, differing only in the position of the sulfate ion along a trigonal axis of the unit cell. One position is assumed in alums with the largest univalent cations, cesium and methylamine, while the second position of the sulfate is taken when the cations are of medium size, such as potassium, ammonium, thallium and rubidium. From their absorption spectra one may venture that cesium sulfate chrome alum has the one structure, while cesium selenate chrome alum has the other. A third, more widely different structure has been found by Lipson and Beevers for alums with small cations. This structure differs from the other two in the orientation of the anion along the trigonal axis. The spectrum of a chrome alum with this structure might well be distinctly unlike the others. Attempts were made, accordingly, to introduce the small ions $Na^+$ and $Ag^+$ into a chrome alum lattice, but without success.

The dielectric measurements of Guillien[11] are of interest in connection with the spectroscopic anomalies of potassium sulfate and ammonium alums. In sulfate alums of iron, chromium and aluminum with ammonium or potassium Guillien finds that the dielectric constant decreases with temperature down to about $-100°$, rises when the temperature is lowered to $-187.5°$ and then very suddenly decreases again. The electric absorption and specific heat also have maxima near $-190°$. The phenomena usually show hysteresis and the maxima seem to be true $\lambda$ points. They are probably to be ascribed to cooperative relaxation of librational restraint upon water molecules or water-containing complexes with rising temperature. In the ammonium chrome alums imposition of this librational restraint upon cooling evidently induces strains in the lattice which are often relieved in the shattering of the crystal. A more stable lattice is formed in which the chromium ions are acted on by fields of slightly different strength and (probably lower) symmetry as is expressed in the changed absorption spectrum. The lattice of the potassium alum is not similarly disrupted and the high and low temperature spectra may exist together.

The nature of the electronic states giving rise to the characteristic doublet or corresponding lines in other $Cr^{+++}$ compounds has not yet been satisfactorily described. Bowen[12] gives the following positions for terms arising from the $3d^3$ configuration of gaseous $Cr^{+++}$.

| | |
|---|---|
| $^4F$ 3/2, 5/2, 7/2, 9/2 | 0, 237, 553, 949 $cm^{-1}$ |
| $^4P$ 1/2, 3/2, 5/2 | 14,058, 14,177, 14,476 $cm^{-1}$ |
| $^2G$ 7/2, 9/2 | 15,056, 15,405 $cm^{-1}$ |
| $^2H$ 9/2, 11/2 | 21,067, 21,320 $cm^{-1}$ |

$^2D$ levels were not found but probably lie not far from $^2H$. The interval $^4F-{}^2G$ of the gaseous ion is nearly equal to the frequency of the sharp lines in the red spectrum of $Cr^{+++}$ compounds. Similarly, the energy difference between $^4F$ and $^2H$ levels of the free ion is nearly the same as the frequency of the blue line absorption spectrum. Hence it has been proposed several times[13] that the line spectra of the chrome alums do in fact represent $^4F-{}^2G$ and $^4F^2-H$ transitions. However, owing to the drastic modification of coupling schemes and selection rules and the splitting and shifting of the energy levels of the free ion in the crystal fields, the above assignment of levels is probably not correct.[13a]

Precise measurements of the magnetic susceptibility have been made only on potassium chromium sulfate alum.[14] The strict linearity of the susceptibility-temperature curve from 1.3° to 290°K makes it probable that there is no

[10] Lipson, Nature **135**, 912 (1935); Proc. Roy. Soc. (London) **A151**, 347 (1935); Lipson and Beevers, Nature **134**, 327 (1934); Proc. Roy. Soc. (London), **A148**, 664 (1934).
[11] Guillien, Comptes rendus **209**, 21 (1939).
[12] Bowen, Phys. Rev. **52**, 1153 (1937).
[13] Deutschbein, Ann. d. Physik **14**, 712 (1932); Joos, Ergeb. exakt. naturwiss. **18**, 78 (1939).
[13a] While this article was in press, papers on the electronic energy levels of the chrome alums have been published by Van Vleck (J. Chem. Phys. **8**, 787 (1940)) and Finkelstein and Van Vleck (*ibid.* **8**, 790 (1940)).
[14] de Haas, Gorter and van den Handel, Proc. Acad. Sci. Amsterdam **33**, 676 (1930); **36**, 158 (1933).

excited electronic level in $Cr^{+++}$ within 200 $cm^{-1}$ of the ground level.[14a] Heat capacity data are not available to add further evidence on this point. The two or more strong, characteristic lines of the chrome alums originate then in transitions from a single lower state to two or more rather closely spaced upper electronic states.[15] The weak lines and the diffuse bands of higher frequency represent simultaneous photo-excitation of the electronic transition and oscillation of the lattice or certain of its constituents. The first (green) continuum may have a similar origin and also may include other electronic jumps and associated secondary structure as yet undetected. The blue absorption lines seem to be the counterpart of the weak sharp lines around 15,100 $cm^{-1}$ and may be associated with a strong, pure electronic transition which is hidden in the continuum.

In absorption spectra of neodymium salts Ewald[16] has found groups of weak, sharp lines repeating strong, sharp, pure electronic multiplets at intervals corresponding to internal vibration frequencies of the anions. Photo-excitation of the characteristic vibrations takes place with moderate probability simultaneously with the electronic transitions of the $Nd^{+++}$ ion in spite of the interposition of neutral molecules of an $Nd(H_2O)_6^{+++}$ complex. As in many neodymium compounds, the anions of the chrome alums are separated from the trivalent ion by an octahedral shell of water molecules.

The fundamental frequencies of the sulfate ion are about 450, 620, 980 and 1100 $cm^{-1}$. The frequencies vary somewhat in different compounds, and removal of degeneracy in asymmetric lattice fields may result in doubling or tripling of the energy states.[17] Characteristic frequencies of the selenate ion are 340, 410, 835 and 870 $cm^{-1}$. None of the sulfate or selenate frequencies appear prominently in the chrome alum spectra. The clearest indications of them are in the 15,200–15,600 $cm^{-1}$ bands of the selenates of K, Rb, Tl and Cs and the sulfates of Rb, Tl and $NH_4$. Most of the bands in this frequency range are common to both selenates and sulfates. The ones which are not are broad, diffuse and weak. Bands present in selenates and absent in sulfates occur shifted 355 and 435 $cm^{-1}$ from the mean frequency of the characteristic doublet, while bands present in sulfates and absent in selenates are at 450 and 645 $cm^{-1}$. Absorption bands surely associated with the higher frequencies of the anion have not been found.

The fundamental frequencies of the water molecule are 1600, 3600 and 3750 $cm^{-1}$. Because of proximity, combination of these frequencies with electronic frequencies of $Cr^{+++}$ might have large probability of occurrence. Corresponding absorption bands would lie in the continuum and indeed may contribute largely to the observed intensity. Other internal vibrations of homopolar complexes can occur only in ammonium, hydroxylamine and methylamine alums. The frequencies are so high (800–3400 $cm^{-1}$)[18] that corresponding absorption would also occur within or close to the continuum. In intensity it would probably be no greater than absorption due to internal oscillation of the anions.

Among the observed weak lines certain of the strongest are of interest because they have nearly the same separation from the pure electronic lines in sulfate and selenate alums of all the classes we have distinguished. Such separations occur at about 330, 570 and 800 $cm^{-1}$. Sometimes the electronic spectrum and its subsidiary structure is repeated exactly at a frequency 330 $cm^{-1}$ higher, but the diffuseness of bands near 570 and 800 $cm^{-1}$ is such that detailed matching of structures is scarcely possible. Lines near 195 $cm^{-1}$ are common to most of the spectra. The electronic spectrum is repeated in lines of moderate strength and good definition at about 110 $cm^{-1}$ in selenate alums of K, Rb, Tl and Cs; at 115 $cm^{-1}$ in sulfate alums of Rb and Tl; at 120 $cm^{-1}$ in cesium sulfate and the

[14a] Van Vleck, J. Chem. Phys. **7**, 61, 72 (1939); Phys. Rev. **57**, 426 (1940).

[15] Crystallographic non-identity of all the $Cr^{+++}$ ions would lead to a difference of energy of the ground states, which, however, would not be revealed necessarily in the magnetic susceptibility-temperature curve of the alum. The upper states, too, would have different energy so that a multiplet could arise in a single transition in different kinds of chromium ions as well as in multiple transitions to a group of levels in a single kind of chromium ion.

[16] Ewald, Ann. d. Physik **34**, 209 (1939).

[17] Hibben, *The Raman Effect and its Chemical Applications* (Reinhold, 1939), p. 387, 396.

[18] Hibben, reference 17, p. 263 ff.

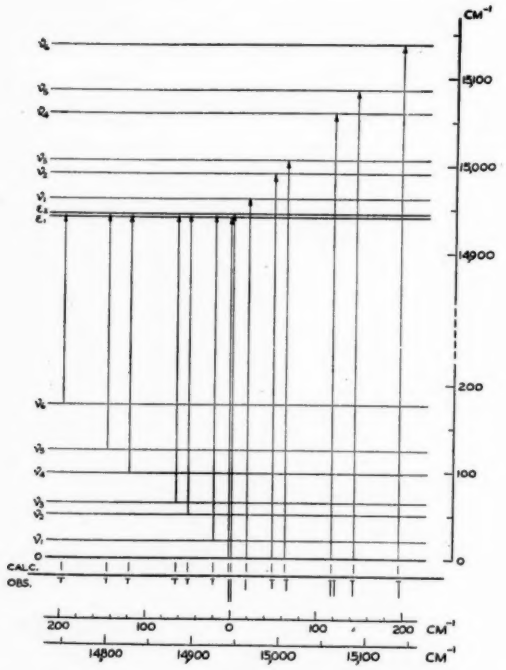


FIG. 5. Partial energy level diagram of $TlCr(SO_4)_2 \cdot 12H_2O$ at 20° and 85°K. Vibrational levels associated with both the lower and upper electronic states and the transitions between them are shown.

methylamine alums; and at 140 in the hydroxylamine and ammonium alums.

Variable low frequency bands (shifted from the electronic spectrum by amounts ranging from a few wave numbers up to perhaps 100 or 150 $cm^{-1}$) presumably arise in mutual oscillation of massive or loosely bound fragments of the lattice, while the higher frequency bands of constant separation from the electronic spectrum (330, 570 $cm^{-1}$, etc.) may be due to the superposition of characteristic librations of a tightly bound electrostatic complex (most probably $Cr(H_2O)_6^{+++}$) upon the electronic spectrum and its attendant low frequency vibrational bands. Raman shifts assignable to internal oscillations in aquo-complexes have not been observed but do appear at frequencies ranging up to 1000 $cm^{-1}$ or more in metal complexes with ammonia, pyridine and ethylene diamine.[19] Potassium aluminum sulfate has Raman shifts of 189 and 322 $cm^{-1}$, which probably correspond to the 195 and 330 $cm^{-1}$ bands we have found. Hellwege[20] has discovered several reflection maxima in the infra-red spectrum of three alums between 56 and 20$\mu$ or between 180 and 500 $cm^{-1}$. From his work it is not at present possible to determine absorption maxima for direct comparison with our results. Furthermore, since Hellwege's experiments were performed at room temperature, some of his reflections may represent combinations of acoustical frequencies (excitable by thermal vibrations but not by light) and optical frequencies, while in our own experiments at 20°K acoustical frequencies except of very low energy do not come in question.

A few temperature sensitive lines often appear on the long wave-length side of the electronic spectrum in the red. Separations of about 115, 200 and 330 $cm^{-1}$ are found in several alums for which Sauer gives data at −78° and +18°. The lines arise in transitions from thermally excited vibrational states associated with the ground state of $Cr^{+++}$. Because of the low intensity and the natural diffuseness of all the absorption lines at −78° and higher temperatures the separations cannot be very accurately defined, but their near identity with photo-excited vibrations associated with the upper electronic state at 20°K is obvious. Similar effects have been observed in the absorption and fluorescence of $Cr^{+++}$ dispersed in various foreign lattices.[13]

In $TlCr(SO_4)_2 \cdot 12H_2O$ at 85°K we find vibrational levels associated with the lower state 19.5, 27, 49, 64, 117.5, 144 and 195.5 $cm^{-1}$ from the mean frequency of the doublet. At 20° we find upper vibrational states at 19.9, 50, 65.6, 117, 142 and 195.5 $cm^{-1}$. Figure 5 is a partial energy diagram of this alum showing the vibrational levels of the lower and upper states and the observed transitions among them.

Three vibrations in the ground state of $NH_3OHCr(SO_4)_2 \cdot 12H_2O$ at 20°K have been found: $\nu_1 = 11.4$, $\nu_2 = 30$, $\nu_3 = 44$. Multiples and combinations of these frequencies added to the two upper electronic states of the characteristic doublet, $\epsilon_1 = 14{,}895.4$ and $\epsilon_2 = 14{,}918.9$, account in a satisfactory manner for all of the first 22 lines of the absorption spectrum (Fig. 6). The doublet separation, 23.5 $cm^{-1}$, is repeated prominently at 139, 273 and 346 $cm^{-1}$, and in the fine structure associated with these lines there is distinguishable to a greater or less

[19] Hibben, reference 17, p. 462.
[20] Hellwege, Ann. d. Physik **34**, 521 (1939).

extent the vibrational pattern close to the doublet.

Repetition of sequences is observable in all the alum spectra. Examples are given graphically in Fig. 7. In Fig. 7-D the ten lines comprising the (electronic) doublet of $TlCr(SO_4)_2 \cdot 12H_2O$ and the first eight (vibrational) lines on the short wave-length side of the doublet are repeated after the 143 $cm^{-1}$ line. Other repetitions, associated with 118, 196 etc., cannot be pointed out with as much assurance of their correctness owing to overlapping and to the width and diffuseness of the lines. In the corresponding rubidium alum there is perfect correspondence among lines appearing in both spectra, but matching lines are not always found, presumably because the proper combination of crystal thickness and exposure time for adequate absorption intensity was not arrived at. This is especially true immediately to the violet of the doublet, where several lines are missing in the rubidium alum. The possibility of unequivocal establishment of repeating sequences at higher frequencies is thus diminished.

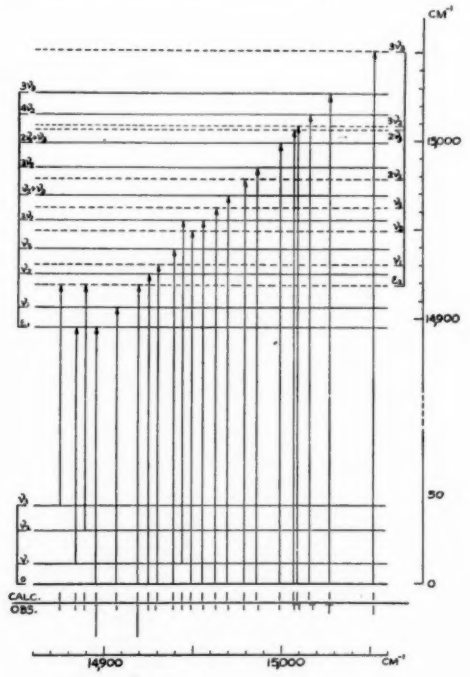


FIG. 6. Partial energy level diagram of $NH_3OHCr(SO_4)_2 \cdot 12H_2O$ at 20°K.

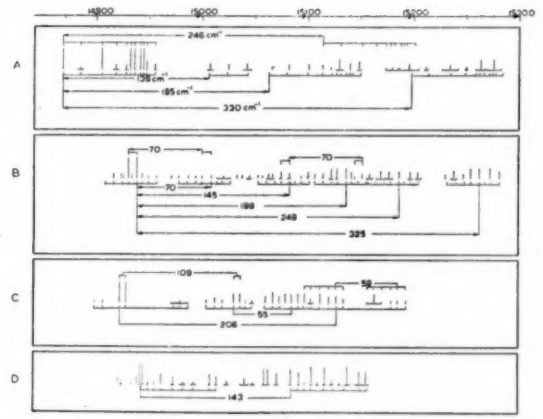


FIG. 7. Repetition of line sequences in some of the alum spectra. A. $NH_4Cr(SO_4)_2 \cdot 12H_2O$ (shattered crystal). B. $NH_4Cr(SO_4)_2 \cdot 12H_2O$ (clear crystal). C. $TlCr(SeO_4)_2 \cdot 12H_2O$. D. $TlCr(SO_4)_2 \cdot 12H_2O$. The intensity of the absorption lines is indicated by the height of the lines in the plot. Lines not crossed at the bottom signify absorption lines whose centers only were measured. The length of the horizontal lines is a measure of the breadth of the absorption lines. Horizontal lines upturned slightly at the ends signify diffuse absorption bands, whose position and breadth is not determinable with high precision.

It will be noticed in Fig. 7 that perfect repetition of the electronic doublet and its closely associated vibrational lines is not always achieved at the higher frequencies. This may be attributable in part to inaccuracy in measurements due to diffuseness or low intensity of the absorption bands. It may also be attributable to an actual small shift in the relative positions of the vibrational energy levels close to an excited electronic level produced by an additional, superimposed vibrational jump of, for example, 195 or 330 $cm^{-1}$. A further possibility of accounting for the observed shift lies in the expectation that vibrational frequencies of the lattice or its constituents will be somewhat dependent upon the electronic state of the $Cr^{+++}$ ion. The magnitude of the vibrational frequencies associated with an electronic jump in a $Cr^{+++}$ ion is a function of the masses of the vibrating units and the force constants of the bonds which link them. The masses are invariant but the force constants may be slightly different for the various electronic states of $Cr^{+++}$ and this would lead to small differences in the spacing of the vibrational levels superposed upon the several electronic states.

# Negative Ion Formation in Iodine Vapor by Electron Impacts

ROLF BUCHDAHL
*The Johns Hopkins University, Baltimore, Maryland*
(Received September 26, 1940)

Using an apparatus similar to the one used by Lozier, the negative ion formation in $I_2$ vapor was investigated as a function of the electron velocity (0–7 ev). The following reaction is responsible for negative ion formation at these velocities: $I_2+e\rightarrow I^-+I$. Measurements of the kinetic energy of the ions for different electron energies show that all the ions are formed by the same reaction. The variation of the yield as a function of the velocity of the electrons can be understood with the help of a potential-curve diagram, by considering transitions from the ground state of the $I_2$ molecule to the ground state of the $I_2^-$ molecule. The probability that an electron colliding with an $I_2$ molecule forms a negative ion varies between $10^{-4}$ and $10^{-3}$. With the aid of an energy cycle one can calculate the electron-affinity of the iodine atom, if one knows the dissociation energy of the neutral molecule, the kinetic energy of the incoming electron, and the kinetic energy of the ions. The value of the electron affinity obtained by this method is $3.0\pm0.2$ ev, which is in agreement with other determinations.

## INTRODUCTION

WHEREAS the formation of positive ions, either by electron collision or irradiation of light, has been the subject of numerous publications[1] in which one has been able to determine the energy necessary to form a positive ion and the probability with which the particular process occurs, there are only few data available in regard to the formation of negative ions.[2] Even for such gases as $Cl_2$, $I_2$, $Br_2$, where the electron affinity[2] of the atom is well known, and where the process leading to negative ion formation has been investigated, ($I_2+e\rightarrow I^-+I$),[3] the yield of this reaction and the variation of the yield with the electron velocity are not well known. The formation of negative ions in iodine vapor, which is the subject of this paper, has been investigated twice before. One paper is by Mohler[4] and the other is by Hey and Leipunski.[5] The large difference between the values of Mohler and Hey and Leipunski in regard to the yield does not seem to be a real one. If one calculates the yield (given by the expression

$$h=\frac{\sigma_i}{\sigma_e}, \qquad (1)$$

where $\sigma_i$ and $\sigma_e$ are, respectively, the cross sections for ion formation and total electron scattering) using the same electron scattering cross section throughout, and if one further makes some correction in the evaluation of Hey and Leipunski's data, one obtains values which are of the same order of magnitude. The fact remains, nevertheless, that the data regarding the variation of the yield with the electron velocity do not agree and that in both cases it is difficult to give a qualitative theoretical interpretation of the observed maxima and minima. The purpose of this investigation is, therefore, to reexamine the variation of the ion formation in $I_2$ vapor as a function of the electron velocity and to measure, at the same time, the kinetic energy of the ions. An attempt is then made to interpret the results from a theoretical point of view.

## DESCRIPTION OF THE APPARATUS

The apparatus used in this investigation is quite similar to the one used by Lozier[6] with

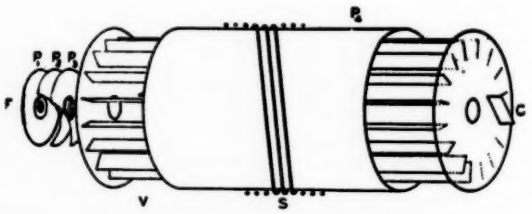


FIG. 1. Schematic representation of the apparatus.

[1] *Handbuch der Physik*, Vol. 23 (1933).
[2] Massey, *Negative Ions* (Cambridge, University Press, 1938).
[3] Hogness and Harkness, Phys. Rev. **32**, 784 (1928).
[4] Mohler, Phys. Rev. **26**, 614 (1925).
[5] Hey and Leipunski, Zeits. f. Physik **66**, 669 (1930).
[6] Lozier, Phys. Rev. **46**, 268 (1934).

which he measured the negative ion formation in $O_2$ and CO.

Electrons which are emitted by a thoriated tungsten filament ($F$) pass three grids ($P_1$, $P_2$ and $P_3$) and travel down the axis of the tube where they are collected on the plate $C$ (see Fig. 1). A solenoid ($S$) establishing a magnetic field parallel to the electron beam fits over the tube. When the magnetic field is strong enough (about 150 gauss), electrons will not move far away from the axis even when they collide with gas molecules. On the other hand, the ions formed by collision of the electrons with the gas molecules will hardly be affected by the magnetic field and will therefore move in all directions. Some of them will get through the vanes ($V$)—there are twelve of them evenly distributed over a circle—and reach the cylinder $P_4$. The purpose of the vanes is a twofold one: (1) To measure the kinetic energy of the formed ions. To do this a variable retarding potential is applied to the outside cylinder. The vanes shield the innermost part of the tube sufficiently so that the velocity of the electrons remains unchanged. (2) To catch those electrons which by multiple reflection or by scattering at right angles to their original direction might have traveled rather far away from the axis.

The filament was heated by an alternating current and was kept at a positive potential with respect to the rest of the apparatus when the heating current was on. When the heating current was off, a negative potential was applied to the filament to give the electrons the desired velocity, so that the electrons actually emitted started from an equal potential surface. The second grid was usually kept at a small positive potential to overcome part of the space charge effects. $P_3$, the vanes and the disk with the small opening at the lower end of the vanes were always kept at the same potential (at ground) so that the electrons were moving in a field-free space when they collided with the gas molecules. A small positive potential was applied to $C$, to make sure that the total electron current actually reached $C$.

The electron current measured at $C$ was of the order of magnitude of $10^{-5}-10^{-4}$ ampere except for measurements below 1 volt, where the current varied between $10^{-6}$ and $10^{-5}$ ampere. The current to $P_4$ was measured by a highly sensitive galvanometer (lower limit $3.10^{-11}$ ampere).

For the few measurements that were made in oxygen, no particular precautions were taken to get it pure. As a matter of fact, air was used and it was assumed that the negative ion formation in air is the same as in oxygen. (Experiments by Bradbury[7] furnish proof for this assumption.) For the measurements with $I_2$, purest chemical iodine available was used; before it was let into the apparatus, the iodine was once more subjected to a vacuum distillation to remove the air adsorbed on the crystals. The pressure range varied between $6.10^{-5}$ and $3.10^{-4}$ mm Hg. In both cases ($O_2$ and $I_2$) the gas was streaming through the apparatus. The pressure of the $I_2$ gas was measured by a quartz fiber manometer. Small changes of the temperature in the cooling flask around the iodine container produced rather noticeable pressure changes. It should be pointed out here that the pressure could be kept constant only within certain limits.

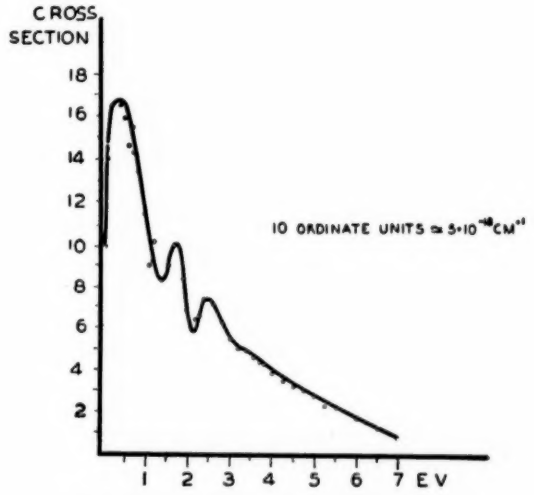


FIG. 2. Capture cross section plotted against energy of electrons in ev.

A serious difficulty in the type of apparatus used is the uncertainty in the total path traveled by the electrons. Two other types of apparatus were constructed, which, however, for various reasons, failed to yield satisfactory results.

In one of these, the electrons originated from a filament situated in the axis of a solenoid, passed first through a slit in a concentric cylinder and then were bent back by the

[7] Bradbury, Phys. Rev. **44**, 883 (1933).

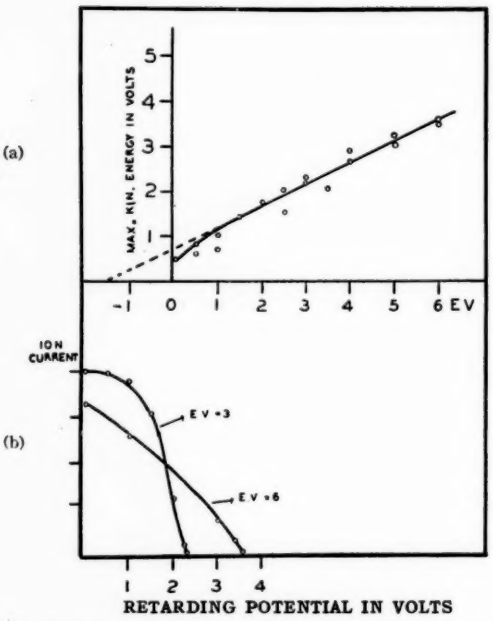


FIG. 3. (a) Maximum kinetic energy of negative ions plotted against energy of electrons in ev. (b) Ordinate: Ion current to $P_4$ (arbitrary units). Abscissa: Retarding potential applied at $P_4$.

magnetic field to the outside of the same cylinder. Ions formed in a field-free space outside of this cylinder were collected on a second concentric cylindrical plate of larger diameter. The apparatus failed because the ion current was masked by the current caused by electrons which succeeded in reaching the outer cylinder, probably because of multiple collisions or reflection.

The uncertainty in regard to the value of the mean free path is a more serious difficulty. To overcome this point, we constructed an apparatus the main part of which is a thick-walled iron cylinder with a slot parallel to the axis of the cylinder. Inside the iron cylinder is a similarly slit thin-walled brass cylinder of slightly smaller diameter. Across the slot of the iron cylinder is a magnetic field of about 250 gauss, strong enough to prevent electrons getting to the outside of the iron cylinder. Electrons emitted by a tungsten filament and focused by a simple electron lens move along the axis inside of the iron cylinder where they collide with the molecules. Those electrons scattered in the process of collision are collected by the brass cylinder whereas the negative ions can easily penetrate the slot and are measured by a plate outside of the iron cylinder. The ratio of the scattered electron current to the negative ion current multiplied by a certain factor due to the geometry of the apparatus, will give immediately the absolute yield of ion formation without involving a knowledge of the mean free path. In order to obtain good results, the stray field inside of the magnetic cylinder must be as small as possible. It was this particular difficulty which made it impossible for the time being to obtain satisfactory results.

## RESULTS

Figure 2 shows the change in capture cross section with electron velocity for $I_2$.* The cross section is defined here in the following way:

$$\sigma_i=\frac{I_i}{I_e\cdot\text{No. of molecules/cm}^3\times d\times f}, \qquad (2)$$

where $d$ is the distance the electrons travel and $f$ is determined by the geometry of the apparatus. Measurements were only made up to about 7.0 ev. At higher velocities positive and negative ions are probably formed simultaneously and the construction of the apparatus did not permit a good analysis of these processes.

To make sure that the current measured at $P_4$ was actually caused by ions formed in the gas phase and to nothing else, several tests were made.

(1) If one measures the current to $P_4$ as a function of the magnetic field (everything being kept constant) with or without a scatterer in the tube, one ought to find that the current to $P_4$ drops rapidly with increasing field. The speed with which it drops depends somewhat on the gas pressure, but sooner or later the current to $P_4$ must become 0, if no ions are formed. On the other hand, if a gas is present that forms positive or negative ions, the current ought to drop also rapidly in the beginning, but then settle down to a constant value over a long range. This was shown to be the case.

(2) If we assume that the negative ions are formed according to the following reaction $I_2+e\rightarrow I^-+I$, it is clear that the maximum kinetic energy of the ions for different electron velocities must have a definite value which one can calculate if one knows the electron affinity and the dissociation energy of the neutral mole-

TABLE I. *Maximum yield of negative ions. $X_2+E\rightarrow X^-+X$ process leading to negative ion formation.*

| GAS | OXYGEN | IODINE | CHLORINE |
|---|---|---|---|
| Lozier | $9.5\cdot10^{-4}$ | | |
| Bradbury | | | $3\cdot10^{-3}$ |
| Bailey | | | $1.5\cdot10^{-3}$ |
| Hey | | $5\cdot10^{-4}$ | |
| Mohler | | $2\cdot10^{-3}$ | |
| Present Results | $1\cdot10^{-3}$ | $8\cdot10^{-4}$ | |

* This curve is the average of three different runs at different pressures.

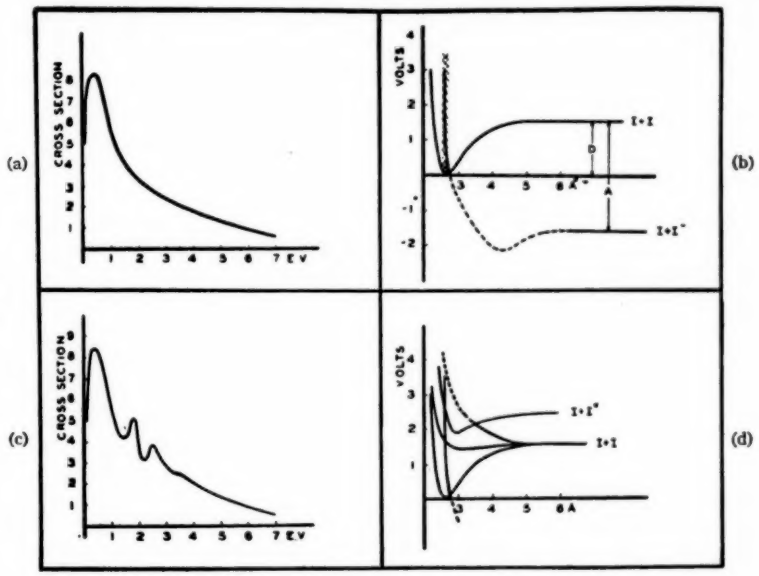


FIG. 4. (a) and (c) Ordinate: $\sigma_i$ (arbitrary units). Abscissa: Energy of electrons in ev. (b) and (d) Ordinate: Volts. Abscissa: Internuclear distance in angstrom units.

cule. All our measurements show that the ions have a kinetic energy which corresponds to the dissociation of the molecular ion into a negative atomic ion and an unexcited* neutral atom. (See Fig. 3(a).) If one extrapolates the straight part of the curve in Fig. 3(a) where it cuts the $x$ axis, one can find the electron affinity of the iodine atom. The value obtained in this manner is $3.0\pm0.2$ which agrees with other determinations by Mayer[8] and Glockler.[9] At this point the question concerning the formation of ions at the filament might arise. It is well known that the $I_2$ molecule dissociates into atoms on a hot tungsten filament above a certain temperature. Negative ions are then formed easily. These ions would then gain the same energy as the electrons, might make collision with neutral $I_2$ molecules and reach $P_4$. The possibility that something like this happens cannot be completely excluded offhand. Nevertheless the geometry of the apparatus makes it quite improbable that many of those ions would reach $P_4$. If so, their maximum kinetic energy ought to be equal to the total energy they have gained. For example, with $V_f=-6$ one ought to find some particles reaching $P_4$ which possess 6-volt kinetic energy or a little less. Figure 3(b) shows that this was never the case.

(3) Our results for oxygen (in the range of 0–10 ev) agree well with the experiments done by Lozier.

## DISCUSSION

### a. Absolute value of yield

To calculate the absolute value of the yield as defined in Eq. (1), we must first know the cross section for ion formation, $\sigma_i$ given by the expression (2). Nevertheless, the value obtained in this manner can only be an approximate one, as we do not know the exact value for $d^*$ (the actual path length of the electrons), because of the fact that all the electrons that have once made collision with a molecule will move on helixes of different sizes instead of straight lines. This remark applies to Mohler's data also and in a similar way to Hey and Leipunski's results. In order to compare our results with the data of Mohler and Hey and Leipunski, we made use of data given by Fisk[10] on the cross section of total electron scattering in chlorine, assuming

* The possibility that some of the collisions will yield a negative atomic ion plus an excited atom will be discussed later.

[8] Mayer and Sutton, J. Chem. Phys. **3**, 20 (1935).

[9] Glockler and Galvin, J. Chem. Phys. **3**, 771 (1935).

* The value of $d$ which was chosen for the evaluation of Eq. (2) was the distance between $P_3$ and the lower end of the vanes. One thus obtains a maximum value for $\sigma_i$.

[10] Fisk, Phys. Rev. **51**, 25 (1937).

that the cross section for iodine is certainly not smaller than that of chlorine. $Q=1500$ cm$^{-1}$ (at 1 mm Hg) was used as an average value for the cross section $\sigma_e$. If one uses this value to calculate the maximum yield, one gets values which are of the same order of magnitude for all three investigations, as one may see from Table I. For comparison, Table I also gives the values for $Cl_2$ and for $O_2$ when the ion formation is caused by the same process: $(X_2+e\rightarrow X^-+X)$. In $O_2$ this process can only take place with electrons of a certain amount of energy as the electron affinity is about 2.8 ev smaller than the dissociation of the neutral molecule. One sees, therefore, that for all processes of negative ion formation which proceed according to the above-mentioned equation, the yield is about the same. On the other hand, the accuracy of the absolute values is small.

**b. Variation of the yield with the electron velocity**

The results of the different authors regarding the variation of the yield with the electron velocity cannot be made to agree satisfactorily. Without discussing the details of the apparatus used by Hey and Leipunski, we shall merely remark that their arrangement does not seem to give good results for the processes due to very slow electrons, mainly because the effect of the earth's magnetic field on these slow electrons cannot be compensated for in a satisfactory way. In regard to Mohler's paper, one must say that because of the high pressure of iodine vapor ($10^{-3}-10^{-2}$ mm Hg) used in his investigation, multiple scattering sets in which might change the shape of the yield curve to a considerable extent. On the other hand, it seems to us that the curves measured with our apparatus could hardly be false. We, therefore, limit ourselves to a theoretical discussion of the result reproduced in Fig. 2.

The reaction $I_2+e\rightarrow I^-+I+E_{(kin)}$ is energetically possible for electrons with zero velocity because the dissociation energy of the iodine molecule is considerably smaller than the electron affinity of the iodine atom. The difference between the electron affinity ($A$) and the dissociation energy ($D$) must be taken up as kinetic energy of the iodine ion and the iodine atom. For electrons with zero velocity the kinetic energy of the ion is $T_k=D-A/2$.* If we temporarily disregard the secondary maxima at 1.75 and 2.5 ev (and possibly at 3.5 ev), we get a curve like the one shown in Fig. 4(a). Electrons with zero velocity give indeed a considerable yield of ion formation according to the equation $I_2+e\rightarrow I^-+I$, but the yield increases with the velocity of the electrons up to 0.4 ev ($\pm 0.15$ ev). We have no reason to doubt the reality of that maximum. For electrons with a velocity higher than 0.4 ev the yield drops sharply but still gives a measurable yield up to 7 ev (the maximum electron velocity used for the investigation in iodine vapor). Bradbury,[11] using the filter method due to Loeb,[12] found a maximum of ion formation in chlorine at 0.75 ev. His measurements do not extend to higher electron velocities.

One can explain this curve in a simple way with the help of the Franck-Condon principle, if one assumes the potential curve of $I_2^-$ to be as shown in Fig. 4(b). The dotted part of the curve is quite uncertain. Following considerations due to Mulliken, one must conclude that the $I_2^-$ molecule has a definite dissociation energy, but the actual depth of that minimum and its accurate position are unimportant for our considerations. On the other hand, the steep part of the curve and the point where this curve cuts the curve for the normal $I_2$ molecule are essential for our interpretation. The maximum at 0.4 ev is then caused by a transition from $I_2+e\rightarrow I_2^-$ corresponding to the perpendicular distance from the minimum of the $I_2$ curve to the $I_2^-$ curve. The rather extended decrease of the curve following the maximum at 0.4 ev indicates that the repulsive part of the $I_2^-$ potential curve must be very steep in that region so that the $I_2^-$ curve runs for a long time inside of the shaded area which corresponds to the zero-point vibration of the $I_2$ molecule. We are here confronted with potential curves which are similar to those which are responsible for the appearance of long continuous absorption spectra

* $D=1.54$ ev; W. G. Brown, Phys. Rev. **38**, 709 (1931).

[11] Bradbury, J. Chem. Phys. **2**, 835 (1934).

[12] Loeb, Phys. Rev. **48**, 684 (1935).

of molecules. (The fact that the iodine vapor was usually at a temperature of about 60°C because of the heating effect of the solenoid, naturally brings a small number of iodine molecules into their first vibrational state; but in first approximation we can neglect that fact.)

We now turn to the discussion of the maxima at 1.75 and 2.5 ev (and possibly at 3.5 ev, our results do not indicate definitely whether or not there is a maximum). (See Fig. 4(c).) Both these values (1.75 and 2.5 ev) agree quantitatively with the perpendicular distance from the ground state of the normal $I_2$ molecule to the first excited states, as one can see from the potential curve diagram (Fig. 4(d)) which is known from spectroscopic work.[13] The transition from the ground state of $I_2$ to the strong repulsive curve of the iodine molecule is about 3.5 ev.[14]

It was obvious to presume that the maxima at 1.75 and 2.5 ev were caused by inelastic collisions of the electrons with the iodine molecules. Two possibilities exist: (1) Because of the inelastic impacts of the electrons the velocity distribution of the primary electrons is changed to such an extent that besides electrons with a velocity of $X$ volts there is at the same time an appreciable amount of electrons present with a velocity of $X-1.75$ and $X-2.5$ volts. As the distance from the filament to the electron collector is of the same order of magnitude as the mean free path, one should have an appreciable amount of these electrons providing the probability of excitation is very great in the region of 1.75 and 2.5 volts. As a matter of fact, this might not be impossible. But if these secondary maxima are caused by electrons which already have been slowed down, they should not lie just at the minimum excitation potential, but should be shifted by an amount of 0.4 ev; because electrons of 0.4 ev have a higher probability to form negative ions than electrons of zero velocity. This reasoning is only justified if we accept definitely the first maximum as given. But even if one doubts this, one has difficulties in interpreting the measurements of the velocity distribution of the ions which are formed. If, for example, the maximum at 2.5 ev is caused by electrons of a velocity of $X-2.5$ volts, then the number of these slowed-down electrons should increase, with increasing electron velocity according to the excitation function. A measurement of the velocity distribution of the ions formed with electrons of 3 ev should, therefore, contain two distinct groups of ions of different velocities, one with a maximum velocity of 2.35 volts and another one with a maximum velocity of 1.7 volts. (Fig. 3(b) shows the results for ions formed with electrons of 3 ev.) Because of the geometry of the apparatus, an exact evaluation of the actual energy distribution of the ions is not possible. Nevertheless it is possible to decide whether or not there are different groups of a definite velocity present. The differentiated curves will indicate these groups even more distinctly. The monotonic shape of these curves seems to be a strong argument against the just-discussed possibility. We therefore come to the conclusion that the secondary maxima are caused by a process which occurs in one elementary act. The possibility that this can occur does exist, as the steep potential curve of the iodine ion molecule cuts the potential curves of the excited neutral molecule at points which lie practically perpendicular above the ground state of the neutral molecule, as it is indicated in Fig. 4(d). This would mean therefore that the same electron which excites or dissociates the iodine molecule is caught by one of the iodine atoms. The monotonic shape of the decrease of the yield with increasing electron velocity will be interrupted at those places where the potential curve of $I_2^-$ cuts the potential curve of the excited iodine molecule. It is important that these cutting points lie directly above the ground state. At 2.5 ev and above the reaction $I_2+I\rightarrow I^-+I^*$ might occur, where $I^*$ is an excited iodine atom. The yield for this reaction will be considerably smaller.

Our interpretation could be checked experimentally if the dependence of the yield could be studied as a function of the pressure over a wide pressure range. Following the interpretation which we prefer, one ought to find that the relative strength of the maxima is independent of the

[13] Brown, Phys. Rev. **38**, 1187 (1931).
[14] Turner, Zeits. f. Physik **65**, 464 (1930).

pressure, whereas according to the first-mentioned and rejected interpretation, they ought to increase quadratically with the pressure. The apparatus used in this investigation unfortunately did not allow us to make measurements at very low pressure.

I am greatly indebted to Professor James Franck, under whose direction this investigation was started, for his continued help and advice. It is a pleasure to acknowledge many helpful discussions with Professor J. E. Mayer and Professor J. A. Bearden.

---

FEBRUARY, 1941 JOURNAL OF CHEMICAL PHYSICS VOLUME 9

# The Differential Diffusion Constant of Calcium Chloride in Aqueous Solution

E. A. HOLLINGSHEAD AND A. R. GORDON
*Chemistry Department, University of Toronto, Toronto, Ontario, Canada*
(Received October 25, 1940)

The differential diffusion constant for calcium chloride in aqueous solution has been measured for concentrations ranging from 0.0025 to 0.5 mole per liter and for temperatures from 15° to 35°C. The relation connecting the diffusion constant at a finite concentration with that at infinite dilution, $k=k_0(1+c\partial \ln f/\partial c)(\eta_0/\eta)$, which holds for moderate concentrations for several 1−1 electrolytes, is valid for this salt only up to 0.01 mole per liter; the corresponding value of $k_0$ is about 1.5 percent less than that computed from the ionic mobilities by the Nernst relation. The activation energy of diffusion for a given concentration decreases with rising temperature as is customary; for a given temperature, however, it decreases with increasing concentration in dilute solutions, and finally becomes independent of concentration.

PREVIOUS papers[1] from this laboratory have reported the differential diffusion constants for hydrochloric and sulphuric acids in aqueous solution as functions of temperature and concentration. The present work was undertaken to obtain similar data for a typical salt of the 2−1 valence type *viz.* calcium chloride.

As in the earlier measurements, diffusion cells of the Northrop-McBain type were employed, the technique of the measurements and the method of analysis of the solutions by interferometer being the same as were used in the previous work. Stock calcium chloride solutions (made up from the twice recrystallized salt and conductivity water) were analyzed by precipitation of silver chloride; all solutions used in the diffusion measurements as well as all reference solutions for the interferometer were made by gravimetric dilution of these stock solutions; weight concentrations were converted to volume concentrations by means of the density data in the *International Critical Tables*. As in the previous measurements, the cells were recalibrated after every three or four calcium chloride runs by diffusing 0.1$N$ KCl solution in water at 25°C; the value of $\bar{k}$ used in the calibration[1a] was $1.842\times10^{-5}$ cm²/sec.

Table I contains the results; the second and third columns give the average initial concentrations of the "inner" and "outer" solutions expressed in moles per liter. The next column gives the square root of the mean concentration of the experiment—the concentration for which the effective diffusion constant $\bar{k}$ (computed by Eq. (2) of reference 1a) is equal to the true differential diffusion constant.[1a,2] The last column gives the average $k$, obtained in each case from measurements in four different cells; the individual values showed in general a mean absolute deviation from the mean of somewhat less than 0.5 percent.

Figure 1 shows the results graphically, the continuous curves of the figure corresponding to the smoothed entries of Table II. Adequate

[1] (a) W. A. James, E. A. Hollingshead and A. R. Gordon, J. Chem. Phys. **7**, 89 (1939); (b) W. A. James and A. R. Gordon, *ibid.* **7**, 963 (1939); (c) E. A. Hollingshead and A. R. Gordon, *ibid.* **8**, 423 (1940).

[2] A. R. Gordon, J. Chem. Phys. **5**, 522 (1937).

thermodynamic data to test the relation previously proposed[2] for 1−1 salts

$$k=k_0(1+c\partial \ln f/\partial c)\cdot(\eta_0/\eta)$$

are only available for calcium chloride for 25°C and for $c\leq 0.1$. The dotted curve of the figure corresponds to this relation, the thermodynamic data being those of Shedlovsky and MacInnes[3] and the viscosities from the *International Critical Tables*.[4] The value selected for $k_0$ is $1.312\times10^{-5}$, slightly less than that computed by the Nernst relation from the ionic mobilities[5] *viz.* $1.335\times10^{-5}$. The figure shows that there is appreciable deviation for $c>0.01$; this is perhaps not surprising when it is remembered that the ionic mobilities of this salt, even for low concentrations, do not obey the rules valid for 1−1 electrolytes.[6]

From Table II it is possible to obtain values of the activation energy of diffusion; at the lowest concentration ($c=0.0025$) the mean activation energies for the temperature differences 15–25° and 25–35° are 4.72 and 4.37 kcal., respectively; with rising concentration the activation energy falls until when $c\geqq 0.04$, it becomes practically independent of concentration at 4.4 and 4.2 kcal., respectively. Thus the activation energy falls with rising temperature as in the other cases studied.[1,7] Its dependence on concentration, however, is different from that found for the acids; for hydrochloric, the energy of activation did not depend on concentration up to 0.2 normal, but then increased, while for sulphuric the activation energy was practically constant for solutions varying from 0.01 to 1.0 mole per liter. This would seem to indicate that the change in the diffusional energy of activation with concentration as well as its absolute value, is, for a given solvent and temperature, a specific property of the diffusing substance.

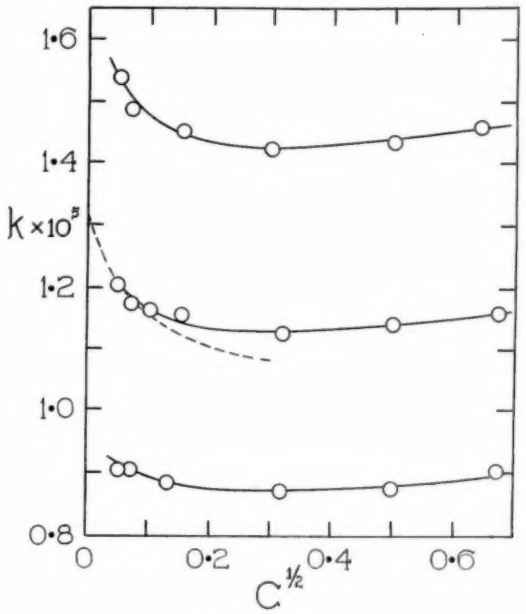


FIG. 1.

TABLE I.

| T°C | $c_0'$ | $c_0''$ | $((c_0'+c_0'')/2)^{\frac{1}{2}}$ | $10^5 k$ |
|---|---|---|---|---|
| 15 | 0.00565 | 0 | 0.053 | 0.904 |
| 15 | .01025 | 0 | .072 | .905 |
| 15 | .0500 | 0 | .158 | .885 |
| 15 | .1522 | 0.0515 | .319 | .870 |
| 15 | .3001 | .2023 | .501 | .874 |
| 15 | .5023 | .4010 | .672 | .901 |
| 25 | .00513 | 0 | .051 | 1.201 |
| 25 | .01024 | 0 | .072 | 1.174 |
| 25 | .02060 | 0 | .101 | 1.161 |
| 25 | .0483 | 0 | .155 | 1.154 |
| 25 | .1517 | .0510 | .318 | 1.129 |
| 25 | .3020 | .1982 | .500 | 1.138 |
| 25 | .5043 | .4034 | .674 | 1.156 |
| 35 | .00559 | 0 | .053 | 1.538 |
| 35 | .01045 | 0 | .072 | 1.488 |
| 35 | .0488 | 0 | .156 | 1.449 |
| 35 | .1491 | .0368 | .305 | 1.423 |
| 35 | .2999 | .2002 | .500 | 1.431 |
| 35 | .4962 | .4000 | .669 | 1.456 |

TABLE II. *$10^5$ k for aqueous solutions of* $CaCl_2$.

| $c^{\frac{1}{2}}$ | 15° | 25° | 35° |
|---|---|---|---|
| 0.05 | 0.913 | 1.204 | 1.530 |
| .10 | .893 | 1.162 | 1.475 |
| .20 | .876 | 1.135 | 1.433 |
| .30 | .871 | 1.128 | 1.422 |
| .50 | .878 | 1.138 | 1.432 |
| .70 | .898 | 1.162 | 1.462 |

[3] T. Shedlovsky and D. A. MacInnes, J. Am. Chem. Soc. **59**, 503 (1937).
[4] Int. Crit. Tab. Vol. **5**, 14 (1929).
[5] D. A. MacInnes, J. Frank. Inst. **225**, 661 (1938).
[6] L. G. Longsworth and D. A. MacInnes, J. Am. Chem. Soc. **60**, 3070 (1938).
[7] H. S. Taylor, J. Chem. Phys. **6**, 331 (1938).

# Theory of Some van der Waals Molecules

RALPH HELLER*
*Sloane Physics Laboratory, Yale University, New Haven, Connecticut*
(Received November 6, 1940)

Using a potential function of the form

$$V(R)=A(\rho)e^{-R/\rho}-\frac{c_1}{R^6}-\frac{c_2}{R^8}-\frac{c_3}{R^{10}}-\frac{c_4}{R^{12}},$$

the vibrational wave number and energy of dissociation of the molecules HgHe, HgNe, HgA, HgKr, HgXe, $Hg_2$, $(O_2)_2$ and $(NO)_2$ in the normal state are calculated. It is found that, if the single value $\rho=0.28$A is chosen, satisfactory agreement is obtained with experimental data except in the case of $(NO)_2$. The latter structure is believed to owe its binding partly to first-order attractive forces.

## INTRODUCTION

SPECTROSCOPIC research as well as results from many other sources strongly indicate the existence of quasi-molecules, such as HgA or $(O_2)_2$, which are not molecules in the ordinary sense because, at least in the gaseous state and under normal conditions, their lifetime is exceedingly small and their concentration minute. These molecules are considered to owe their existence to the so-called van der Waals forces and are therefore spoken of as van der Waals molecules. They show very flat potential minima (depth $\Delta\backsimeq 0.01\div 0.1$ ev) at relatively large interatomic distances ($R_0\backsimeq 3\div 4$A).

The subject of van der Waals forces has been thoroughly dealt with recently in a paper by London[1] and in Margenau's[2] review article.

The present investigation is concerned with the eight molecules HgHe, HgNe, HgA, HgKr, HgXe, $Hg_2$, $(O_2)_2$ and $(NO)_2$ in the gaseous phase and the lowest energy state. The two last-named molecules can be safely treated as consisting of two bodies inasmuch as the two atoms in each normal $O_2$[NO] molecule are fairly tightly bound (energy of dissociation slightly above 5 ev[3]) and their separation of 1.21[1.15]A[3] is much smaller than the intermolecular distance, $R_0$ say, of $(O_2)_2$[$(NO)_2$]. Disregarding the contributions of permanent quadrupole and higher moments of Hg, $O_2$ and NO, whose magnitude is not known at present but is probably small, the dipole-dipole terms in the alignment and induction effects are utterly negligible as compared to the dispersion effect in the case of nitric oxide, whose permanent dipole moment is somewhat less than $0.2(10)^{-18}$ e.s.u.,[4] and they are zero for the other molecules, whose constituents carry no permanent dipole moments. Thus only the dispersion forces will be considered in the attractive part of the potential.

In addition to the second-order attractive forces, the first-order contribution must be taken into account. In London's[5] original calculation of the depth of the potential minimum the repulsive potential was approximated by a vertical line drawn at a distance equal to the sum of the gas kinetic radii of the interacting atoms. The depth of the potential at the minimum was also computed by Ekstein and Magat,[6] who improved on London's calculations by employing a term $bR^{-n}$ to represent the repulsive potential; and the same type of potential function was used by Wohl[7] and by Salow.[8] We shall, following Born and Mayer's[9] treatment of the alkali-halide crystals, write the repulsive potential in the

* Part of a dissertation presented to the Faculty of the Graduate School of Yale University in candidacy for the degree of Doctor of Philosophy.

[1] F. London, Trans. Faraday Soc. **33**, 8 (1937).

[2] H. Margenau, Rev. Mod. Phys. **11**, 1 (1939).

[3] G. Herzberg, *Molecular Spectra and Molecular Structure, I* (New York, 1939), Table 36.

[4] C. P. Smyth and K. B. McAlpine, J. Chem. Phys. **1**, 60 (1933); H. E. Watson, G. Gundo Rao and K. L. Ramaswamy, Proc. Roy. Soc. London **A143**, 558 (1934).

[5] F. London, Zeits. f. physik. Chemie **B11**, 222 (1930) [$Hg_2$, HgA, HgKr].

[6] H. Ekstein and M. Magat, Comptes rendus **199**, 264 (1934) [$Hg_2$].

[7] K. Wohl, Zeits. f. physik. Chemie **B14**, 36 (1931) [$(O_2)_2$].

[8] H. Salow, Dissertation (Berlin, 1935), pp. 40–48 [$(O_2)_2$].

[9] M. Born and J. E. Mayer, Zeits. f. Physik **75**, 1 (1932).

form $Ae^{-R/\rho}$, where $A$ and $\rho$ are positive constants. Detailed quantum-mechanical calculations[10] indicate that such an expression may be expected to be a fair approximation in a certain region about the potential minimum.

That the first-order potential energy will always lead to repulsion is by no means evident as far as the molecules $(O_2)_2$ and $(NO)_2$ are concerned, their (paramagnetic!) constituents possessing unsaturated spin moments (normal state: $^3\Sigma$ and $^2\Pi$, respectively). In the absence of theoretical information as to the size of the first-order attractive forces, however, they will be considered to be negligible. As regards the validity of this assumption, the reader is referred to the last paragraph in the section on the molecule $(NO)_2$.

## The Potential Energy Function $V(R)$

Denote by $R$ the (variable) distance between the centers of positive charge of the two normal-state atoms or groups of atoms forming a van der Waals molecule. Their mutual potential energy, $V(R)$, will be the sum of the repulsive potential, $Ae^{-R/\rho}$, and the attractive dispersion potential, $\Delta E^{(2)}$ say.

For two electrically neutral charge distributions $I$ and $II$ representing normal atoms or molecules the dispersion-force potential is of the form

$$\Delta E^{(2)} = -\sum_{i=1}^{\infty} \frac{c_i}{R^{2(i+2)}}. \tag{1}$$

The coefficient of the leading term, $-c_1/R^6$, which represents the dipole-dipole interaction, is given by London's general expression,[5] which for two atoms or groups of atoms in the normal state reads

$$c_1 = \frac{3}{32\pi^4}\frac{e^4 h}{m_0{}^2}\sum_{k,\,l}\frac{f_k{}^I f_l{}^{II}}{\nu_k{}^I \nu_l{}^{II}(\nu_k{}^I+\nu_l{}^{II})}, \tag{2}$$

where $e$ and $m_0$ are charge and mass of the electron, the summation is extended over all energy states $k$ (for atom $I$) and $l$ (for atom $II$), and the $\nu$'s and $f$'s are the frequencies and oscillator strengths associated with the transitions from the ground state to the excited state labeled $k$ or $l$ and are available from the most complete experimental Sellmeier-type dispersion formulas for substance $I$ or $II$. Approximate values for the coefficients of the higher powers of $R^{-2}$ in the expansion (1) are found by means of a perturbation calculation, using Margenau's[11] harmonic oscillator model, the result being

$$c_2 = \frac{45}{8}\frac{1}{e^2}\alpha_0{}^I\alpha_0{}^{II}h\nu^I h\nu^{II}\left(\frac{\alpha_0{}^I}{f^I}\frac{h\nu^I}{2h\nu^I+h\nu^{II}} + \frac{\alpha_0{}^{II}}{f^{II}}\frac{h\nu^{II}}{2h\nu^{II}+h\nu^I}\right); \tag{3}$$

$$c_3 = \frac{105}{4}\frac{1}{e^4}\alpha_0{}^I\alpha_0{}^{II}h\nu^I h\nu^{II}\left[\left(\frac{\alpha_0{}^I}{f^I}\right)^2\frac{(h\nu^I)^2}{3h\nu^I+h\nu^{II}} + \frac{3}{2}\frac{\alpha_0{}^I}{f^I}\frac{\alpha_0{}^{II}}{f^{II}}\frac{h\nu^I h\nu^{II}}{2h\nu^I+2h\nu^{II}} + \left(\frac{\alpha_0{}^{II}}{f^{II}}\right)^2\frac{(h\nu^{II})^2}{3h\nu^{II}+h\nu^I}\right]; \tag{4}$$

$$c_4 = \frac{4725}{32}\frac{1}{e^6}\alpha_0{}^I\alpha_0{}^{II}h\nu^I h\nu^{II}\left[\left(\frac{\alpha_0{}^I}{f^I}\right)^3\frac{(h\nu^I)^3}{4h\nu^I+h\nu^{II}} + 2\frac{\alpha_0{}^I}{f^I}\frac{\alpha_0{}^{II}}{f^{II}}h\nu^I h\nu^{II}\left(\frac{\alpha_0{}^I}{f^I}\frac{h\nu^I}{3h\nu^I+2h\nu^{II}} + \frac{\alpha_0{}^{II}}{f^{II}}\frac{h\nu^{II}}{3h\nu^{II}+2h\nu^I}\right) + \left(\frac{\alpha_0{}^{II}}{f^{II}}\right)^3\frac{(h\nu^{II})^3}{4h\nu^{II}+h\nu^I}\right]. \tag{5}$$

Here $\nu^j, f^j$ and $\alpha_0{}^j (j=I, II)$ are the characteristic frequency, oscillator strength and static molecular polarizability of atom $j$ as given by experimental one-term Sellmeier-type dispersion formulas. For a medium with a one-term dispersion formula there exists the relation

$$\alpha_0{}^j = \frac{e^2}{4\pi^2 m_0}\frac{f^j}{(\nu^j)^2} \quad (j=I, II). \tag{6}$$

The coefficients of higher powers in $R^{-2}$ than $R^{-12}$ in (1) are neglected.

The derivation of (3), (4), and (5) is similar to Margenau's,[11] the difference being that the two constituents $I$ and $II$ of the molecule will here be allowed to be different and that higher terms will be included in the classical Coulombian interaction energy. For two neutral charge

[10] L. Pauling, Zeits. f. Krist. **67**, 377 (1928); H. Brück, Zeits. f. Physik **51**, 707 (1928); P. Gombás, Zeits. f. Physik **93**, 378 (1934).

[11] H. Margenau, J. Chem. Phys. **6**, 896 (1938).

TABLE I. *List of the principal numerical data.* ($\rho = 0.28A$.)

| MOLECULE | $c_1$ (EV $\times A^6$) | $c_2$ (EV $\times A^8$) | $c_3$ (EV $\times A^{10}$) | $c_4$ (EV $\times A^{12}$) | $R_0$ (A) | $R_m$ (A) | $\rho^*$ (A) | $A$ (EV) | WAVE NUMBER $\tilde{\nu}_0$ ($CM^{-1}$) | ZERO-POINT ENERGY ($10^{-3}$ EV) | ENERGY OF DISSOCIATION‡ ($10^{-3}$ EV) |
|---|---|---|---|---|---|---|---|---|---|---|---|
| Hg He | 9.12 | 33.85 | 130.4 | 623.9 | 3.28 | 3.1 | 0.3627 | 689.7 | 46.6 | 2.88 ($\epsilon_0$)<br>2.53 ($\epsilon_1$) | 3.01 ($D_0$)<br>3.36 ($D_1$) |
| Hg Ne | 17.62 | 65.37 | 251.6 | 1202 | 3.09 | 3.0 | 0.3459 | 1237 | 31.5 | 1.95 ($\epsilon_0$)<br>1.88 ($\epsilon_1$) | 11.22 ($D_0$)<br>11.30 ($D_1$) |
| Hg A | 66.09 | 257.8 | 1055 | 5409 | 3.39 | 3.35 | 0.3998 | 6601 | 35.9 *30*[37a] | 2.20 ($\epsilon_0$)<br>2.16 ($\epsilon_1$) | 27.5 ($D_0$) *25*[37a]<br>27.5 ($D_1$) 63($\Delta$)[5] |
| Hg Kr | 95.80 | 380.2 | 1624 | 8714 | 3.46 | 3.4 | 0.4056 | 10275 | 31.7 *30*[37a] | 1.96 ($\epsilon_0$)<br>1.93 ($\epsilon_1$) | 38.1 ($D_0$) *35*[37a]<br>38.1 ($D_1$) 75($\Delta$)[5] |
| Hg Xe | 150.6 | 610.1 | 2759 | 15687 | 3.66 | 3.65 | 0.4442 | 22375 | 28.1 | 1.74 ($\epsilon_0$)<br>1.72 ($\epsilon_1$) | 41.9 ($D_0$)<br>41.9 ($D_1$) |
| $Hg_2$ | 143.3 | 781.2 | 4049 | 26430 | 3.2$_6$ | 3.2 | 0.3512 | 16133 | 35.2 *36*[23] | 2.18 ($\epsilon_0$)<br>2.16 ($\epsilon_1$) | 86.0 ($D_0$) *65÷91*[23]<br>86.0 ($D_1$) 86($\Delta$)[5]<br>84($\Delta$)[6] |
| $(O_2)_2$ | 34.69 | 70.54 | 222.5 | 883.4 | 3.48 | 3.4 | 0.4397 | 2806 | 34.4 48[6] | 2.13 ($\epsilon_0$)<br>2.04 ($\epsilon_1$) | 10.77 ($D_0$) *5.6*[e]<br>10.86 ($D_1$) *10*[g]<br>16($\Delta$) [7, p. 62]<br>10($D_0$)[8] |
| $(NO)_2$ | 34.66 | 83.28 | 268.9 | 1094 | 3.68 | 3.6 | 0.4662 | 3857 | 30.5 | 1.89 ($\epsilon_0$)<br>1.80 ($\epsilon_1$) | 7.90 ($D_0$) *56* [37, p. 1792]<br>7.99 ($D_1$) *35*[45] |

‡ References e and g are to footnotes to Table II.

distributions each of which has its positive charge localized at one point this energy, up to and including the term in $R^{-6}$, is

$$U^{I,II}(R) = U_{pp} + U_{p\Theta} + (U_{\Theta\Theta} + U_{p\Omega}) + (U_{\Theta\Omega} + U_{p\Phi}), \quad (7)$$

where, in a form convenient for the computation,

$$U_{pp} = \frac{e^2}{R^3} \sum_{st} (\mathbf{r}_s \cdot \boldsymbol{\varrho}_t - 3 z_s \zeta_t);$$

$$U_{p\Theta} = \frac{3}{2} \frac{e^2}{R^4} \sum_{st} [r_s^2 \zeta_t - z_s \rho_t^2 + (2\mathbf{r}_s \cdot \boldsymbol{\varrho}_t - 5 z_s \zeta_t)(z_s - \zeta_t)];$$

$$U_{\Theta\Theta} = \frac{3}{4} \frac{e^2}{R^5} \sum_{st} [r_s^2 \rho_t^2 - 5(z_s^2 \rho_t^2 + r_s^2 \zeta_t^2) - 15 z_s^2 \zeta_t^2 + 2(\mathbf{r}_s \cdot \boldsymbol{\varrho}_t - 5 z_s \zeta_t)^2];$$

$$U_{p\Omega} = \frac{1}{2} \frac{e^2}{R^5} \sum_{st} [-3(r_s^2 + \rho_t^2)(\mathbf{r}_s \cdot \boldsymbol{\varrho}_t - 5 z_s \zeta_t) + 5(z_s^2 + \zeta_t^2)(3\mathbf{r}_s \cdot \boldsymbol{\varrho}_t - 7 z_s \zeta_t)];$$

$$U_{\Theta\Omega} = \frac{5}{4} \frac{e^2}{R^6} \sum_{st} [3(r_s^2 \zeta_t - z_s \rho_t^2)(2\mathbf{r}_s \cdot \boldsymbol{\varrho}_t - 7 z_s \zeta_t) + 7(r_s^2 \zeta_t^3 - z_s^3 \rho_t^2) + 3\{r_s^2 \rho_t^2 + 21 z_s^2 \zeta_t^2 + 2\mathbf{r}_s \cdot \boldsymbol{\varrho}_t (\mathbf{r}_s \cdot \boldsymbol{\varrho}_t - 7 z_s \zeta_t)\}(z_s - \zeta_t)];$$

$$U_{p\Phi} = \frac{5}{8} \frac{e^2}{R^6} \sum_{st} [3(z_s \rho_t^4 - r_s^4 \zeta_t) - 6(z_s r_s^2 - \zeta_t \rho_t^2)(2\mathbf{r}_s \cdot \boldsymbol{\varrho}_t - 7 z_s \zeta_t) + 7(z_s^3 - \zeta_t^3)(4\mathbf{r}_s \cdot \boldsymbol{\varrho}_t - 9 z_s \zeta_t)].$$

$\mathbf{R}$ points from $I$ to $II$, $\mathbf{r}_s = (x_s, y_s, z_s)[\boldsymbol{\varrho}_t = (\xi_t, \eta_t, \zeta_t)]$ is the position vector of the $s$th [$t$th] electron $e$ of multipole $I(II)$ referred to the respective center as origin, and the $z$'s and $\zeta$'s are taken along $R$. The subscripts $p$, $\Theta$, $\Omega$ and $\Phi$ affixed to the $U$'s refer to the (instantaneous) dipole, quadrupole, octupole and fourth-order pole moments whose interaction is represented by these components of (7).

When the matrix elements of (7) are calculated with the use of oscillator eigenfunctions, employing different stiffness constants $(4\pi^2 m_0/h)\nu^j \equiv \beta^j (j = I, II)$ for the two constituents of the molecule, and then substituted into the formula for the second-order perturbation energy of the normal state and finally the value of $\beta^j$ is expressed by means of (6), there results

$$\Delta E^{(2)} = -\frac{c_1^0}{R^6} - \frac{c_2}{R^8} - \frac{c_3}{R^{10}} - \frac{c_4}{R^{12}},$$

complete up to and including the term in $R^{-12}$, with $c_2$, $c_3$ and $c_4$ given by (3), (4) and (5), whereas the coefficient

$$c_1^0 = \frac{3}{2} \alpha_0^I \alpha_0^{II} h\nu^I h\nu^{II} \frac{1}{h\nu^I + h\nu^{II}}, \quad (8)$$

already derived by London,[5] is the special case of the accurate expression (2) for substances with one-term dispersion formulas.

The numerical factors in the energy denominators of the coefficients (8), (3), (4), and (5) indicate in an obvious way the combination of poles which has given rise to the corresponding term. Note that, owing to the inclusion of the dipole-octupole interactions, the coefficient (4) of the term in $R^{-10}$ in the special case of two alike atoms or molecules is 7/3 times the corresponding coefficient as found by Margenau,[11] who did not consider the interactions involving poles higher than quadrupoles. It will be seen that the effect of the term in $R^{-12}$, here included for completeness, is small.

In Table I will be found the values of the coefficients $c_1$ to $c_4$ given by (2) to (5) as computed from the following experimental dispersion formulas: the three-term formulas of Wolfsohn[12] for mercury, Larsén[13] for argon, Ladenburg and

[12] G. Wolfsohn, Zeits. f. Physik **83**, 234 (1933).
[13] T. Larsén, Zeits. f. Physik **88**, 389 (1934).

Wolfsohn[14] for oxygen; the two-term formulas of Kronjäger[15] for krypton and xenon, and Koch[16] for nitric oxide; the one-term formulas of Quarder, Herzfeld and Wolf[17] for argon and of C. and M. Cuthbertson[18] for mercury and oxygen, krypton and xenon, helium and neon and nitric oxide.

The potential energy function of a van der Waals molecule is thus

$$V(R)=Ae^{-R/\rho}-\frac{c_1}{R^6}-\frac{c_2}{R^8}-\frac{c_3}{R^{10}}-\frac{c_4}{R^{12}}. \tag{9}$$

It will have a minimum at some interatomic distance $R_m$ if and only if

$$A=\frac{2}{R_m{}^7}\left(3c_1+4\frac{c_2}{R_m{}^2}+5\frac{c_3}{R_m{}^4}+6\frac{c_4}{R_m{}^6}\right)\cdot\rho e^{R_m/\rho} \tag{10}$$
$$=A(\rho)$$

and

$$\rho<\frac{c_1+\frac{4}{3}\frac{c_2}{R_m{}^2}+\frac{5}{3}\frac{c_3}{R_m{}^4}+2\frac{c_4}{R_m{}^6}}{c_1+\frac{12}{7}\frac{c_2}{R_m{}^2}+\frac{55}{21}\frac{c_3}{R_m{}^4}+\frac{26}{7}\frac{c_4}{R_m{}^6}}\frac{R_m}{7}\equiv\rho^*. \tag{11}$$

A more detailed study shows that (since $\rho$ and the $c$'s are all positive) the equality sign in (11) cannot be admitted as it would lead to a point of inflection instead of a minimum, also that, providing (10) and (11) hold, (9) has its maximum at some point $R_M<R_m$ and has no other (finite) $R$ where the tangent is horizontal. Since the values of the parameter $\rho$ that we will have occasion to use are about $\frac{3}{4}$ times the maximum value $\rho^*$ defined by (11) and hence small enough to permit the maximum of $V(R)$ to rise fairly high above the $R$ axis, the potential function has the shape shown in Fig. 1. It is sufficient for our purpose and will be assumed that $V(R)$ is trustworthy over the classical range of vibration for the lowest vibrational level and thence up to infinite separation. The depth $\Delta$ of the potential (9) at the minimum is

$$-V(R_m)=\frac{c_1}{R_m{}^6}\left(1-\frac{6\rho}{R_m}\right)+\frac{c_2}{R_m{}^8}\left(1-\frac{8\rho}{R_m}\right)$$
$$+\frac{c_3}{R_m{}^{10}}\left(1-\frac{10\rho}{R_m}\right)+\frac{c_4}{R_m{}^{12}}\left(1-\frac{12\rho}{R_m}\right) \tag{12}$$
$$\equiv\Delta,$$

and the second derivative at the minimum is

$$V''(R_m)=\frac{2}{\rho R_m{}^7}\left[3c_1\left(1-\frac{7\rho}{R_m}\right)+4\frac{c_2}{R_m{}^2}\left(1-\frac{9\rho}{R_m}\right)\right.$$
$$\left.+5\frac{c_3}{R_m{}^4}\left(1-\frac{11\rho}{R_m}\right)+6\frac{c_4}{R_m{}^6}\left(1-\frac{13\rho}{R_m}\right)\right], \tag{13}$$

$\rho$ being bounded by (11) and the subtrahends in the parentheses expressing the effect of the repulsive part of the potential energy.

## The Zero-Point Vibrational Energy

Let $\nu_0$ stand for the classical frequency of vibrations with infinitely small amplitude of a diatomic molecule about the equilibrium position, which then coincides with the separation $R_m$ corresponding to the minimum of the potential function. As $V''(R_m)=\mu(2\pi\nu_0)^2$, where $\mu$ is the molecule's reduced mass, the wave number associated with $\nu_0$ is

$$\bar{\nu}_0=\frac{\nu_0}{c}=\frac{1}{2\pi c}\left(\frac{V''(R_m)}{\mu}\right)^{\frac{1}{2}} \tag{14}$$

with $V''(R_m)$ given by (13).

In zeroth approximation the potential function (9) can be replaced by a Hooke's law potential.

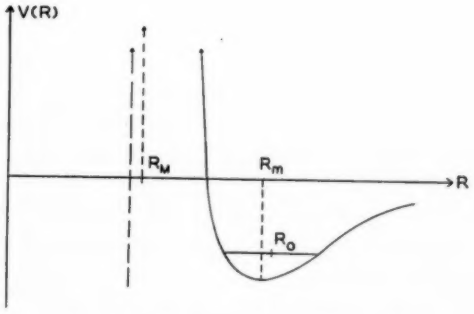


FIG. 1. The potential function $V(R)$.

[14] R. Ladenburg and G. Wolfsohn, Zeits. f. Physik **79**, 42 (1932).
[15] W. Kronjäger, Zeits. f. Physik **98**, 17 (1935).
[16] J. Koch, Arkiv f. Matematik **18**, No. 3 (1924).
[17] B. Quarder, Ann. d. Physik [4], **74**, 255 (1924); K. F. Herzfeld and K. L. Wolf, *ibid.* [4], **76**, 71 (1925).
[18] C. and M. Cuthbertson: Proc. Roy. Soc. London **A83**, 151 (1909) [$O_2$, Hg]; **A84**, 13 (1910) [Kr, Xe]; **A135**, 40 (1932) [He, Ne]; Trans. Roy. Soc. London **A213**, 1 (1913) [NO].

The pure vibration energy of the molecule in the lowest energy state is then known to be

$$\epsilon_0=\tfrac{1}{2}h\nu_0=\tfrac{1}{2}hc\cdot\tilde{\nu}_0 \qquad (15)$$

with the small amplitude wave number $\tilde{\nu}_0$ from (14).

The potential function (9) is not a parabola, however; and it will be shown in Fig. 3 for the case of the quasi-molecule HgHe that the Morse potential function $M(R)$ which best fits our function $V(R)$ represents its asymmetry over a considerable range of the variable $R$ around the minimum value $R_m$ very well. One may thus expect the zero-point vibrational energy, $\epsilon_1$ say, on the Morse potential to be a better approximation than the oscillator energy (15), in terms of which it may be written

$$\epsilon_1=\epsilon_0\left(1-\frac{1}{4}\frac{\epsilon_0}{\Delta}\right), \qquad (16)$$

where $\Delta$ is the depth (12) of the potential minimum and the subtrahend in the parenthesis expresses the effect on the vibrational energy of the asymmetry of $V(R)$ about $R_m$,—an effect that is almost negligible for all the molecules here considered except HgHe.

### Determination of $R_m$ and $\rho$

The energy of dissociation of a van der Waals molecule in the state of lowest electronic and vibrational energies is

$$\Delta-\epsilon_0\equiv D_0 \qquad (17)$$

in zeroth approximation, and

$$\Delta-\epsilon_1\equiv D_1 \qquad (18)$$

in first approximation, $\Delta$ standing for the depth (12) of the potential at the minimum.

The quantities $\nu_0$, $\epsilon_0$, $\epsilon_1$, $D_0$, $D_1$, as well as the potential curve (9, 10) and the Morse curve best fitting it, depend on the coefficients $c_1$ to $c_4$, which have already been expressed and computed as functions of the constants of experimental dispersion formulas; on the molecule's reduced mass $\mu$; on the separation $R_m$, by means of which the constant $A(\rho)$ could be eliminated in the potential; and on $\rho$.

The asymmetry of the potential curve $V(R)$, already responsible for the slight depression of the vibrational level $\epsilon_1$ as against $\epsilon_0$, makes itself felt, moreover, in that the distance $R_m$, corresponding to the minimum of the potential function $V(R)$, cannot be expected exactly to equal the equilibrium separation, $R_0$ say, of the molecule in its normal state, though the relative difference should be small. To correlate $R_m$ and $R_0$, a graphic procedure, suggested by Kane,[19] will be employed. He identified the midpoint of the classical range of oscillation of the lowest vibrational level with the equilibrium distance $R_0$. (See Fig. 1.) So we will have to choose $R_m$ such that, taking some value of $\rho$ satisfying the minimum condition (11), that midpoint comes just at the equilibrium distance $R_0$. We shall feel contented, however, when the difference between midpoint and $R_0$ does not exceed one percent of $R_0$.

The equilibrium distance $R_0$ ought to be deduced from the spectroscopic constant for rotation in the lowest vibrational state, $B_0=h/(8\pi^2\mu R_0^2)$. Unfortunately, however, the rotational structure of the band spectra of the van der Waals molecules under discussion is missing or (in the case of $Hg_2$) unresolved, and hence the $B_0$ constants are not known. To find approximate values for $R_0$ for the various molecules, recourse will be had to crystal and related data. It is to be hoped that these $R_0$ values are not much in error.

The values adopted for $R_0$ are listed in Table I. For the five mercury-rare gas compounds, we shall take the arithmetic mean of the distances between two nearest neighbors at or near 0°K in the crystal lattices of mercury, 2.98A as found by extrapolation with the aid of density measurements[20] of the value given by Neuburger,[21] and of the inert gases; for helium this is[22] 3.57A (at 1.45°K), whereas the values used for the remaining rare gases differ by less than one percent from those employed by Kane.[19] Mercury being a metal, the true equilibrium distance of two normal Hg atoms forming an isolated $Hg_2$

[19] G. Kane, J. Chem. Phys. **7**, 603 (1939). [$R_m$ and $R_0$, p. 607; $R_0$ values, first row of Table V and p. 605, where reference d ought to read: W. H. Keesom and H. H. Mooy, Proc. Roy. Acad. Amst. **33**, 447 (1930), being Comm. Leiden No. 209b.]

[20] A. Sapper and W. Biltz, Zeits. f. anorg. allgem. Chemie **198**, 184 (1931).

[21] M. C. Neuburger, Zeits. f. anorg. allgem. Chemie **212**, 40 (1933).

[22] W. H. Keesom and K. W. Taconis, Physica **5**, 161 (1938); being Comm. Leiden No. 250e.

molecule ought to be somewhat larger than the crystal value, 2.98A; and we shall adopt the value $3.2_0$A, also employed by Kuhn,[23] which is an average of the atomic diameter of Hg as determined from the density of liquid mercury assuming closest tetrahedral packing (3.25A) and from the amalgams[24] Ag-Hg (3.09A) and Pb-Hg (3.24 ÷ 3.28A). For oxygen, we shall use Vegard's[25] x-ray value, 3.48A, for the intermolecular distance of two $O_2$ molecules forming a pair in γ-oxygen at about 48°K. As to nitric oxide, for which no x-ray measurements are available, $R_0$ will be set equal to the arithmetic mean, 3.68A,* of Vegard's value for oxygen and the smallest distance[26] between the centers of two neighboring $N_2$ molecules at 21°K in α-nitrogen.

Except for having an upper bound in accordance with the minimum condition (11), the positive quantity $\rho$ is a disposable parameter. The energy of dissociation and the vibrational wave number are known spectroscopically for the molecules HgA, HgKr and $Hg_2$ in the lowest vibrational level of the electronic ground state. For each of the three molecules the computed data come out in good agreement with the two spectroscopic values if, and only if, the adjustable parameter is taken very nearly equal to 0.28A. The same value of $\rho$ will be adopted for the five remaining molecules; for, as regards energies of dissociation and vibrational wave numbers, no experimental data are available excepting estimates from nonspectroscopical sources of the dissociation energies of $(O_2)_2$ and $(NO)_2$.

The dependence of the zero-point energy (15) and energy of dissociation (17) on the value chosen for the parameter $\rho$ is shown in Fig. 2, which is plotted for HgA but is representative of the functions $\epsilon_0(\rho)$ and $D_0(\rho)$ for the other molecules as well. It is seen that the energy of dissociation is not very sensitive to a change of $\rho$ over a considerable part of its range, whereas the zero-point energy (or the vibrational wave number) depends much more strongly on the value of that parameter.**

## HgA AND HgKr

The spectra of the molecules HgA and HgKr are well known from Oldenberg's[27] measurements in fluorescence, and recently the spectrum of HgA has also been obtained in absorption[28] and in an electrical discharge.[29] Oldenberg[27a] suggested that these bands are caused by transitions from some fixed vibrational state of the excited molecule Hg′A or Hg′Kr to all the vibrational levels of the normal molecule and from this interpretation derived the experimental values given in Table I for wave number and dissociation energy of these two molecules.

As an example for the actual computation of the vibrational wave number and energy of dissociation of a normal van der Waals molecule, consider the molecule HgA. Refer to the corresponding row in Table I. The equilibrium distance is taken as $R_0 = 3.39$A. Try $R_m = 3.35$A. Using the known $c$'s, the zero-point energy $\epsilon_0$ from (15) and energy of dissociation (17) are computed and plotted in Fig. 2 as a function of the parameter $\rho$, whose upper limit $\rho^*$ as given by (11) will also be found in Table I. Choosing $\rho = 0.28$A, the calculated values as listed are obtained for the vibrational wave number (14) as well as the zero-point and dissociation energies in zeroth (15, 17) and first (16, 18) approximations. Next the constant $A(\rho)$ given by (10) is computed and the potential energy function $V(R)$ from (9) plotted; it is similar in shape to the $V(R)$ curve for the molecule HgHe shown in Fig. 3. Since the midpoint of the classical range of oscillations for the lowest vibrational level $\epsilon_0$ or $\epsilon_1$ comes at

[23] H. Kuhn, Proc. Roy. Soc. London **A158**, 230 (1937).
[24] V. M. Goldschmidt, Zeits. f. physik. Chemie **133**, 397 (1928).
[25] L. Vegard, Nature **136**, 720 (1935); Zeits. f. Physik **98**, 1 (1935). Also: W. H. Keesom and K. W. Taconis, Physica **3**, 141 (1936); being Comm. Leiden No. 240d.
* It so happens that 3.68A is just the product of the diameter of an NO molecule as deduced from the critical temperature and pressure, by the correction factor 1.30. For the five inert gases, the departure from 1.30 of the ratio of the x-ray value of the distance of two nearest neighbors (at or near 0°K) to the ($p_{crit}$, $T_{crit}$) atomic diameter does not exceed 4.2 percent.
[26] M. C. Neuburger, Zeits. f. Krist. **93**, 1 (1936). (On p. 15, replace his reference number 105 by 109.)

** In Fig. 2, $R_m$ rather than $R_0$ is kept constant (having been chosen such that the midpoint of the level $\epsilon_0$ or $\epsilon_1$ agrees with $R_0$ for values of $\rho$ not too far off 0.28A). Also the approximation of the zero-point energy by (15) [or even (16)] is unreliable for $\rho$ values so small that the ratio $\epsilon_0/\Delta$ becomes comparable to unity. The curves are, therefore, approximate only except in the neighborhood of $\rho = 0.28$A.
[27] (a) O. Oldenberg, Zeits. f. Physik **55**, 1 (1929); (b) H. Kuhn and O. Oldenberg, Phys. Rev. **41**, 72 (1932).
[28] H. Kuhn, Proc. Roy. Soc. London **A158**, 212 (1937).
[29] W. M. Preston, Phys. Rev. **51**, 298 (1937).

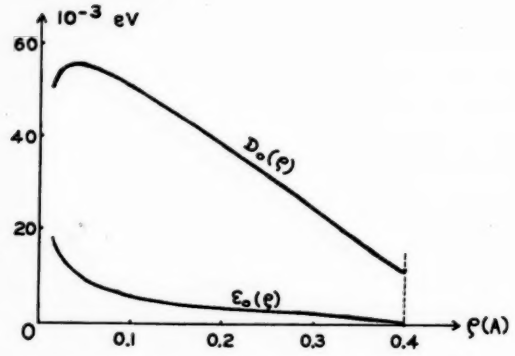


FIG. 2. $\epsilon_0(\rho)$ and $D_0(\rho)$ for HgA. ($R_0=3.39$A; $R_m=3.35$A; $\rho^*=0.3998$A.)

about 3.37A, in sufficient agreement with $R_0$, the choice for $R_m$ has been appropriate. The value 0.28A has been selected for the parameter $\rho$ in order to obtain approximate agreement between Oldenberg's spectroscopic data for the vibrational wave number and energy of dissociation and the values here calculated.

The procedure followed is analogous for the other molecules treated in this paper. As to the results for the molecule HgKr, see the corresponding row in Table I. It also lists the results of previous theoretical investigations.

## $Hg_2$

Mercury vapor is practically monatomic.[30] That two Hg atoms in the normal state ($6^1S_0$) can form a van der Waals molecule $Hg_2(^1\Sigma_g^+)$ follows, however, from the band spectrum to which gaseous mercury gives rise. This spectrum consists of a multitude of continua and more or less diffuse bands and has been discussed in detail in a recent excellent monograph of Finkelnburg.[31] As to the spectroscopic values for the energy of dissociation and vibrational frequency, reference is made to a paper by Kuhn,[23] who, incidentally, found 0.02 percent for the fraction by weight $\tau$ of $Hg_2$ in mercury vapor at a pressure of about 8 mm Hg and at 448°K.

The numerical data pertaining to the molecule $Hg_2$ are assembled in Table I.

[30] A. Kundt and E. Warburg, Ber. **8**, 945 (1875); Ann. d. Physik [2] **157**, 353 (1876).

[31] W. Finkelnburg, *Kontinuierliche Spektren* (*Struktur und Eigenschaften der Materie*, Vol. 20 (Berlin, 1938)).

## HgHe, HgNe AND HgXe

Unlike HgA and HgKr, the spectra of HgHe, HgNe and HgXe, observed in fluorescence by Oldenberg,[27] and in the case of HgHe in an electrical discharge by Preston,[29] are continua which show no structure (except for HgNe on the short wave-length side of the mercury line λ2537). The absence of a diffuse structure on the long wave-length side in the HgXe spectrum may have been caused by strong scattering[27b] from the quartz bulb used. On Oldenberg's[27a] hypothesis, according to which such a structure represents the vibrational quanta of the molecule in its lowest electronic state, the experimental fact that the structure is missing in the HgHe spectrum is what should be expected from the present calculation inasmuch as, in view of Fig. 3 and the numerical data in Table I, the ratio of zero-point vibrational energy and depth of the potential minimum is so big ($\epsilon_0/\Delta=48.9\%$; $\epsilon_1/\Delta=42.9\%$) as to suggest that the first *excited* vibrational level would not be stable. But the absence of a structure on the long wave-length side in the spectrum of HgNe cannot be accounted for in this way.

## $(O_2)_2$

The molecule $(O_2)_2$ is perhaps the most interesting of all known van der Waals molecules.[32] That $(O_2)_2$ molecules exist in gaseous oxygen, and in the liquid and solid phases as well, follows conclusively from the continuous absorption bands, some of which are responsible for the pale blue color of compressed, liquid and solid oxygen. Particulars regarding the absorption spectrum caused by $(O_2)_2$ can be found in Finkelnburg's[31] monograph and in the recent dissertations of Guillien[33] and Herman.[34]

[32] It has no connection with a hypothetical compound, $O_4$, called *oxozone*, with great chemical activity, which C. Harries (Chem.-Zeitung **31**, 609 (1907); Liebig's Ann. **374**, 293 (1910); **390**, 235 (1912); Zeits. f. Elektrochemie **17**, 631 (1911); **18**, 130 (1912); Ber. **45**, 936 (1912)) claimed was contained in an appreciable quantity in gaseous and liquid ozone. This substance never has been isolated; and E. H. Riesenfeld and G. M. Schwab (Ber. **55**, 2088 (1922)), who succeeded in preparing pure gaseous, liquid and solid ozone, have stated that there is no evidence for the existence of oxozone.

[33] R. Guillien, Ann. de physique [11] **8**, 555 (1937); being his Thèse (Paris, 1937).

[34] L. Herman, Ann. de physique [11] **11**, 548 (1939); being his Thèse (Paris, 1939).

The spectroscopic evidence is corroborated by the results of a good many other investigations, magnetic and otherwise, concerning the physical properties of oxygen. Some of these are listed in Table II.

## $(NO)_2$

Table II contains also some information regarding magnetic data which suggest the existence of the dimer $(NO)_2$ of the "odd" molecule NO. There is, in addition, some evidence from chemical sources that it is the molecule $(NO)_2$ that serves as the intermediary product in the oxidation of nitric oxide.

This reaction, of considerable importance at one stage in the preparation of nitric acid from nitric oxide and also in the theory of the lead chamber process, is of the third order and has a small negative temperature coefficient.[35] As recent experiments of Porret[36] proved the reaction rate constant to be practically independent of the pressure of an added foreign gas (nitrogen), Kassel's[37] statistical theory of trimolecular mechanisms does not seem applicable to this reaction. If, instead, the reaction proceeds in two bimolecular steps, the intermediary substance may be either $NO_3$ or $(NO)_2$. The existence of $NO_3$ is assured both spectroscopically[38] and on the basis of chemical kinetics,[39] though it has not yet been isolated;[40] but the complete absence[41] of its characteristic lines in the absorption spectrum of a mixture of nitric oxide and oxygen would appear to rule it out as the intermediate in the reaction under consideration (unless one postulate[42] *ad hoc* the existence of an *isomer* of $NO_3$). The belief, now held by Bodenstein,[43] that the intermediate is the dimer $(NO)_2$ is strongly supported[43a, b] by the close analogy and parallelism in the chemical behavior of the reactions of nitric oxide with oxygen, bromine[44a] and chlorine.[44b]

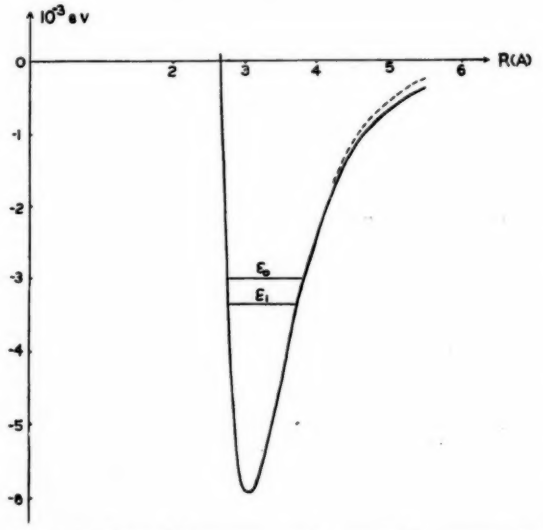


FIG. 3. Potential energy and zero-point energy for HgHe. ($R_0$=3.28A; $R_m$=3.1A; $\rho$=0.28A.) ———: $V(R)$; — — —: Morse curve $M(R)$.

From the temperature dependence of the reaction rate constant as deduced from Bodenstein's older measurements of the rate of the oxidation of nitric oxide, the energy of dissociation of an $(NO)_2$ molecule has been estimated by Kassel[37] to be $56(10)^{-3}$ ev and by Christiansen[45] to be $35(10)^{-3}$ ev. This estimate is several times larger than the value of about 8 millivolts† computed by the present author, suggesting that first-order attractive forces arising from the tendency for saturation of the spin moments of two normal ($^2\Pi$) NO molecules may be present, as was already pointed out by Briegleb[46] in an attempt to explain the discrepancy between the experimental and computed second virial coefficient of nitric oxide (at 273°K). $(NO)_2$ would not then be a pure van der Waals molecule. It is interesting

[35] M. Bodenstein and L. Wachenheim, Zeits. f. Elektrochemie **24**, 183 (1918) [273÷363°K]; M. Bodenstein and Frl. Lindner, Zeits. f. physik. Chemie **100**, 87 (1922) [414÷662°K]; F. Matthes, Dissertation (Berlin, 1933) [143÷273°K]; E. Briner, W. Pfeiffer and G. Malet, J. chim. phys. **21**, 25 (1924) [90÷348°K].

[36] D. Porret, Dissertation (Berlin, 1937), pp. 1–6.

[37] L. S. Kassel, J. Phys. Chem. **34**, 1777 (1930); also: *Kinetics of Homogeneous Gas Reactions* (New York, 1932), Section 9.1.

[38] P. E. M. Berthelot, Comptes rendus **92**, 82 (1881); the references in footnotes 2 and 3 of Sprenger, reference 39; also P. Hautefeuille and J. Chappuis, Comptes rendus **92**, 946 (1882), and J. Chappuis, Ann. Éc. Norm. Sup. [2], **11**, 137 (1882); E. J. Jones and O. R. Wulf, J. Chem. Phys. **5**, 873 (1937).

[39] G. Sprenger, Zeits. f. Elektrochemie **37**, 674 (1931), and the papers cited in his footnote 1. (Decomposition of ozone in the presence of nitrogen pentoxide.) See also: G. M. Calhoun and R. H. Crist, J. Chem. Phys. **5**, 301 (1937); **7**, 719 (1939); and G. v. Elbe and B. Lewis, J. Am. Chem. Soc. **59**, 2022 (1937); **61**, 1350 (1939).

[40] A. Klemenc and W. Neumann, Zeits. f. anorg. allgem. Chemie **232**, 216 (1937).

[41] H. J. Schumacher and G. Sprenger, Zeits. f. angew. Chemie **42**, 697 (1929).

[42] F. Swarts, *5e Conseil de Chimie*, Instituts Solvay (Paris, 1935), p. 37.

[43] M. Bodenstein, (a) reference 42, p. 1 ff.; (b) Helv. Chim. Acta **18**, 743 (1935); (c) Zeits. f. physik. Chemie **A175**, 294 (1935).

[44] (a) W. Krauss, Zeits. f. physik. Chemie **A175**, 295 (1935); (b) W. Krauss and M. Saracini, *ibid.* **A178**, 245 (1936). The announced simultaneous discussion of the three reactions of nitric oxide has not been published as yet.

[45] J. A. Christiansen, reference 42, p. 31.

† Just as for the other molecules, $\rho$=0.28A has been assumed. No matter what particular value is taken for the parameter $\rho$, however, the calculated energy of dissociation would never exceed 13 millivolts.

[46] G. Briegleb, Zeits. f. physik. Chemie **B23**, 127 (1933).

TABLE II. *Some experimental evidence for the existence of* $(O_2)_2$ *and* $(NO)_2$. ($\tau$ *denotes the fraction by weight of the dimer in the undiluted substance.*)

| PHENOMENON | PHASE | AUTHOR | REMARKS |
|---|---|---|---|
| | | *Oxygen* | |
| 1. Departure from reduced equation of state | Gas | E. C. Wiersma and C. J. Gorter[a] | |
| 2. Anomalous Faraday effect | Gas | R. Serber[b] | |
| 3. Deviations from Curie's law of paramagnetism | Gas | H. R. Woltjer, C. W. Coppoolse and E. C. Wiersma[c]; E. C. Wiersma, W. J. de Haas and W. H. Capel[d] | |
| | Liquid | G. N. Lewis[e] | $D=5.6$ mv; $\tau=40\%$ at 77°K; $\tau$(extrap.) $=0.03\%$ at 293°K and 1 atmos. |
| 4. Cotton-Mouton effect | Liquid | P. Lainé[f,g] | |
| 5. Kerr effect | Liquid | R. Guillien [h; 33, p. 619/20, 643] | |
| 6. Concentration dependence of extinction coefficient | Liquid | R. Guillien [33, p. 578] | $\tau=40\%$ at 77°K |
| 7. Heat of mixing of liquid oxygen and nitrogen | Liquid | P. Lainé[g] | $D=10$ mv |
| 8. Structure of $\gamma$-oxygen | Solid | L. Vegard[25] | $R_0=3.48$A |
| 9. Magnetic susceptibility | Solid | A. Perrier and H. Kamerlingh Onnes[i] | |
| | | *Nitric Oxide* | |
| 1. Faraday effect | Gas, Liquid | H. Bizette and B. Tsaï[j] | $\tau=93\%$ at 110°K |
| 2. Magnetic susceptibility | Liquid | H. Bizette and B. Tsaï[k] | $\tau=97\%$ at 110°K |
| | Solid | E. Lips[l] | |

[a] Physica **12**, 316 (1932); being Comm. Leiden, Suppl. No. 73c.
[b] Phys. Rev. **41**, 489 (1932).
[c] Proc. Roy. Acad. Amst. **32**, 1329 (1929); being Comm. Leiden No. 201d.
[d] Proc. Roy. Acad. Amst. **34**, 494 (1931); being Comm. Leiden No. 215b.
[e] J. Am. Chem. Soc. **46**, 2027 (1924).
[f] J. de physique [7] **6**, 14S, 62S (1935).
[g] *Biréfringence magnétique* (Paris, 1936), p. 35, 44.
[h] Physica **3**, 895 (1936); being Comm. Leiden No. 242d.
[i] Proc. Roy. Acad. Amst. **16**, 894 (1913); being Comm. Leiden No. 139c.
[j] Comptes rendus **204**, 1638, 1965 (1937).
[k] Comptes rendus **206**, 1288 (1938).
[l] Helv. Phys. Acta **8**, 247, 380 (1935).

to note that Wohl's[7] second virial coefficient of oxygen (from 121 to 373°K) is in excellent agreement with experiment, and that the experimental and theoretical values in Table I for the energy of dissociation of the molecule $(O_2)_2$ are fairly concordant, although no first-order forces had been assumed for the attraction between two normal $(^3\Sigma)$ $O_2$ molecules.

## DISCUSSION

The main numerical results have been assembled in Table I. The three last columns, giving the vibrational wave number, zero-point energy, and energy of dissociation, are subdivided, showing the results of the present investigation on the left-hand side and the data obtained by other authors to the right. Experimental results are indicated by figures printed in *italics*. The results derived from a potential energy function, on the other hand, are differentiated, except for the wave numbers, by means of the symbols $(\epsilon_0)$ or $(D_0)$, $(\epsilon_1)$ or $(D_1)$, or $(\Delta)$, according as they were computed with the aid of the oscillator zero-point energy $\epsilon_0$, the Morse zero-point energy $\epsilon_1$, or are depths of the potential at the minimum.

It is believed that the repulsive law $Ae^{-R/\rho}$, successfully employed by Born and Mayer[9] for ionic crystals, has proved satisfactory for the van der Waals molecules here under discussion.

If the term in $R^{-12}$ in the attractive part of the potential (9, 10) were replaced by zero, the error thus introduced would be only 2.1 percent or less in the depth $\Delta$ of the potential minimum and less than 5.3 percent in the zero-point energy $\epsilon_0$ (or $\epsilon_1$) or wave number $\tilde{\nu}_0$ for the eight molecules considered (assuming $\rho=0.28$A). However, the contribution of the terms in $R^{-8}$ and $R^{-10}$, which were first considered by Margenau[47] and in which the dipole-octupole interaction has been included in this paper, is appreciable at $R=R_m$.

[47] H. Margenau, Phys. Rev. **38**, 747 (1931).

It is of interest to observe how a change in the polarizability of the constituents is counteracted by a corresponding change in size and especially in reduced mass of the van der Waals molecule such that the vibrational wave number $\tilde{\nu}_0$ is nearly the same for the eight molecules, varying from 28.1 $cm^{-1}$ (HgXe) to 46.6 $cm^{-1}$ (HgHe). A similar result has already been obtained by Salow[8] for the molecules $O_2Z$ ($Z=O_2$, He, Ne, A, $N_2$, $CO_2$), his $\tilde{\nu}_0$'s ranging from 39 $cm^{-1}$ ($O_2Ne$) to 95 $cm^{-1}$ ($O_2(CO_2)$). The spectroscopic values for normal-state diatomic molecules with a chemical bond, on the other hand, extend all the way from about 42 $cm^{-1}$ ($Cs_2$) up to about 4400 $cm^{-1}$ ($H_2$).[3]

ACKNOWLEDGMENT

In conclusion I am happy to express my thanks and appreciation to Professor Henry Margenau for suggesting this work and for his helpful interest in its progress.

---

FEBRUARY, 1941 JOURNAL OF CHEMICAL PHYSICS VOLUME 9

# The Entropy of Formic Acid. The Heat Capacity from 15 to 300°K. Heats of Fusion and Vaporization

J. W. STOUT* AND LEON H. FISHER
*Department of Chemistry, University of California, Berkeley, California*

(Received November 7, 1940)

The heat capacity of solid and liquid formic acid has been measured from 15 to 300°K. The melting point is 281.40°K (0°C = 273.10°K). The heat of fusion is 3031 cal. $mole^{-1}$ and the heat of vaporization at 298.10°K is 4754 cal. $mole^{-1}$. (1 mole = 46.0260 grams.) The vapor pressure at 298.10°K is 4.31 cm of mercury. From the third law of thermodynamics and the calorimetric data the entropy has been calculated. To the value obtained from the calorimetric measurements an entropy of $R/2$ ln 2, due to the random orientation of hydrogen bonds in the solid which has been predicted by Pauling, has been added. This gives 31.51 cal. $deg.^{-1}$ $mole^{-1}$ for the entropy of the liquid at 298.10°K and 47.46 for the entropy of 46.0260 grams of gas, $P=4.31$ cm, in equilibrium with the liquid at 298.10°K. These are the values that should be used in thermodynamic calculations.

THIS paper presents the results of a low temperature calorimetric investigation of formic acid, leading to values for the entropy of the liquid and the gas. The value of the entropy obtained is compared with those deduced from free energy and heat changes.

The measurements were made in a calorimeter of laboratory designation Gold Calorimeter IV. The resistance thermometer was calibrated during the measurements by comparison with standard copper-constantan thermocouple W-21. The calorimeter and the calibration of the thermocouple have been described by Kemp and Giauque.[1] The apparatus and methods of measurement and calculation have been described in previous papers[2] from this laboratory. The ice point was taken as 273.10°K, and the defined calorie, 4.1833 international joules, was used throughout.

## PREPARATION AND PURITY OF FORMIC ACID

Since the commercially available formic acid contained an objectionable amount of acetic acid, which might have proved difficult to remove, it was decided to prepare the sample by the reaction of a formate with a mineral acid. Phosphoric acid was chosen since it has a negligible vapor pressure and preliminary experiments had shown that it does not rapidly

* Fellow of the Lalor Foundation, 1938–39. Now at the Massachusetts Institute of Technology.

[1] Kemp and Giauque, J. Am. Chem. Soc. **59**, 79 (1937).

[2] (a) Giauque and Wiebe, J. Am. Chem. Soc. **50**, 101 (1928). (b) Giauque and Johnston, J. Am. Chem. Soc. **51**, 2300 (1929). (c) Giauque and Egan, J. Chem. Phys. **5**, 45 (1937).

TABLE I. *Melting point of formic acid 0°C=273.10°K.*

| TIME | % MELTED | $T$, °K. RESISTANCE THERMOMETER | $T$, °K. THERMOCOUPLE |
|---|---|---|---|
| *4–25–39* | | | |
| 9:26 P.M. | Heated into melting point | | |
| 11:25 P.M. | 8 | 281.365 | 281.36 |
| *4–26–39* | | | |
| 12:31 A.M. | 8 | 281.360 | 281.36 |
| 10:36 A.M. | 8 | 281.358 | 281.35 |
| 11:37 A.M. | Supplied heat | | |
| 12:22 P.M. | 19 | 281.385 | 281.38 |
| 2:04 P.M. | 19 | 281.386 | 281.38 |
| 3:21 P.M. | 19 | 281.387 | 281.38 |
| 5:28 P.M. | Supplied heat | | |
| 6:01 P.M. | 56 | 281.392 | 281.39 |
| 8:15 P.M. | 56 | 281.387 | 281.39 |
| 10:10 P.M. | 56 | 281.391 | 281.39 |
| 11:16 P.M. | 56 | 281.388 | 281.39 |
| | | Accepted value | 281.40±.05 |

decompose formic acid as does concentrated sulfuric acid. 85 percent phosphoric acid was heated to 250°C to drive off some of the water and then cooled to room temperature. This acid was then added to ammonium formate and the formic acid was distilled off. During the distillation the temperature of the flask was kept below 50°C. The formic acid so prepared contained an appreciable amount of water which was satisfactorily removed by distilling the sample into a bulb containing anhydrous calcium sulfate (Drierite) which had been pumped under a high vacuum at 250°C. No decomposition of the formic acid such as was observed in preliminary experiments with phosphorus pentoxide or concentrated sulfuric acid was found with the anhydrous calcium sulfate. The sample was then distilled at room temperature through a small fractionating column and the middle fraction selected for the measurements.

The preparation and purification of the formic acid was performed in an all-glass system from which air had been evacuated. All stopcocks were lubricated with Apiezon grease. We observed no evidence of reaction of the Apiezon grease with formic acid such as has been reported by Ramsperger and Porter[3] for ordinary stopcock grease. To avoid the slow decomposition of liquid formic acid to which Coolidge[4] has called attention, the sample was kept constantly frozen

TABLE II. *The heat capacity of formic acid. 0°C=273.10°K, molecular weight 46.0260.*

| $T$, °K | APPROX. $\Delta T$ | $C_p$ CAL. DEG.$^{-1}$ MOLE$^{-1}$ | $T$, °K | APPROX. $\Delta T$ | $C_p$ CAL. DEG.$^{-1}$ MOLE$^{-1}$ |
|---|---|---|---|---|---|
| 15.05 | 2.1 | 0.479 | 163.49 | 7.3 | 11.02 |
| 17.27 | 2.2 | 0.673 | 170.63 | 7.0 | 11.23 |
| 19.61 | 2.5 | 0.936 | 177.74 | 7.3 | 11.46 |
| 22.28 | 2.7 | 1.235 | 184.94 | 7.0 | 11.69 |
| 25.15 | 3.0 | 1.540 | 192.12 | 7.3 | 11.88 |
| 28.28 | 3.2 | 1.908 | 199.30 | 7.0 | 12.10 |
| 31.43 | 3.1 | 2.308 | 206.21 | 6.8 | 12.33 |
| 34.63 | 3.3 | 2.740 | 213.07 | 7.1 | 12.57 |
| 38.31 | 4.0 | 3.196 | 220.31 | 6.8 | 12.79 |
| 42.59 | 4.6 | 3.670 | 227.55 | 7.1 | 13.06 |
| 47.39 | 5.1 | 4.163 | 234.84 | 6.8 | 13.31 |
| 52.64 | 5.4 | 4.707 | 241.89 | 6.6 | 13.53 |
| 57.98 | 5.2 | 5.212 | 248.78 | 6.4 | 13.70 |
| 63.16 | 5.2 | 5.652 | 255.57 | 6.2 | 13.94 |
| 68.56 | 5.6 | 6.114 | 262.12 | 5.9 | 14.17 |
| 74.32 | 6.0 | 6.592 | 268.56 | 5.7 | 14.40 |
| 80.47 | 6.3 | 7.071 | 274.92 | 5.4 | 15.24* |
| 86.88 | 6.6 | 7.522 | 281.40 | Melting point | |
| 93.82 | 7.2 | 7.963 | 275.28 | 4.2 | 23.39 |
| 100.79 | 6.7 | 8.368 | 279.68 | 4.1 | 23.49 |
| 107.72 | 7.2 | 8.747 | 284.16 | 4.0 | 23.55 |
| 114.83 | 7.0 | 9.099 | 286.42 | 4.0 | 23.53 |
| 121.63 | 6.6 | 9.422 | 286.46 | 4.0 | 23.63 |
| 128.51 | 7.4 | 9.701 | 289.32 | 4.4 | 23.62 |
| 135.68 | 7.0 | 10.02 | 290.76 | 4.0 | 23.63 |
| 141.99 | 5.5 | 10.25 | 294.90 | 3.6 | 23.66 |
| 148.09 | 6.6 | 10.47 | 299.79 | 3.5 | 23.68 |
| 155.65 | 8.4 | 10.74 | | | |

* High because of premelting.

[3] Ramsperger and Porter, J. Am. Chem. Soc. **48**, 1267 (1926).
[4] Coolidge, J. Am. Chem. Soc. **50**, 2166 (1928).

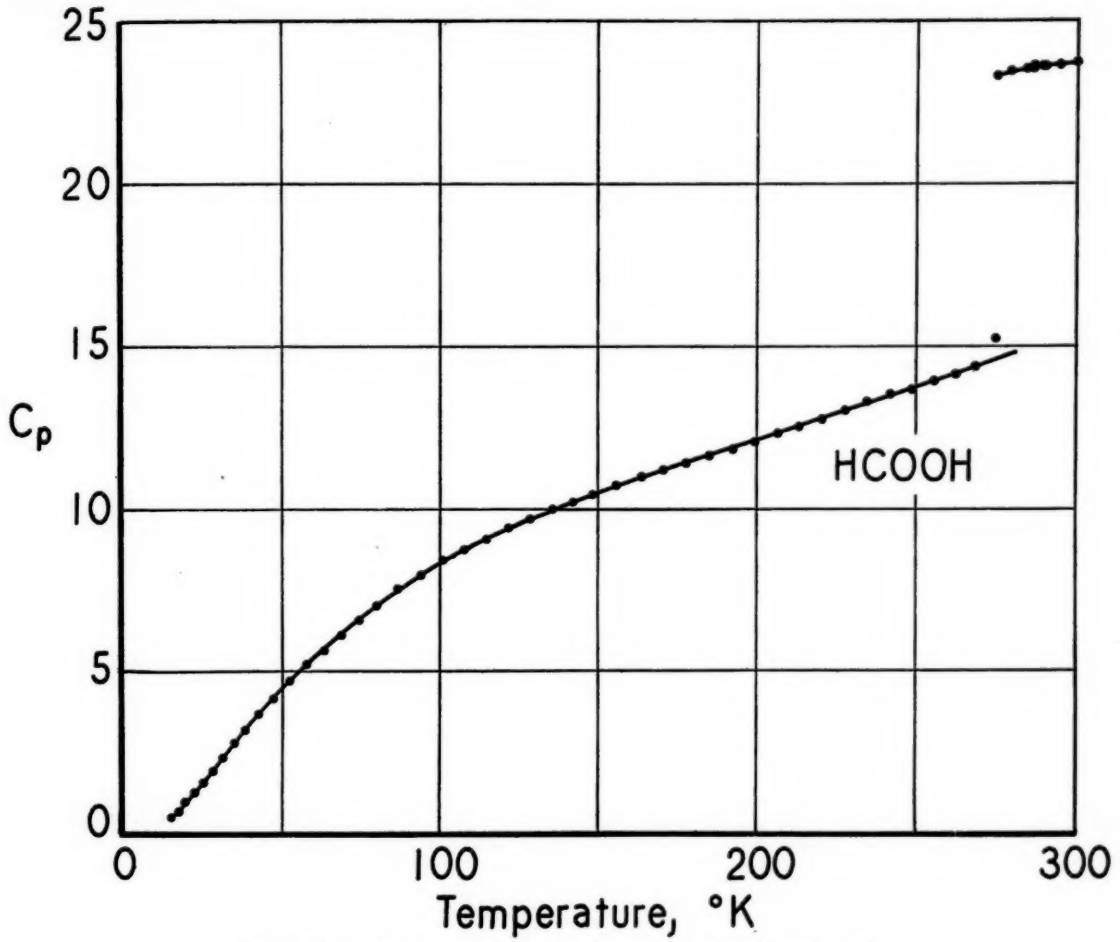


FIG. 1. Heat capacity in calories per degree per mole of formic acid.

except during transfer and during the measurements above the melting point.

The purity of the formic acid was estimated from a series of short heat capacity measurements immediately below the melting point. The amount of liquid-soluble solid-insoluble impurity was six parts per 100,000 on a molal basis. The same value may be obtained from the change of the melting point with fraction melted.

## THE MELTING POINT

A summary of the melting point observations is given in Table I. The temperatures measured by the resistance thermometer are given to 0.001° only because of the high relative accuracy. In calculating the accepted value of the melting point, correction has been made for the lowering of the melting point because of the impurity present. Of previous determinations of the melting point the most recent is that of Coolidge[5] who obtained the value 8.25°C as compared to our value of 8.30°C (281.40°K).

## THE HEAT CAPACITY OF FORMIC ACID

The amount of formic acid present during the measurements of the heat capacities and the heats of fusion was determined by distilling the sample into an evacuated glass bulb which was weighed. All weights have been corrected to vacuum. 156.041 g or 3.3903 moles of formic acid were used for the measurements. The heat capacity observations were corrected for vaporization into the small volume of the calorimeter

[5] Coolidge, J. Am. Chem. Soc. 52, 1874 (1930).

TABLE III. *The heat capacity of formic acid. Values from a smooth curve through the observations. 0°C=273.10°K, molecular weight 46.0260.*

| T, °K | $C_p$ CAL. DEG.$^{-1}$ MOLE$^{-1}$ | DEVIATION G. L. AND P. −THIS RES. % | T, °K | $C_p$ CAL. DEG.$^{-1}$ MOLE$^{-1}$ | DEVIATION G. L. AND P. −THIS RES. % |
|---|---|---|---|---|---|
| 15 | 0.474 | | 170 | 11.21 | |
| 20 | .980 | | 180 | 11.51 | +9.1 |
| 25 | 1.527 | | 190 | 11.82 | +10.6 |
| 30 | 2.124 | | 200 | 12.13 | +11.5 |
| 35 | 2.781 | | 210 | 12.46 | |
| 40 | 3.384 | | 220 | 12.81 | |
| 45 | 3.921 | | 230 | 13.14 | |
| 50 | 4.439 | | 240 | 13.47 | +14.5 |
| 60 | 5.381 | | 250 | 13.78 | +15.5 |
| 70 | 6.241 | +13.7 | 260 | 14.10 | +16.2 |
| 80 | 7.033 | +10.0 | 270 | 14.43 | +16.8 |
| 90 | 7.725 | +6.7 | 280 | 14.75 | |
| 100 | 8.325 | | 281.40 | Melting point | |
| 110 | 8.862 | | | Liquid | |
| 120 | 9.338 | | 275 | 23.38 | |
| 130 | 9.779 | | 280 | 23.49 | |
| 140 | 10.17 | | 290 | 23.61 | −0.5 |
| 150 | 10.55 | | 300 | 23.68 | |
| 160 | 10.89 | | | | |

TABLE IV. *Heat of fusion of formic acid. Melting point 281.40°K, molecular weight 46.0260.*

| RUN | TEMP. RANGE, °K | HEAT INPUT CAL. MOLE$^{-1}$ | $\int C_p dT$ CAL. MOLE$^{-1}$ | PREMELTING CAL. MOLE$^{-1}$ | $\Delta H$ FUSION CAL. MOLE$^{-1}$ |
|---|---|---|---|---|---|
| 1 | 279.50–286.67 | 3214.3 | 186.4 | 4.7 | 3032.6 |
| 2 | 278.11–283.71 | 3156.3 | 127.8 | 2.7 | 3031.2 |
| 3 | 278.36–284.04 | 3159.3 | 132.6 | 2.9 | 3029.6 |
| | | | | This research, mean | 3031±3 |
| | | | | Berthelot[1] | 2524 |
| | | | | Coolidge[2] | 3035 |

[1] Berthelot, Ann. Chim. Phys. [5] 4, 74 (1875).
[2] Cf. reference 5 of text.

and line. In order to insure thermal equilibrium about 2 cm pressure of helium was admitted to the calorimeter at 250°K. No evidence of poor thermal conductivity of the solid, such as has been mentioned by Gibson, Latimer and Parks[6] was observed. Except for the runs immediately below the melting point, thermal equilibrium in the calorimeter was attained within five minutes after the addition of energy.

The heat capacity measurements on solid and liquid formic acid are presented in Table II and represented graphically in Fig. 1. Two points on the heat capacity of the supercooled liquid are included.

Values read from a smooth curve through the observations are given in Table III. These values are believed accurate to 0.2 percent above 35°K, to 1 percent at 20°K and to 5 percent at 15°K. In Table III the earlier measurements of Gibson, Latimer and Parks[6] are compared with our results.

[6] Gibson, Latimer and Parks, J. Am. Chem. Soc. 42, 1533 (1920).

## THE HEAT OF FUSION

The results of the measurements of the heat of fusion are given in Table IV. The runs were started several degrees below the melting point and ended at a temperature above. Corrections were made for the heat capacity of the solid before melting and the heat capacity of the liquid afterwards. Small corrections were also applied for the amount of premelting in the solid at the start of the run. For comparison the values of the heat of fusion obtained by previous investigators are also listed in Table IV.

## THE HEAT OF VAPORIZATION

Since the vapor pressure of formic acid at 298°K is only some 4.3 cm, it was not possible

to collect the sample vaporized in an absorption bulb open to the atmosphere as is ordinarily done with a gas vaporizing at its normal boiling point. The procedure adopted was to utilize the pressure drop through a glass capillary to maintain the pressure in the calorimeter at that corresponding to the desired temperature of vaporization. The formic acid was condensed in evacuated glass bulbs which were cooled in a bath of carbon dioxide and methyl alcohol. The glass bulb, which was attached to the line from the calorimeter by means of a ground glass joint, was removed and weighed before and after the heat of vaporization. All weights have been corrected to vacuum. Corrections have been applied for the difference in the amount of formic acid present in the gas space above the calorimeter before and after the heats of vaporization. The electrical energy introduced into the calorimeter was corrected for the heat exchanged with the surroundings and for the change in temperature of the calorimeter and contents between the start and end of the energy input (labeled $\int C_{cal} dT$ in Table V). In correcting the values of the heat of vaporization at the measured average temperatures to 298.10°K the value 4 cal. mole$^{-1}$ deg.$^{-1}$ for the change in heat of vaporization with temperature, derived from the measurements of Coolidge[5] was used.

Several different rates of evaporation were used in order to determine if slowness in the attainment of equilibrium between single and double molecules in the gas appreciably affected the value obtained. Capillary *A*, 0.1 cm I.D. and 44 cm long was used for runs 1, 2 and 3 and capillary *B*, 0.1 cm I.D. and 69 cm long for runs 4 and 5. Runs 6 and 7 were taken using the two capillaries in parallel. The data on the heat of vaporization are presented in Table V. The heats of vaporization at the slowest rate are slightly larger than the others but since the difference is of the order of the expected experimental error we have adopted the mean of all the measurements as the best value. The value obtained from a smooth curve drawn through the observations of Coolidge[5] is included for comparison in Table V.

During the equilibrium periods before and after each heat of vaporization the vapor pressure of the liquid formic acid in the calorimeter was measured. The readings were made with a cathetometer used as a comparison instrument with a standard meter bar mounted in a case with the mercury manometer. The pressure readings were corrected to international cm of mercury. The average value of the pressure of liquid formic acid was 4.31 cm at 298.10°. This is to be compared with the value 4.29 cm obtained from a smooth curve through the measurements of Coolidge[5] and that of 4.16 in the *International Critical Tables*.[7] Coolidge[4] has called attention to the marked lowering in the vapor pressure of formic acid produced by small amounts of water.

### The Entropy from Calorimetric Data

The entropy was calculated by graphical integration of $\int_0^T C_p d \ln T$ plus the entropies of fusion and vaporization. A summary of the entropy calculation is given in Table VI.

Gibson, Latimer and Parks[6] obtained 24.30 cal. deg.$^{-1}$ mole$^{-1}$ for the entropy of the solid at the melting point compared to our value of 18.68. About 4 cal. deg.$^{-1}$ mole$^{-1}$ of the discrepancy is caused by the extrapolation from the lowest measured point of Gibson, Latimer and Parks at 70.8°K to the absolute zero.

Pauling[8] has pointed out that the entropy obtained from low temperature calorimetric measurements on formic acid should be too low by $\frac{1}{2}R \ln 2$ per mole of monomer caused by a random orientation of the two hydrogen bonds present in a dimer molecule in the solid. A similar random orientation of hydrogen bonds has been confirmed experimentally in the case of $H_2O$[9] and $D_2O$.[10] If the predicted random orientation in formic acid occurs, as seems very likely, an entropy of 0.69 cal. deg.$^{-1}$ mole$^{-1}$ should be added to the values listed in Table VI for the liquid and the gas.

The entropy of the gas listed in Table VI is the sum of the entropies of the monomer and the dimer present in 46.0260 g of gas under its saturation vapor pressure, 4.31 cm, at 298.10°K, the entropy of each species being calculated at its partial pressure. Careful measurements of the equilibrium between the monomer and the

[7] Int. Crit. Tab. Vol. III, p. 215.
[8] Pauling, J. Am. Chem. Soc. **57**, 2680 (1935).
[9] Giauque and Stout, J. Am. Chem. Soc. **58**, 1144 (1936).
[10] Long and Kemp, J. Am. Chem. Soc. **58**, 1829 (1936).

TABLE V. *Heat of vaporization of formic acid, molecular weight 46.0260.*

| RUN | $T$, °K | MOLES EVAP. | TIME OF ENERGY INPUT, MIN. | ELEC. ENERGY CAL. MOLE$^{-1}$ | HEAT EXCHANGE CAL. MOLE$^{-1}$ | $\int C_{cal} dT$ CAL. MOLE$^{-1}$ | $\Delta H_T$ CAL. MOLE$^{-1}$ | $\Delta H_{298.10}$ CAL. MOLE$^{-1}$ |
|---|---|---|---|---|---|---|---|---|
| 1 | 297.99 | 0.21482 | 56 | 4817.9 | 4.1 | −75.9 | 4746.1 | 4747 |
| 2 | 298.17 | .21801 | 56 | 4737.1 | 3.9 | +12.8 | 4753.8 | 4754 |
| 3 | 298.15 | .22031 | 56 | 4685.9 | 2.4 | 67.2 | 4755.5 | 4755 |
| 4 | 298.10 | .21945 | 94 | 4732.1 | 14.8 | 15.9 | 4762.8 | 4763 |
| 5 | 298.15 | .22181 | 94 | 4678.6 | 15.6 | 66.3 | 4760.5 | 4760 |
| 6 | 297.74 | .22229 | 42 | 4610.0 | 27.2 | 108.9 | 4746.1 | 4748 |
| 7 | 297.69 | .21715 | 42 | 4713.0 | 35.8 | 0.0 | 4748.8 | 4750 |
| | | | | | | | Mean | 4754±5 |
| | | | | | | | Coolidge[5] | 4805 |

dimer in the gas have been reported by Ramsberger and Porter[3] and by Coolidge.[4] These measurements do not, however, permit an estimation of $\Delta S$ of the dissociation reaction more closely than about 1 cal. deg.$^{-1}$ mole$^{-1}$. A more accurate treatment of the dissociation equilibrium and the answer to the question of random orientation of hydrogen bonds in solid formic acid must be postponed until values of the vibrational frequencies of at least the gaseous monomer molecule have been obtained.

The equilibrium

$$HCOOH(l) = H_2O(l) + CO(g) \qquad (1)$$

has been studied by Branch[11] and the equilibrium

$$HCOOH(l) = H_2(g) + CO_2(g) \qquad (2)$$

by Bredig, Carter and Enderli.[12] Parks and Huffman[13] employing a heat of combustion of liquid formic acid based on the measurements of Berthelot and Matignon[14] and Jahn[15] have calculated $\Delta S^0_{298.10} = 30.3$ cal. deg.$^{-1}$ mole$^{-1}$ for reaction (1) and 47.9 cal. deg.$^{-1}$ mole$^{-1}$ for (2). Using the $S^0_{298.10}$ values, $H_2O(l) = 16.75$,[16] $CO(g) = 47.32$,[17] $H_2(g) = 31.23$,[18] and $CO_2(g) = 51.07$,[19] one obtains for $S^0_{298.10}$ of liquid formic acid 33.8 cal. deg.$^{-1}$ mole$^{-1}$ from reaction (1) and 34.4 from reaction (2). The lack of agreement with the value 30.82+0.69=31.51 obtained from our measurements combined with the assumption of random orientation of hydrogen bonds in the solid is probably due to inaccuracy in the heats of combustion.

TABLE VI. *The entropy of formic acid, molecular weight 46.0260.*

| | |
|---|---|
| 0–15°K, Debye extrapolation | 0.164 |
| 15–281.40°K, Graphical | 18.517 |
| Fusion 3031/281.40 | 10.771 |
| 281.40–298.10°K, Graphical | 1.365 |
| $S$ of liquid at 298.10°K | 30.82±0.1 |
| Vaporization 4754/298.10 | 15.95 |
| $S$ of 46.0260 g of actual gas ($P$=4.31 cm) in equilibrium with the liquid at 298.10°K | 46.77±0.1 cal. deg.$^{-1}$ mole$^{-1}$ |

[11] Branch, J. Am. Chem. Soc. **37**, 2316 (1915).

[12] Bredig, Carter and Enderli, Monats. F. Chem. **54**, 1023 (1929).

[13] Parks and Huffman, *The Free Energies of Some Organic Compounds* (Chemical Catalog Co., 1932).

[14] Berthelot and Matignon, Comptes rendus **114**, 1145 (1892).

[15] Jahn, Wied. Ann. **37**, 408 (1889).

[16] Rossini, Knowlton and Jonston, J. Research Nat. Bur. Stand. **24**, 369 (1940).

[17] Clayton and Giauque, J. Am. Chem. Soc. **54**, 2610 (1932); **55**, 5071 (1933).

[18] Giauque, J. Am. Chem. Soc. **52**, 4816 (1930).

[19] Giauque and Egan, J. Chem. Phys. **5**, 45 (1937).

# A Note on Bethe-Kirkwood's Partition Function for a Binary Solid Solution

T. S. CHANG
*Department of Physics, Central University, Chungking, China*
(Received December 5, 1940)

A symmetrical method of finding the Thiele semi-invariants $\lambda_n$ in the partition function for a binary solid solution is described. In addition to the first four $\lambda$'s already known, $\lambda_5$ and $\lambda_6$ are calculated.

IN studying the equilibrium properties of a binary solid solution consisting of $N_A A$ atoms and $N_B B$ atoms and inhabiting a lattice of the type $AB$ (a lattice which can be divided into two interpenetrating sublattices, say $\alpha$ sublattice and $\beta$ sublattice), we are faced with the construction of the partition function* $F(\theta, T)$

$$\sum_X f(N, \tfrac{1}{2}N\theta, N_A-\tfrac{1}{2}N\theta, X) \times\exp\left\{-\frac{(V_{AA}+V_{BB}-2V_{AB})X}{kT}\right\}, \quad (1)$$

where $V_{AA}$, $V_{BB}$ and $V_{AB}$ are the interactions between $AA$, $BB$ and $AB$ pairs of nearest neighbors, and $f(N, \frac{1}{2}N\theta, N_A-\frac{1}{2}N\theta, X)$ is the number of ways of arranging $N_A$ particles on a lattice of the type $AB$ consisting of $N$ sites in total, with $\frac{1}{2}N\theta$ particles on the $\alpha$ sublattice, $N_A-\frac{1}{2}N\theta$ particles on the $\beta$ sublattice, and further with the particles forming $X$ pairs of nearest neighbors or first neighbors. At $T=\infty$, $F(\theta, T)$ is simply

$$\sum_X f(N, \tfrac{1}{2}N\theta, N_A-\tfrac{1}{2}N\theta, X)$$

or

$$\binom{\frac{1}{2}N}{\frac{1}{2}N\theta}\binom{\frac{1}{2}N}{N_A-\frac{1}{2}N\theta},$$

so we can put $\log F(\theta, T)$ as

$$\log\binom{\frac{1}{2}N}{\frac{1}{2}N\theta}\binom{\frac{1}{2}N}{\frac{1}{2}N\theta'}+\lambda_1\alpha+\lambda_2\frac{\alpha^2}{2!}+\lambda_3\frac{\alpha^3}{3!}+\cdots, \quad (2)$$

where $\alpha$ stands for $-(V_{AA}+V_{BB}-2V_{AB})/kT$ and $\theta'$ for $2N_A/N-\theta$. By an ingenious method Kirkwood has been able to obtain $\lambda_1$, $\lambda_2$ and $\lambda_3$.[1] He gave for the special case $N_A=\frac{1}{2}N$, $\lambda_1=\frac{1}{2}Nz\theta(1-\theta)$, $\lambda_2=\frac{1}{2}Nz\theta^2(1-\theta)^2$, $\lambda_3=-\frac{1}{2}Nz\theta^2\times(1-\theta)^2(1-2\theta)^2$, where $z$ is a coordination number of the lattice denoting the number of first neighbors of a site. A subsequent paper by Bethe and Kirkwood[2] gave

$$\lambda_4=\tfrac{1}{2}Nz\theta^2(1-\theta)^2(1-6\theta+6\theta^2)^2 +3N\{\sum_{a'=1\neq a}^{\frac{1}{2}N} z_{aa'}^2-z^2\}\theta^4(1-\theta)^4, \quad (3)$$

where $z_{aa'}$ is another coordination number denoting the number of first neighbors common to the sites $a$ and $a'$.

In a paper by the writer,[3] where $\lambda_1$, $\lambda_2$ and $\lambda_3$ are given for the general case $N_A\neq\frac{1}{2}N$, it is unfortunately remarked that $\lambda_4$ and the higher $\lambda$'s cannot be found by continuing Kirkwood's method. This is due to the fact that the introduction of coordination numbers other than $z$ was then not considered. In the present note, $\lambda_4$, $\lambda_5$ and $\lambda_6$ will be given for the general case. An attempt to calculate them is worth while, for, at the critical point of the setting in of the long distance order, the higher moments such as $\lambda_5$ and $\lambda_6$ do not seem to converge quickly, as can be seen below.

Since

$$F(\theta_1 T)=\sum_X f\left(1+\alpha X+\frac{\alpha^2}{2!}X^2+\frac{\alpha^3}{3!}X^3+\cdots\right),$$

we can write

$$F(\theta, T)=(\sum_X f) \times\left(1+\alpha M_1+\frac{\alpha^2}{2!}M_2+\frac{\alpha^3}{3!}M_3+\cdots\right), \quad (4)$$

where

$$M_1=\langle X\rangle, \quad M_2=\langle X^2\rangle, \quad M_3=\langle X^3\rangle, \quad \cdots$$

* The interactions between more distant neighbors and the factor in the partition function caused by vibrations and excitations are left out for simplicity.

[1] Kirkwood, J. Chem. Phys. **6**, 70 (1938).

[2] Bethe and Kirkwood, J. Chem. Phys. **7**, 578 (1939).

[3] Chang, Proc. Roy. Soc. **173**, 48 (1939).

with $\langle u\rangle$ denoting the *a priori* average of $u$ over the $\sum xf$ ways of arrangements. In the first paper by Kirkwood, $X$ is written as $\sum_a \nu_a n_a$, where $\nu_a$ denotes the number of $A$ atoms in the site $a$ of the $\alpha$ sublattice and is accordingly either zero or unity, and $n_a$ denotes the number of $A$ atoms among the first neighbors of the site $a$, the summation being taken over all $a$'s. The problem therefore reduces to the calculation of $\langle(\sum \nu_a n_a)^n\rangle$. In the paper by Bethe and Kirkwood, $X$ is written as

$$\sum_{a,b} \lambda_{ab}\zeta_a\eta_b, \tag{5}$$

where $\zeta_a$ denotes the number of $A$ atoms in the site $a$ of the $\alpha$ sublattice, $\eta_b$ the number of $A$ atoms in the site $b$ of the $\beta$ sublattice, and $\lambda_{ab}$ is an element of a neighbor matrix which is unity if sites $a$ and $b$ are first neighbors and zero otherwise. The authors have not shown how to calculate $\langle(\sum\lambda_{ab}\zeta_a\eta_b)^n\rangle$, but simply referred to Kirkwood's paper for the calculation of $\langle(\sum\nu_a n_a)^n\rangle$. Needless to say, the values found for $\langle(\sum\lambda_{ab}\zeta_a\eta_b)^n\rangle$ and $\langle(\sum\nu_a n_a)^n\rangle$ are necessarily the same. However, we shall describe below how to calculate $\langle(\sum\lambda_{ab}\zeta_a\eta_b)^n\rangle$, for two reasons. First, such a calculation enables us to keep the symmetry between the two sublattices always in sight, and second, it can be easily adapted (or generalized) to include interactions between more distant neighbors,* or to cases with other types of superlattice formations. For example, if we study the superlattice formations of the type $AB_3$ with the help of neighbor matrices similar to $\lambda_{ab}$ in nature and restrict ourselves to the task of finding $\lambda_1$, $\lambda_2$ and $\lambda_3$, we find that this can easily be done, the labor required being much less than that required in applying Bethe's method.[4] As a latent heat phenomena instead of a discontinuity of the specific heat is the main feature there and the amount of the latent heat does not depend so sensitively on $\lambda_2$, $\lambda_3$, etc., we shall omit here discussions on superlattice formations of the type $AB_3$.

Consider $\langle(\sum\lambda_{ab}\zeta_a\eta_b)^2\rangle$ for definiteness. A binomial expansion gives

$$\sum_{a,b}{}^{2}\lambda_{ab}\langle\zeta_a{}^2\eta_b{}^2\rangle+\sum_{a,a',b}\lambda_{ab}\lambda_{a'b}\langle\zeta_a\zeta_{a'}\eta_b{}^2\rangle+\sum_{a,b,b'}\lambda_{ab}\lambda_{ab'}\langle\zeta_a{}^2\eta_b\eta_{b'}\rangle+\sum_{a,a',b,b'}\lambda_{ab}\lambda_{a'b'}\langle\zeta_a\zeta_{a'}\eta_b\eta_{b'}\rangle, \tag{6}$$

where $a$ and $a'$, as well as $b$ and $b'$, denote different sites. We first replace $\langle\zeta_a\cdots\eta_b\cdots\rangle$ by $\langle\zeta_a\cdots\rangle\langle\eta_b\cdots\rangle$, since the *a priori* average of a product of $\zeta$'s and $\eta$'s is the product of the *a priori* averages of $\zeta$'s and $\eta$'s. Next, we replace $\langle\zeta_a{}^2\rangle=\langle\zeta_a\rangle$ by $\theta_1$, $\langle\zeta_a\zeta_{a'}\rangle$ by $\theta_2$, $\langle\eta_b{}^2\rangle=\langle\eta_b\rangle$ by $\theta_1'$, $\langle\eta_b\eta_{b'}\rangle$ by $\theta_2'$, since $\langle\zeta_a\rangle$ is the same for different $a$ sites, $\langle\zeta_a\zeta_{a'}\rangle$ is the same for whatever pairs of $a$ and $a'$ sites, etc. After the replacement, (6) becomes

$$\sum_{a,b}{}^{2}\lambda_{ab}\theta_1\theta_1'+\sum_{a,a',b}\lambda_{ab}\lambda_{a'b}\theta_2\theta_1'+\sum_{a,b,b'}\lambda_{ab}\lambda_{ab'}\theta_1\theta_2'+\sum_{a,a',b,b'}\lambda_{ab}\lambda_{a'b}\theta_2\theta_2'.$$

Hence we need to find $\theta_1$, $\theta_2$, $\theta_1'$, $\theta_2'$, and $\sum\lambda_{ab}^2$ (or $\sum\lambda_{ab}$), $\sum\lambda_{ab}\lambda_{a'b}$, $\sum\lambda_{ab}\lambda_{ab'}$, $\sum\lambda_{ab}\lambda_{a'b'}$, each of the last four being a summation over all the suffices that appear in it. In finding $\langle(\sum\lambda_{ab}\zeta_a\eta_b)^n\rangle$, similar replacements can be done, and we are left with quantities of two kinds. Quantities of the first kind are $\theta_1$, $\theta_2$, $\cdots$ and $\theta_1'$, $\theta_2'$, $\cdots$, where $\theta_n$ is $\langle\zeta_a\zeta_{a'}\cdots\zeta_a(n-1)\rangle$, $a$, $a'$, $\cdots$ being any $n$ different sites among the $\alpha$ sublattice. Quantities of the second kind are summations of the products of a succession of $\lambda_{ab}$'s.

The different $\theta$'s can be found as follows. In the first place, $\theta_1$ is nothing but $\theta$. From the relation

$$(\tfrac{1}{2}N\theta)^2=\langle(\sum_a\zeta_a)^2\rangle=\sum_a\langle\zeta_a{}^2\rangle+\sum_{a,a'}\langle\zeta_a\zeta_a'\rangle=\tfrac{1}{2}N\theta_1+\tfrac{1}{2}N(\tfrac{1}{2}N-1)\theta_2,$$

we get

$$\theta_2=\tfrac{1}{2}N\theta(\tfrac{1}{2}N\theta-1)/\tfrac{1}{2}N(\tfrac{1}{2}N-1).$$

* An example is provided by the subsequent paper, which includes second-neighbor interactions in the calculation of $\lambda_1$, $\lambda_2$ and $\lambda_3$.

[4] Peierls, Proc. Roy. Soc. **154**, 207 (1936).

From the relation

$$(\tfrac{1}{2}N\theta)^3=\langle(\sum_a \zeta_a)^3\rangle=\sum_a\langle\zeta_a{}^3\rangle+3\sum_{a,\,a'}\langle\zeta_a{}^2\zeta_{a'}\rangle+\sum_{a,\,a',\,a''}\langle\zeta_a\zeta_{a'}\zeta_{a''}\rangle,$$

$$=\tfrac{1}{2}N\theta_1+\tfrac{3}{2}N(\tfrac{1}{2}N-1)\theta_2+\tfrac{1}{2}N(\tfrac{1}{2}N-1)(\tfrac{1}{2}N-2)\theta_3,$$

we get

$$\theta_3=\tfrac{1}{2}N\theta(\tfrac{1}{2}N\theta-1)(\tfrac{1}{2}N\theta-2)/\tfrac{1}{2}N(\tfrac{1}{2}N-1)(\tfrac{1}{2}N-2).$$

In general

$$\theta_n=\tfrac{1}{2}N\theta(\tfrac{1}{2}N\theta-1)\cdots(\tfrac{1}{2}N\theta-n+1)/\tfrac{1}{2}N(\tfrac{1}{2}N-1)\cdots(\tfrac{1}{2}N-n+1). \tag{7}$$

In a similar way we can show $\theta_1'=\theta'$, $\cdots$, and

$$\theta_n'=\tfrac{1}{2}N\theta'(\tfrac{1}{2}N\theta'-1)\cdots(\tfrac{1}{2}N\theta'-n+1)/\tfrac{1}{2}N(\tfrac{1}{2}N-1)\cdots(\tfrac{1}{2}N-n+1).$$

The different summations of the product of two $\lambda_{ab}$'s can be found as follows. In the first place we have from the definition of $\lambda_{ab}$ and $z$,

$$\lambda_{ab}^2=\lambda_{ab},\quad \sum_a\lambda_{ab}=\sum_b\lambda_{ab}=z, \tag{8}$$

and hence $\sum_{a,b}\lambda_{ab}=\frac{1}{2}Nz$. Now we have the relation

$$\sum_{a,\,a',\,b}\lambda_{ab}\lambda_{a'b}=\sum_{a,\,b}(\lambda_{ab}\sum_{a^*}\lambda_{a^*b})-\sum_{a,\,b}\lambda_{ab}^2,$$

where in the summation over $a^*$, $a^*$ may correspond to any site in the $\alpha$ sublattice, not necessarily different from the site $a$. Hence

$$\sum_{a,\,a',\,b}\lambda_{ab}\lambda_{a'b}=\sum_{a,\,b}\lambda_{ab}z-\sum_{a,\,b}\lambda_{ab}=\tfrac{1}{2}Nz(z-1). \tag{9}$$

This is also the value of $\sum_{a,\,b,\,b'}\lambda_{ab}\lambda_{ab'}$ due to the symmetry between the $\alpha$ and $\beta$ sublattices. Further we have the relation

$$\sum_{a,\,a',\,b,\,b'}\lambda_{ab}\lambda_{a'b'}=\sum_{a,\,b,\,b'}(\lambda_{ab}\sum_{a^*}\lambda_{a^*b'})-\sum_{a,\,b,\,b'}\lambda_{ab}\lambda_{ab'}=\sum_{a,\,b,\,b'}\lambda_{ab}z-\tfrac{1}{2}Nz(z-1),$$

from which we get

$$\sum_{a,\,a',\,b,\,b'}\lambda_{ab}\lambda_{a'b'}=\tfrac{1}{4}N^2z^2-\tfrac{1}{2}Nz(2z-1). \tag{10}$$

In a similar way, we can get the summation of the products of three $\lambda_{ab}$'s. Because of the symmetry between the $a$'s and the $b$'s, there are only four significantly different products, i.e., $\sum\lambda_{ab}\lambda_{ab'}\lambda_{ab''}$, $\sum\lambda_{ab}\lambda_{ab'}\lambda_{a'b}$, $\sum\lambda_{ab}\lambda_{ab'}\lambda_{a'b''}$ and $\sum\lambda_{ab}\lambda_{a'b'}\lambda_{a''b''}$.* They are given by†

$$\sum\lambda_{ab}\lambda_{ab'}\lambda_{ab''}=\sum(\lambda_{ab}\lambda_{ab'}\sum_{b^*}\lambda_{ab^*})-2\sum\lambda_{ab}\lambda_{ab'}=\tfrac{1}{2}Nz(z-1)(z-2),$$

$$\sum\lambda_{ab}\lambda_{ab'}\lambda_{a'b}=\sum(\lambda_{ab}\lambda_{ab'}\sum_{a^*}\lambda_{a^*b})-\sum\lambda_{ab}\lambda_{ab'}=\tfrac{1}{2}Nz(z-1)^2,$$

$$\sum\lambda_{ab}\lambda_{ab'}\lambda_{a'b''}=\sum(\lambda_{ab}\lambda_{ab'}\sum_{a^*}\lambda_{a^*b''})-\sum\lambda_{ab}\lambda_{ab'}\lambda_{ab''}=\tfrac{1}{2}Nz(z-1)(\tfrac{1}{2}Nz-3z+2),$$

$$\sum\lambda_{ab}\lambda_{a'b'}\lambda_{a''b''}=\sum(\lambda_{ab}\lambda_{a'b'}\sum_{a^*}\lambda_{a^*b''})-2\sum\lambda_{ab}\lambda_{a'b'}\lambda_{ab''}=\tfrac{1}{8}N^3z^3+\tfrac{3}{4}N^2z^2(-2z+1)$$

$$+Nz(5z^2-6z+2). \tag{11}$$

By using the same method we can express the summations of the products of four or five $\lambda_{ab}$'s in terms of $z$ and a quantity $y$ defined as $(2/N)\sum\lambda_{ab}\lambda_{ab'}\lambda_{a'b}\lambda_{a'b'}$ which may be considered as a new coordination number. Continuing this method further, we express the summations of products of six

* It is understood from now on that all summations without subscripts under the summation sign are summations over all the subscripts in the summand, and summations with subscripts under the summation sign are taken over these subscripts only.

† For clarity, we repeat that in the summation over $a^*$ (or $b^*$), $a^*$ (or $b^*$) may correspond to any site in the $\alpha$ (or $\beta$) sublattice, not necessarily different from $a$ or $a'$ or $a''$ (or $b$, $b'$, $\cdots$), while in summations over $a$, $a'$, $\cdots$ (or $b$, $b'$, $\cdots$), the $a$'s (or $b$'s) are necessarily different sites.

or seven $\lambda_{ab}$'s in terms of $z$, $y$ and two quantities $\gamma_1$ and $\gamma_2$, defined as $(2/N)\sum\lambda_{ab}\lambda_{ab'}\lambda_{ab''}\lambda_{a'b}\lambda_{a'b'}\lambda_{a'b''}$ and $(2/N)\sum\lambda_{ab}\lambda_{ab'}\lambda_{a'b'}\lambda_{a'b''}\lambda_{a''b''}\lambda_{a''b}$. The writing out of expressions for all such summations is cumbersome and will be omitted. Evidently we can continue the method still further to find summations of products of eight or more $\lambda_{ab}$'s with the introduction of other coordination numbers of the same nature as $y$, $\gamma_1$ and $\gamma_2$, but this will not be done here.

With the $\theta$'s and the summations of products of three, four, five, or six $\lambda_{ab}$'s completely determined, we obtain $M_1$, $M_2$, $\cdots$ up to $M_6$. Expanding the $M$'s in powers of $N^{-1}$, substituting the expanded series into (4), and comparing the $F(\theta, T)$ so obtained with (2), we find

$$\begin{aligned}
&\lambda_1=\tfrac{1}{2}Nz\theta\theta', \quad \lambda_2=\tfrac{1}{2}Nz\theta\theta'(1-\theta)(1-\theta'), \quad \lambda_3=\tfrac{1}{2}Nz\theta\theta'(1-\theta)(1-\theta')(1-2\theta)(1-2\theta'),\\
&\lambda_4=\tfrac{1}{2}Nz\theta\theta'(1-\theta)(1-\theta')(1-6\theta+6\theta^2)(1-6\theta'+6\theta'^2)+3N(y-z)\theta^2\theta'^2(1-\theta)^2(1-\theta')^2,\\
&\lambda_5=\tfrac{1}{2}Nz\theta\theta'(1-\theta)(1-\theta')(1-2\theta)(1-2\theta')(1-12\theta+12\theta^2)(1-12\theta'+12\theta'^2)\\
&\qquad\qquad +30N(y-z)\theta^2\theta'^2(1-\theta)^2(1-\theta'^2)(1-2\theta)(1-2\theta'),\\
&\lambda_6=\tfrac{1}{2}Nz\theta\theta'(1-\theta)(1-\theta')\{1-30\theta(1-\theta)(1-2\theta)^2-30\theta'(1-\theta')(1-2\theta')^2\}\\
&\quad +15N(13y+17z)\theta^2\theta'^2(1-\theta)^2(1-\theta')^2+30N(\gamma_1-30y-28z)\theta^2\theta'^2(1-\theta)^2(1-\theta')^2\\
&\qquad \times\{\theta(1-\theta)+\theta'(1-\theta')\}+60N(\gamma_2-4\gamma_1+66y+42z)\theta^3\theta'^3(1-\theta)^3(1-\theta')^3,
\end{aligned} \tag{12}$$

where terms of the order smaller than $N$ are not written out. It is seen that the $\lambda$'s are linear in the coordination numbers $z$, $y$, $\gamma_1$ and $\gamma_2$, meaning that they do not contain powers of $y$, $z$, $\gamma_1$ and $\gamma_2$, nor their products. Whether this holds for the higher $\lambda$'s remains to be seen, but it seems very plausible.

The connection between the coordination numbers $y$, $\gamma_1$ and $\gamma_2$ and the number $z_{aa'}$ of first neighbors common to the sites $a$ and $a'$ is as follows. Since $z_{aa'}$ is nothing but $\sum_b\lambda_{ab}\lambda_{a'b}$, we have

$$\sum\lambda_{ab}\lambda_{ab'}\lambda_{a'b}\lambda_{a'b'}=\sum(\lambda_{ab}\lambda_{a'b}\sum_{b^*}\lambda_{ab^*}\lambda_{a'b^*})-\sum\lambda_{ab}\lambda_{a'b},$$

whereupon

$$\sum\lambda_{ab}\lambda_{ab'}\lambda_{a'b}\lambda_{a'b'}=\tfrac{1}{2}N\{\textstyle\sum_{a'}z_{aa'}^2-z(z-1)\},$$

or

$$y=\textstyle\sum_{a'}z_{aa'}^2-z(z-1). \tag{13}$$

In a similar way we can prove

$$\begin{aligned}
\gamma_1&=\textstyle\sum_{a'}z_{aa'}^3-3\sum_{a'}z_{aa'}^2+2z(z-1),\\
\gamma_2&=\textstyle\sum_{a'\,a''}z_{aa'}z_{a'a''}z_{a''a}-3(z-2)\sum_{a'}z_{aa'}^2+2z(z-1)(z-2).
\end{aligned} \tag{14}$$

These equations furnish us a way of obtaining the numerical values of these coordination numbers. We have, for simple cubic systems, $z=6$, $y=24$, $\gamma_1=0$ and $\gamma_2=264$, and for body-centered cubic systems, $z=8$, $y=96$, $\gamma_1=144$ and $\gamma_2=1776$.

The calculation of the critical point for the setting in of a long distance order and the accompanying discontinuity $\Delta C_v$ of the specific heat can be carried out in the usual manner. For the special case $N_A=\frac{1}{2}N$, the results are

$$\alpha \text{ at the critical point } T_c \text{ or } \alpha_c=-\frac{4}{z}\left\{1+\frac{1}{z}+\frac{4}{3}\frac{1}{z^2}+\left(\frac{y}{z}+2\right)\frac{1}{z^3}+\left(\frac{4y}{z}+\frac{16}{5}\right)\frac{1}{z^4}+\left(\frac{\gamma_2}{z}-\frac{2\gamma_1}{3z}+10\frac{y}{z}+\frac{16}{3}\right)\frac{1}{z^5}+\cdots\right\}, \tag{15}$$

$$\Delta C_v \text{ in } k \text{ per atom}=\frac{3}{2}\left\{1+\frac{1}{z}+\frac{2}{3}\frac{1}{z^2}+\left(\frac{3y}{z}\right)\frac{1}{z^3}+\left(\frac{6y}{z}-\frac{52}{45}\right)\frac{1}{z^4}+\left(\frac{5\gamma_2}{z}-\frac{40\gamma_1}{3z}-\frac{26}{3}\frac{y}{z}-\frac{28}{9}\right)\frac{1}{z^5}+\cdots\right\}. \tag{16}$$

In the expansion we have considered $y$, $\gamma_1$ and $\gamma_2$ as of the order $z$, though strictly speaking we should not do so, as $y$, $\gamma_1$ and $\gamma_2$ are much larger than $z$.

The fifth and the sixth terms in the above expansions are directly affected by what values $\lambda_5$ and $\lambda_6$ take. It is easily seen that owing to the large value of $y$, $\gamma_1$ and $\gamma_2$ the convergence of the above series is slow. For example, the third term in the bracket in (16) is $2/(3z^2)$, amounting to 0.0104 for body-centered cubic systems, while the fifth and the sixth terms for the same lattice structure are 0.0173 and 0.0233 respectively. Thus, for a thorough investigation, a knowledge of the higher $\lambda$'s is necessary. Neglecting the dotted terms in (15) and (16), we have

$-\alpha$ at $T_c=0.838$, $\Delta C_v$ in $k$ per atom $=1.92$ for simple cubic systems,
$-\alpha$ at $T_c=0.598$, $\Delta C_v$ in $k$ per atom $=1.87$ for body-centered cubic systems,

which are not significantly different from values obtained earlier.[1]

In any effort to coordinate the change of configurations with the change of the vibrations of the atoms in the binary solid solution,[5] it is necessary to construct the partition function with a factor $Y$ corresponding to the vibrations of the solution, $Y$ depending in general on $\theta$, $X$ and $T$. Thus in the construction of the partition function it is necessary to know explicitly the function $f(N, \frac{1}{2}N\theta, \frac{1}{2}N\theta', X)$. This function can be found from the $\lambda$'s as follows.

Replacing the summation (1) by the maximum term, and equating its logarithm to (2), we have

$$\log f(N, \tfrac{1}{2}N\theta, \tfrac{1}{2}N\theta', X)+X\alpha=\log \binom{\frac{1}{2}N}{\frac{1}{2}N\theta}\binom{\frac{1}{2}N}{\frac{1}{2}N\theta'}+\sum \lambda_n \frac{\alpha^n}{n!}, \tag{17}$$

where $X$ is a function of $\theta$, $\theta'$ and $\alpha$ given by

$$(\partial/\partial X) \log f(N, \tfrac{1}{2}N\theta, \tfrac{1}{2}N\theta', X)+\alpha=0. \tag{18}$$

An alternative way of looking at the Eqs. (17) and (18) is to consider (17) as an equation between $f$, $\theta$, $\theta'$ and $X$, with $\alpha$ considered as a function of $\theta$, $\theta'$ and $X$ determined by (18). This provides us at once a method of determining $f$. After eliminating $\alpha$ from (17) and (18), we obtain

$$\log f=\log \binom{\frac{1}{2}N}{\frac{1}{2}N\theta}\binom{\frac{1}{2}N}{\frac{1}{2}N\theta'}+\sum c_n\{\tfrac{1}{2}Nz\theta\theta'(1-\theta)(1-\theta')\}^{1-n}(X-\tfrac{1}{2}Nz\theta\theta')^n, \tag{19}$$

where

$$\begin{aligned}
&c_0=c_1=0, \quad c_2=-\tfrac{1}{2}, \quad c_3=\tfrac{1}{6}\{(1-\theta)^2-\theta^2\}\{(1-\theta')^2-\theta'^2\},\\
&c_4=-\frac{1}{12}\{(1-\theta)^3+\theta^3\}\{(1-\theta')^3+\theta'^3\}+\frac{1}{4}\frac{y}{z}\theta\theta'(1-\theta)(1-\theta'),\\
&c_5=\frac{1}{20}\{(1-\theta)^4-\theta^4\}\{(1-\theta')^4-\theta'^4\},\\
&c_6=-\frac{1}{30}\{(1-\theta)^5+\theta^5\}\{(1-\theta')^5+\theta'^5\}-\frac{1}{6}\left(\frac{4\gamma_1}{z}-\frac{\gamma_2}{z}+3\frac{y^2}{z^2}\right)\theta^2\theta'^2(1-\theta)^2(1-\theta')^2\\
&\qquad\qquad +\frac{1}{12}\frac{\gamma_1}{z}\theta\theta'(1-\theta)(1-\theta')\{\theta(1-\theta)+\theta'(1-\theta')\}.
\end{aligned} \tag{20}$$

The higher $C$'s can be obtained when $\lambda_7$ and the higher $\lambda$'s are determined. A similar calculation of $f$ from an expression of $F(\theta_1 T)$ deduced from the equilibrium properties of the solid solution calculated by Bethe's method has been done in reference 3. If we expand the formula for $\log f$ given there in

[5] Chang, Proc. Camb. Phil. Soc. **35**, 265 (1939).

powers of $(X-\frac{1}{2}Nz\theta\theta')^n$ and put the expansion in the form (19), the coefficients $C_0, \cdots$ up to $C_6$ are exactly the same as those given by (20), except that all terms containing $y$ or $\gamma_1$ or $\gamma_2$ are no longer present. In fact, if we put the expression for $\log F(\theta_1 T)$ deduced from the equilibrium properties obtained by Bethe's method in the form (2), the $\lambda$'s are exactly the same as those given by (12), with $y$, $\gamma_1$ and $\gamma_2$ put equal to zero. This accounts for the agreement of the present formula for $\log f$ and the formula given there when we remove all terms containing $y$ or $\gamma_1$ or $\gamma_2$. It is almost needless to add that if we expand the values of $\alpha_c$ and $\Delta C_v$ obtained by Bethe's method in powers of $z^{-1}$, we obtain (15) and (16) after removing all terms in them which contain $y$ or $\gamma_1$ or $\gamma_2$.

In conclusion, the writer wishes to express his thanks to Dr. J. S. Wang of Southwestern Associated University and Mr. S. K. Kao of this university for their interest and helpful discussions.

---

FEBRUARY, 1941 JOURNAL OF CHEMICAL PHYSICS VOLUME 9

# Second-Neighbor Interactions and the Critical Behavior of Binary Solid Solutions

T. S. CHANG
*Department of Physics, Central University, Chungking, China*
(Received December 5, 1940)

The Thiele semi-invariants $\gamma_1$, $\gamma_2$ and $\gamma_3$ of a binary solid solution are calculated with the assumption that there are second-neighbor interactions as well as first-neighbor interactions. The results give a decrease of the critical temperature $T_c$ at which the superlattice sets in, an increase of the local order $\sigma$ at $T_c$, an increase of the discontinuity of the specific heat, thus in general agreement with the results obtained by applying Bethe's method to the same problem.

THE configurational partition function $F(\theta, T)$ of a binary solid solution consisting of $N_A A$ atoms and $N-N_A B$ atoms and inhabiting a lattice of the type $AB$ (a lattice consisting of two interpenetrating sublattices, referred to as $\alpha$ and $\beta$ sublattices) for configurations with $\frac{1}{2}N\theta A$ atoms on one of the sublattices, say $\alpha$ sublattice, can be put into the form[1]

$$\binom{\frac{1}{2}N}{\frac{1}{2}N\theta}\binom{\frac{1}{2}N}{\frac{1}{2}N\theta'} \exp\left\{\sum \frac{\gamma_n}{n!}\left(-\frac{1}{kT}\right)^n\right\}, \quad (1)$$

where $\theta'$ stands for $2N_A/N-\theta$ and $\gamma_n$ are to be determined. When all interactions between the atoms are those between the first neighbors, the first six $\gamma_n$ have been determined and are exactly $(V_{AA}+V_{BB}-2V_{AB})^n$ times the $\lambda_n$ given in reference 1, $V_{AA}$, $V_{BB}$ and $V_{AB}$ denoting the interaction between $AA$, $BB$ and $AB$ pairs of first neighbors. As shown there, the convergence of the series $\sum\gamma_n(n!)^{-1}(-kT)^{-n}$ at the critical point is slow, and for an accurate determination of the behavior of the setting-in of a long distance-order at the critical point, it is necessary to find $\gamma_7$, $\gamma_8$, etc. Before we undertake to find $\gamma_7$, $\gamma_8$, it is advisable to know what effects the introduction of second- or third-neighbor interactions has upon the lower $\gamma$'s, say $\gamma_1$, $\gamma_2$ and $\gamma_3$. If the effect is large, it will be unwise to calculate $\gamma_7$, $\gamma_8$ with second- or third-neighbor interactions neglected, since they will depend on the second- or third-neighbor interactions to a greater extent.

In the following, we introduce second-neighbor interactions $V_{AA}^{(2)}$, $V_{BB}^{(2)}$ and $V_{AB}^{(2)}$ and calculate $\gamma_1$, $\gamma_2$ and $\gamma_3$ following a method given in reference 1. The same problem has been studied by using Bethe's second approximation.[2,3] The result given there is that, if $V_{AA}^{(2)}+V_{BB}^{(2)}-2V_{AB}^{(2)}$ is also positive, just as $V_{AA}+V_{BB}-2V_{AB}$, the critical temperature $T_c$ is lowered, the local order $\sigma$ at $T_c$, say $\sigma_c$, is increased, and the discontinuity

[1] See the preceding paper entitled "A note to Bethe-Kirkwood's partition function of a binary solid solution," J. Chem. Phys. **9**, 169 (1941).

[2] H. A. Bethe, Proc. Roy. Soc. **150**, 552 (1935).
[3] T. S. Chang, Proc. Roy. Soc. **161**, 546 (1937).

$\Delta C_v$ in the specific heat considerably increased. The mere knowledge of $\gamma_1$, $\gamma_2$ and $\gamma_3$ for cases with or without second-neighbor interactions cannot give us the precise amount of changes in $T_c$ or $\sigma_c$ or $\Delta C_v$, since the series $\sum\gamma_n(n!)^{-1}(-kT)^{-n}$ converges slowly in both cases, meaning that the higher $\gamma$'s are equally important in determining $T_c$, $\sigma_c$ and $\Delta C_v$. But as can be seen below, the results calculated with $\gamma_1$, $\gamma_2$ and $\gamma_3$ and with the higher $\gamma$'s neglected points clearly to a decrease of $T_c$, an increase of $\sigma_c$ and an increase of $\Delta C_v$, which is in agreement with the results obtained by Bethe's method.

Denoting the number of $AA$ pairs of first neighbors by $X$, the number of $AA$ pairs of second neighbors by $Y$, $-(V_{AA}+V_{BB}-2V_{AB})/kT$ by $\alpha$, and $-(V_{AA}^{(2)}+V_{BB}^{(2)}-2V_{AB}^{(2)})/kT$ by $t\alpha$, we may write $F(\theta, T)$ as

$$\binom{\frac{1}{2}N}{\frac{1}{2}N\theta}\binom{\frac{1}{2}N}{\frac{1}{2}N\theta'}\left\{1+\alpha M_1+\frac{\alpha^2}{2!}M_2+\cdots\right\}, \quad (2)$$

where $M_1=\langle(X+tY)\rangle$, $M_2=\langle(X+tY)^2\rangle$, $\cdots$, $\langle u\rangle$ denoting the *a priori* average of $u$ over all configurations with $\frac{1}{2}N\theta A$ atoms on the $\alpha$ sublattice. Introducing $\zeta_a$ as the number of $A$ atoms in the site $a$ of the $\alpha$ sublattice and $\eta_b$ as the number of $A$ atoms in the site $b$ of the $\beta$ sublattice, we have

$$X=\sum_{a,b}\lambda_{ab}\zeta_a\eta_b, \quad (3)$$

$$Y=\tfrac{1}{2}\{\sum_{a,a'}\mu_{aa'}\zeta_a\zeta_{a'}+\sum_{b,b'}\mu_{bb'}\eta_b\eta_{b'}\}, \quad (4)$$

where $\lambda_{ab}$ is a first-neighbor matrix which is defined to be unity if the sites $a$ and $b$ are first neighbors and zero otherwise and $\mu_{aa'}$ (or $\mu_{bb'}$) is a second-neighbor matrix which is defined to be unity if the sites $a$ and $a'$ (or $b$ and $b'$) are second neighbors and zero otherwise. Further we introduce the coordination numbers $z_1$, $z_2$, $z_{112}$ and $z_{222}$ defined by

$$\begin{aligned} z_1&\equiv\sum_a\lambda_{ab}=\sum_b\lambda_{ab},\\ z_2&\equiv\sum_{a'}\mu_{aa'}=\sum_{b'}\mu_{bb'},\\ z_{112}&\equiv\left(\frac{2}{N}\right)\sum_{a,a',b}\lambda_{ab}\lambda_{a'b}\mu_{aa'},\\ z_{222}&\equiv\left(\frac{2}{N}\right)\sum_{a,a',a''}\mu_{aa'}\mu_{a'a''}\mu_{a''a}, \end{aligned} \quad (5)$$

where $a$, $a'$ and $a''$ as well as $b$ and $b'$ denote different sites. Then it is possible to calculate $M_1$, $M_2$ and $M_3$ exactly in the same way as given in reference 1, i.e., we first replace $\langle\zeta\cdots\eta\cdots\rangle$ by $\langle\zeta\cdots\rangle\langle\eta\cdots\rangle$, and then $\langle\zeta_a\rangle$ by $\theta_1$, $\langle\zeta_a\zeta_{a'}\rangle$ by $\theta_2$, $\langle\zeta_a\zeta_{a'}\zeta_{a''}\rangle$ by $\theta_3$, $\langle\eta_b\rangle$ by $\theta_1'$, $\langle\eta_b\eta_{b'}\rangle$ by $\theta_2'$, etc., obtaining finally only quantities such as the $\theta$'s and the summations of products of $\lambda_{ab}$'s and $\mu$'s. The $\theta$'s are given in reference 1, and regarding the summations of products of $\lambda_{ab}$'s and $\mu$'s, we meet the following kinds in the calculation of $M_1$, $M_2$ and $M_3$, i.e.,

(i) Summations of products of one $\lambda_{ab}$ and one $\mu$,
(ii) Summations of products of two $\lambda_{ab}$'s and one $\mu$,
(iii) Summations of products of one $\lambda_{ab}$ and two $\mu$'s,
(iv) Summations of products of two or three $\lambda_{ab}$'s,
(v) Summations of products of two or three $\mu$'s.

By following a method sketched in the reference 1, we can express summations of products of the first and the third types in terms of $z_1$ and $z_2$, those of the second type in terms of $z_1$, $z_2$ and $z_{112}$, those of the fourth type in terms of $z_1$, and those of the fifth type in terms of $z_2$ and $z_{222}$. After obtaining these summations and also the $\theta$'s, we obtain $M_1$, $M_2$ and $M_3$ in terms of $\theta$, $\theta'$ and the coordination numbers $z_1$, $z_2$, $z_{112}$ and $z_{222}$.

If we proceed further to find the higher $M$'s, we must introduce other coordination numbers. It can be seen that quite generally, each coordination number is connected with a summation of the products of $\lambda_{ab}$'s and $\mu$'s, say the summation of

$$\lambda_{ij}\lambda_{..}\cdots\mu_{kl}\mu_{..}\cdots,$$

in which, if we consider $\lambda_{ij}$ as something connecting the subscripts $i$ and $j$ and $\mu_{kl}$ as something connecting the subscripts $k$ and $l$, we can find two or more chains of $\lambda_{ab}$'s and $\mu$'s, with no $\lambda_{ab}$ or $\mu$ in common, connecting any one of the subscripts to any other. Each of the subscripts occurs therefore at least twice, and the whole summation is of the order $N/2$. We can thus define the corresponding coordination numbers as $2/N$ times the respective summations. For example, in finding $M_4$, we meet the coordination

numbers

$$z_{1122}\equiv\frac{2}{N}\sum\lambda_{ab}\lambda_{a'b'}\mu_{aa'}\mu_{bb'},$$

$$z'_{1122}\equiv\frac{2}{N}\sum\lambda_{ab}\lambda_{a'b}\mu_{aa''}\mu_{a'a''},$$

$$z_{1111}\equiv\frac{2}{N}\sum\lambda_{ab}\lambda_{ab'}\lambda_{a'b}\lambda_{a'b'},$$

$$z_{2222}\equiv\frac{2}{N}\sum\mu_{aa'}\mu_{a'a''}\mu_{a''a'''}\mu_{a'''a}.$$

It is needless to say that the number of coordination numbers increases very rapidly when we go into the higher $M$'s.

Substituting the found values of $M_1$, $M_2$ and $M_3$ into (2), expanding in powers of $N^{-1}$, and then comparing (2) with (1), we get

$$-\frac{\gamma_1}{kT}=\alpha\{\tfrac{1}{2}Nz_1\theta\theta'+\tfrac{1}{4}Nz_2t(\theta^2+\theta'^2)\},$$

$$\frac{\gamma_2}{(kT)^2}=\alpha^2\{\tfrac{1}{2}Nz_1\theta\theta'(1-\theta)(1-\theta')+\tfrac{1}{4}Nz_2t^2[\theta^2(1-\theta)^2+\theta'^2(1-\theta')^2]\},$$

$$-\frac{\gamma_3}{(kT)^3}=\alpha^3\{\tfrac{1}{2}Nz_1\theta\theta'(1-\theta)(1-\theta')(1-2\theta)(1-2\theta')+\tfrac{3}{2}Nz_{112}t\theta\theta'(1-\theta)(1-\theta')[\theta(1-\theta)+\theta'(1-\theta')]$$
$$+\tfrac{1}{4}Nz_2t^3[\theta^2(1-\theta)^2(1-2\theta)^2+\theta'^2(1-\theta')^2(1-2\theta')^2]+\tfrac{1}{2}Nz_{2222}t^3[\theta^3(1-\theta)^3+\theta'^3(1-\theta')^3]\},\quad(6)$$

where terms of an order smaller than $N$ are not written out. It can be noted that all the $\gamma$'s are linear in the coordination numbers just as the $\lambda$'s in reference 1.

The numerical values of such coordination numbers for simple cubic systems and body-centered cubic systems are as follows:

for simple cubic systems

$$z_1=6,\quad z_2=12,\quad z_{112}=24,\quad z_{222}=0;$$

for body-centered systems

$$z_1=8,\quad z_2=6,\quad z_{112}=24,\quad z_{222}=0.$$

Since $z_{222}$ is zero for both cases, we shall leave out the term in $-\gamma_3/(kT)^3$ containing $z_{222}$. Because of the large value of $z_2$ and $z_{112}$, the effect of increasing $t$ from 0 to some value such as 0.1 is already noticeable. For example, for simple cubic systems, at $\theta=\frac{2}{5}$, $\theta'=\frac{3}{5}$, $\gamma_3$ is changed by 1.44 times.

The calculation of the critical point $T_c$ and the discontinuity $\Delta C_v$ in the specific heat can be carried out in the usual manner. For the particular case $N_A=\frac{1}{2}N$, we have

$$\alpha \text{ at } T_c \text{ or } \alpha_c=-\frac{4}{(z_1-z_2t)}\left\{1+\frac{z_1+z_2t^2}{(z_1-z_2t)^2}-\frac{1}{3}\frac{2z_1+9z_{112}t-2z_2t^3}{(z_1-z_2t)^3}+\frac{2(z_1+z_2t^2)^2}{(z_1-z_2t)^4}+\cdots\right\},\quad(7)$$

$$\Delta C_v \text{ in } k \text{ per atom}=\frac{3}{2}\left\{1+\frac{z_1+z_2t^2}{(z_1-z_2t)^2}-\frac{16z_1+18z_{112}t-16z_2t^3}{3(z_1-z_2t)^3}+6\frac{(z_1+z_2t^2)^2}{(z_1-z_2t)^4}+\cdots\right\}.\quad(8)$$

The local order $\sigma$ can be defined by $\bar{X}=\frac{1}{8}Nz_1(1-\sigma)$ for this special case, $\bar{X}$ being the equilibrium value of $X$ for the binary solution. Now $\bar{X}$ is given by $(\partial/\partial\alpha)\log F(\theta, T)$, where in the differentiation $t\alpha$ is kept constant. Hence we get at $T_c$, where $\theta=\theta'=\frac{1}{2}$,

$$\bar{X}=\frac{1}{8}Nz_1\left(1+\frac{1}{4}\alpha_c+\frac{1}{8}\frac{z_{112}}{z_1}t\alpha_c^2\right),$$

and accordingly,

$$\sigma_c=-\frac{\alpha_c}{4}-\frac{1}{8}\frac{z_{112}}{z_1}t\alpha_c^2,$$

or

$$\frac{1}{(z_1-z_2t)}\left\{1+\frac{z_1+z_2t^2}{(z_1-z_2t)^2}-\frac{2z_{112}t}{z_1(z_1-z_2t)}\right\}.\quad(9)$$

Thus, if $t$ is positive, $T_c$ is decreased, $\sigma_c$ increased, and $\Delta C_v$ increased, but the increase of $\Delta C_v$ does not seem to be large enough to bring the calculated results into agreement with experiments. The above expansions are in series of $(z_1-z_2t)^{-1}$, and this makes the increase or decrease at once obvious. We can, of course, expand in $z_1^{-1}$, and then the increase or decrease will be shifted to a lower term.

Finally, the writer wishes to thank Mr. S. K. Kao for helpful discussions.

# Granulation, Phase Change, and Microstructure

## Kinetics of Phase Change. III*

MELVIN AVRAMI
*Columbia University, New York, New York*

(Received August 6, 1940)

The theory of the preceding papers is generalized and the notation simplified. A cluster of molecules in a stable phase surrounded by an unstable phase is itself unstable until a critical size is reached, though for statistical reasons a distribution of such clusters may exist. Beyond the critical size, the cluster tends to grow steadily. The designation "nuclei" or "grains" is used according as the clusters are below or above the critical size. It is shown that a comprehensive description of the phenomena of phase change may be summarized in Phase Change, Grain Number and Microstructure Formulas or Diagrams, giving, respectively, the transformed volume, grain, and microstructure densities as a function of time, temperature, and other variables. To facilitate the deduction of formulas for these densities the related densities of the "extended" grain population are introduced. The extended population is that system of interpenetrating volumes that would obtain if the grains granulated and grew through each other without mutual interference. The extended densities are much more readily derivable from an analysis of the fundamental processes of granulation and growth. It is shown that, under very general circumstances, the densities of the actual grain population may be expressed simply in terms of the extended population.

### A. NUCLEI AND GRAINS

IN the previous papers[1] we have developed a treatment of the transformation mechanism which we may now generalize. At the same time, it is desirable to simplify some of the previous notations. To recapitulate: It appears that the grains of a new phase generally originate at certain centers or heterogeneities in the old phase. In these it is desirable to distinguish between two stages. For even though, in the supercooled (or superheated) condition, the *internal* free energy of the new phase is lower than in the old, the additional opposing free energy change, involved in the creation of an interface, makes a cluster of the new phase below a certain critical size (function of the thermodynamic conditions) incapable of steady growth. Only if a cluster larger than the critical size occurs, e.g., through spontaneous or stimulated fluctuations, will it grow steadily.

Now, in previous investigations,[1] we have used the name "germ nuclei" to refer to such activable regions before they reach the critical size, and "growth nuclei" for those which have reached and passed the critical size. It is possible, and perhaps desirable for psychological reasons, to simplify the terminology by calling the former simply "nuclei" and the latter "grains" (or "new grains" if necessary for specificity).

This we shall do in the future, *confining the term "nucleus" to a cluster of the new phase smaller than the critical size, the term "grain" to a cluster larger than the critical size.* The region (originally a nucleus) around which a grain has grown may be referred to as the "*grain center.*" A nucleus or grain may have foreign matter (inclusion) as a core, or it may form on a foreign surface and thus not be entirely surrounded by the old phase, but, in any case, the specifications for the critical size may be worked out.[1(a)] It has been suggested that the process of passing from the nucleus to the grain stage shall be termed "granulation."† The "*granulation rate*" is the number of nuclei, per unit time and unit volume, which "pop," i.e., pass through the critical size, and, becoming grains, embark upon a career of steady growth.

Several recent investigators[2] have discussed the necessary existence, in equilibrium, of clusters of one phase in another before the temperature

* Publication assisted by the Ernest Kempton Adams Fund for Physical Research of Columbia University.

[1] (a) J. Chem. Phys. **7**, 1103 (1939); (b) *ibid.* **8**, 212 (1940); referred to as K.P.C. I and II, respectively.

† This replaces the term "nucleation" which was used in K.P.C. I in conformity with the current somewhat vague terminology. It seems logical, to confine the term nucleation to the process of becoming a nucleus.

[2] In particular J. Frenkel, J. Chem. Phys. **7**, 538 (1939); W. Band, *ibid.* **7**, 324 (1939); J. E. Mayer and S. F. Streeter, *ibid.* **7**, 1019 (1939). A connection has also been established with the general statistical mechanical treatment given by Mayer and his collaborators.

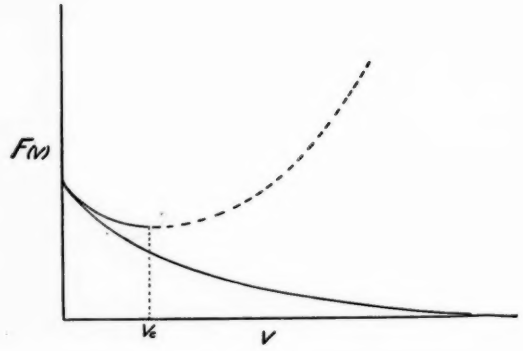


FIG. 1.

for macroscopic transition is reached.†† These "heterophase clusters" are nuclei in our sense of the word. In the case of a substance free from foreign particles, they are the only nuclei present. Their typical size-frequency density (i.e., number of given size per unit volume), at a certain temperature $T_1$ above the transition point, is indicated by the solid curve in Fig. 1. Below the transition point, the critical size diminishes from infinity to some finite value. Thus, if we quench suddenly from $T_1$ to a supercool temperature $T_2$, for which the critical nucleus size is $v_c$, all clusters larger than $v_c$, present at $T_1$, are effective grains and start growing steadily. Those below the critical size shift their frequency statistically and, it can be shown, generally increase in number, so that at a later time the frequency is given by a curve like the dotted one in Fig. 1. The general kinetics of the processes involved will be analyzed in a later paper. For the present, the underlying physical situation may be described as follows: Any particular nucleus below the critical size has a higher tendency to dissolve than to grow. But when we consider the entire group of a particular size, we find that the tendency of its majority to dissolve is more than balanced by the minority tendency of the *larger group* of next smaller size to grow. The granulation rate, at any time, is the number of clusters per unit volume which pass through the "bottleneck" $v_c$ per unit time.

Sometimes, the distribution with which we start was not in equilibrium at the pretreatment temperature. Also, it may be non-uniform, so that the resulting density varies in space. The considerations in this paper will, however, apply generally to these and other industrially important cases where the transforming substance contains foreign heterogeneities which catalyze the reaction by providing adsorbing-activating surfaces on which nuclei and grains form. These, like the heterophase clusters, may be present from the beginning of the reaction, and are therefore determined by its "prehistory"; or they may be introduced physically, or formed chemically, during the reaction, and are therefore functionals of its history.

### B. Volume, Grain, and Frequency Densities

We may arrange observations on the kinetics of transformation under the following headings. First we consider the *volume density* $V$ of the new phase (i.e., fraction of unit volume of space occupied), as a function of time $t$, position $P$, initial temperature $T_0$, and as a functional of the prehistory and of the subsequent type of thermal treatment $T(t, T_0, P)$. For given prehistory and type of history (e.g., isothermal, linear cooling, "seeding" at a certain time, etc.), and for the unit volume around a given point, a three-dimensional diagram relating $V$, $t$, and $T_0$ may be constructed. We shall call this the "*Volume Diagram*" or "*Phase Change Diagram*" in contrast with the familiar Phase Equilibrium Diagrams to which it reduces in the cross section at infinite time (system with isothermal history). The analytical representation of

$$V \equiv V(t, T_0, P)$$

will be called the "*Phase Change Formula.*" It is to be remarked that $V$ corresponds to the variable, "degree of advancement" of a reaction, used by De Donder-Rysselbergh[3] and Guggenheim[4] in various thermodynamic studies.

A second important type of relation is that giving the *grain density* $N$ (i.e., number of grain centers per unit volume)* as a function of $t$, $T_0$,

†† For simplicity of speech, and in conformity with the usual experimental conditions, we consider pressure kept constant and temperature as the controlling variable. Also, we take the new phase as the one stable at lower temperatures, and therefore speak of supercooling. The generalization can be made without difficulty.

[3] De Donder-Rysselbergh, *Affinity* (Stanford University Press, 1936).

[4] Guggenheim, J. Chem. Phys. **7**, 103 (1939).

* This is a reversal of the notation in the two earlier papers, where $N'$ was used to designate grain density and $N$ was used for nucleus density. Since we shall deal

$P$, $T(t, T_0, P)$, and the prehistory. Again, for given prehistory, type of history, and location, we may construct a three-dimensional "*Grain-Number Diagram*" between $N$, $t$, and $T_0$. The analytical representation of

$$N \equiv N(t, T_0, P)$$

will be called the "*Grain-Number Formula.*"

The grain-number diagram or formula is of great importance in the theory of microstructures resulting from given treatment. For a given type of crystal habit, a quantitative description of microstructure may be given by the *volume-frequency density* $F(v)dv$, i.e., the number, per unit volume, of centers of grains (or nuclei) with volume between $v$ and $v+dv$. This, too, is a function of time, position, initial temperature, etc. Fixing the prehistory, history, and location, we still have one more variable here, and it would be necessary to use a four-dimensional plot to represent the frequency density as a function of both time and temperature. If, however, we fix the initial temperature, we may set up a three-dimensional diagram between $F$, $v$, and $t$. This may be called the microstructure-time diagram. A more important diagram will be that giving the volume-frequency density, after infinite (or very long) time, as a function of initial temperature. This we shall designate the "*Microstructure Diagram.*" The general formula for $F$ will be called the "Microstructure Formula." By definition, the relations

$$N = \int_{v_c}^{\infty} F(v)dv \tag{1}$$

and

$$V = \int_{0}^{\infty} vF(v)dv \tag{2}$$

must subsist.†

In some cases (crystalline aggregates), the orientation $\eta$ (abbreviation for the two direction-specifying coordinates) of the individual grains with respect to some fixed direction in space may be distinguished. In others, where the grains are isotropic and possess complete spherical symmetry (drops and bubbles), this distinction is lost. In the anisotropic grain case, a more detailed description of the system may be given by taking into account the distribution in orientation of the grains. This leads to an orientation-dependent grain density

$$N(\eta, t, T_0, P)d\eta,$$

and an orientation-dependent frequency density

$$F(\eta, v, t, T_0, P)d\eta.$$

The previously given $N$ and $F$ may be regarded as orientation-averaged densities, and it is with these that we shall work in the following unless otherwise specified. We note that all the subsequent analysis may be carried through equally well with the orientation-dependent densities.

The deduction of formulas for $V$, $N$, and $F$ is considerably facilitated by the conception of related "extended densities" which we shall now develop. As a transformation proceeds, two phenomena occur: (1) Some nuclei are reached and enveloped by growing grains and become inoperative for production of new grains. (2) The growing grains impinge upon one another and interact; the possible forms of this interaction will be discussed later. Those grains which would have appeared up to any given time, if their nuclei did not lie in occupied regions, will be referred to as "phantom grains." [1(b)] The grains (phantoms included), taken in the fullest extent they would have, had their growth been unimpeded and unmodified by impingement upon one another, will be referred to as "extended grains." To visualize the extended-grain population, we may imagine a representative geometrical system of interpenetrating volumes obeying exactly the same laws as the physical system except that the volumes *granulate and grow through each other.* For brevity, we shall use the adjective "extended," and the superior symbol $\sim$, to designate any attribute of the representative geometrical system.†† Thus, the "*extended volume-frequency density*" $\tilde{F}(\tilde{v})d\tilde{v}$ is the number per unit volume of (phantom-included) grains or nuclei of extended volume between $\tilde{v}$ and $\tilde{v}+d\tilde{v}$. The "*extended grain density*" $\tilde{N}$ is the total number

primarily with grain density, it is desirable to make this simplification even at the risk of some difficulty in comparing with I and II.

† The "*nucleus density*" has the obvious correlative definition $\int_0^{v_c} F(v)dv$. Formula (2) is correct only if the unit volume is large compared with the grain sizes or the space gradient of grain density; see Eq. (5) below.

†† This is a simplification of the notation in the previous papers in which the subscript $_{ex}$ was employed.

larger than $\tilde{v}_c$ in the unit volume, i.e.,

$$\tilde{N}=\int_{v_c}^{\infty}\tilde{F}(\tilde{v})d\tilde{v}. \qquad (1')$$

Similarly, the *extended volume density* $\tilde{V}$ is the fraction of unit volume of space occupied by the extended population. By definition then, over a volume large compared with the size of an average grain

$$\tilde{V}=\int_{0}^{\infty}\tilde{v}F(\tilde{v})d\tilde{v}. \qquad (2')$$

Evidently $\tilde{V}$ can become larger than unity.

(1′) and (2′) enable us to compute $\tilde{N}$ and $\tilde{V}$ when $\tilde{F}$ is given. If, on the other hand, $\tilde{N}$ and the law of growth of the individual extended grain is easily found (a frequent case), $\tilde{V}$ and $\tilde{F}$ may be calculated therefrom. $V$, $N$, and $F$ may then be calculated, so that a knowledge of $\tilde{N}$ and the law of growth of the individual grain is all that is required for the determination of the kinetics of a granular aggregate (sections C and D).

The introduction of the extended densities considerably facilitates the theoretical treatment of transformation kinetics. The problem can now be split into two parts. First, an analysis of the microkinetic processes of granulation and growth leads to the determination of the extended densities as a function of position, time, initial temperature, and as a functional of the prehistory and type of history.* Then, by the formulas to be developed in this paper, the observable macrokinetic quantities, $V$, $N$, and $F$, of the *actual* grains of the new phase may be deduced.

## C. Average Densities and Their Relations

It is necessary at this point to refine our concepts somewhat. So far, we have applied the term "density" to numbers or quantities found in unit volume, without pausing to consider the dependence upon the absolute size of the unit volume. We obtain a useful, statistically suitable, definition of density for point distributions in the following manner: Subdivide the space containing the points or grain centers into "physically small" cells $\Omega$ with positions indicated by subscript capital letters. Each is further subdivided into "geometrically small" subcells $\Delta\omega$ (positions designated by small letters) which may become infinitesimal. Let $N_Q$ denote the number of centers contained in $\Omega_Q$. The average

$$N(Q)=N_Q/\Omega_Q$$

will be referred to as the "average density around $Q$" or, simply, the "*density around Q.*" The absolute size of $\Omega$ is arbitrary within the limits set by the following conditions: (1) It shall be large enough to contain sufficiently many centers so that changing its dimensions continuously alters the density within only slowly. (2) It shall be small enough so that the average number of centers in the subcells $\Delta\omega$ does not vary appreciably from one side of $\Omega$ to the other. A further analysis of the concept of average density leads to some very interesting questions which we shall not discuss here. For the present purpose, the rough verbal restrictions given in (1) and (2) will suffice. We merely note that, for a sufficiently fine-grained distribution, the $\Omega$ will be small enough to serve, approximately, as elements of integration. We shall assume this in the following, replacing the individual $\Omega$ by $d\Omega$ whenever a summation is required.

It is clear that, though the average density may vary in a complex manner from one region of space to another, the centers within a cell may be very simply distributed. A particularly important case, *which includes most physical situations*, is where the numbers in the subcells are distributed about the local average $N$ according to the laws of chance; i.e., the probability of finding $m$ centers in any $\Delta\omega$ is given by the Bernoulli distribution function:

$$\binom{N}{m}(\Delta\omega)^m(1-\Delta\omega)^{N-m}.$$

The distribution is then said to be "*locally random.*" This includes the many important

* We shall show elsewhere that information about prehistory and type of history corresponds to boundary conditions for the system of differential equations governing the nucleation and growth processes of the extended population. This system is also representable by a partial differential equation of the same form as that which appears in the theory of heat conduction in a heterogeneous bar or electric propagation in a non-uniform cable. When this is set up and solved under appropriate boundary conditions, it yields the extended densities. On the other hand, the latter may often be found directly by elementary methods, as in K.P.C. I and II, where assumptions holding in special cases are made.

systems where the gradient of grain density is very sharp, even infinitely sharp, as when the nuclei are distributed upon certain surfaces (walls or grain boundaries of the old phase). We shall investigate the case of local randomness in detail below.

We return now to consideration of the quantities discussed in the previous section. It is clear that practically useful descriptions of frequency and grain distributions will be in terms of average densities. Also, a theoretical treatment is likely to yield information only about such average densities. In related fashion the probable or average "*extended volume density around a point* $P$" $\tilde{V}(t, P)$ may be defined by the average number of extended grains which have grown through $d\Omega_P$.† This may be expressed in terms of the integral of $\tilde{N}$ over the entire region of influence of $P$

$$\tilde{V}(t, P) = \int \tilde{N}(t', Q) d\Omega_Q, \tag{3}$$

where $t'$ is a retarded time something like that appearing in field theories (electromagnetism, etc.). The retardation $t-t'$ is the time required for the "propagation" or growth of a grain with linear velocity $G$ from its origin at $Q$ to its terminus $P$ at time $t$. $G$ is a function of temperature, concentration, etc., i.e., in general of position and time. Expressing $Q$ in terms of spherical coordinates $r$, $\theta$, $\varphi$ about $P$ as origin, we obtain the more explicit form (letting $d\psi = \sin\theta d\theta d\varphi$)

$$\tilde{V}(t, P) = \int_0^{\pi} \int_0^{2\pi} \int_0^{\bar{r}} \tilde{N}(t', r, \theta, \varphi) r^2 dr d\psi, \tag{3'}$$

where $\bar{r}$ denotes the radius of the region of influence for $P$ (i.e., $t'=0$). If external conditions remain constant in time so that $G$ is a function only of position $\rho$, $\theta$, $\varphi$ then

$$t' = t - \int_0^r \frac{d\rho}{G}.$$

If the temperature is changing so that $G$ is also a function of the time $w$, $t'$ must be found from the conditions that, in the integral of the differential equation

$$d\rho = -G(\rho, \theta, \varphi, w) dw,$$

$w=t$ at $\rho=0$ and $w=t'$ at $\rho=r$. This then expresses $t'$ as a function of $r$, $t'(r, \theta, \varphi; t)$. On the other hand, if we so wish, the differential equation may be integrated to give $r$ as a function of $t'$, $r(\theta, \varphi, t'; t)$, and $r$ may be replaced in (3') by $t'$ as an independent variable.

For anisotropic grains $G$ depends also on the grain orientation, so that $\tilde{N}(t', Q)$ in the integral of (3) should be replaced by an average over the densities in the various orientations, each associated with a different value of the retarded time $t'$, i.e.,

$$\tilde{V}(t, P) = \int\int \tilde{N}(\eta, t'_\eta, Q) d\eta d\Omega_Q \tag{4}$$

or

$$\tilde{V}(t, P) = \int_0^{\pi} \int_0^{2\pi} \int_0^{\bar{r}} \int \tilde{N}(\eta; t'_\eta, r, \theta, \varphi) d\eta r^2 dr d\psi. \tag{4'}$$

This may be applied to various cases of distribution of the grain centers, e.g., uniformly random distribution in space;[1(b)] random distribution on foreign surfaces (ingot walls in solidification, electrode plates in electrolytic deposition, etc.); random distribution on internal grain surfaces of the old phase as in grain boundary nucleation.

We shall not discuss the general problem of evaluating (4') here, but three limiting cases previously considered[1(b)] recommend themselves to our attention. In the first, where the growth is polyhedral, i.e., approximately equal in all directions, $t_\eta'$, is the same for all directions, and

$$\int \tilde{N}(\eta, t_\eta', Q) d\eta = \tilde{N}(t', Q)$$

with $G$ in $t'$ representing the rate of radial growth of the pseudospherical grain. In this case, as is to be expected, (4) reduces to (3).

In the second case, that of *plate-like* growth, the grain grows primarily parallel to a single plane, i.e., its (small) thickness $h$ does not change

† It is evident that, upon integration over any macroscopic volume, the density so defined yields the correct total extended volume. Thus, for instance, the average extended volume in a macroscopic unit volume is the integral over the volume

$$\tilde{V} = \int d\Omega_P \int \tilde{N}(t', Q) d\Omega_Q.$$

This is the integral equivalent of formula (7) in K.P.C. I.

appreciably while it grows planarly from its center with radial velocity $G$. If the plate grows in the shape of a circular sector with constant angle $\gamma$ (radians), the cross section of the advancing face of the plate at distance $r$ from its origin in $\gamma rh$. Supposing, also, that the distribution of orientations is random, the probability of a grain with center at $Q$ intercepting the element of volume $d\Omega_P$ at $P$, is the ratio of the area intercepted by the plate on the sphere of radius $r$ to the area of the sphere itself, i.e.,

$$h\gamma r/4\pi r^2 = h\gamma/4\pi r,$$

where $r$ is the distance $PQ$. Thus, out of the total $\tilde{N}(t', Q)$ of grains which had appeared around $Q$ at $t'$, only the fraction

$$\frac{h\gamma}{4\pi r}\tilde{N}(t', Q)$$

is effective. Similarly, in the third case, that of *lineal* or needle-like growth at the rate $G$ with approximately constant cross section $a$, the probability of a grain, originating at $Q$, intercepting $d\Omega_P$ is

$$\frac{a}{4\pi r^2}$$

and the effective orientation-averaged grain density is

$$\frac{a}{4\pi r^2}\tilde{N}(t', Q).$$

For brevity, let us designate the factor in front of $\tilde{N}$ in (4') by $\sigma r^{k-1}/4\pi$ so that

$$\tilde{V}(t, P) = \frac{\sigma}{4\pi}\int_0^{\pi}\int_0^{2\pi}\int_0^{\tilde{r}} r^{k-1}\tilde{N}(t', r, \theta, \varphi)drd\psi, \tag{4''}$$

where

| | | |
|---|---|---|
| $\sigma = 4\pi$ | $k = 3$ | for polyhedral growth |
| $\sigma = h\gamma$ | $k = 2$ | for platelike growth |
| $\sigma = a$ | $k = 1$ | for lineal growth. |

Integrating (4'') by parts with respect to $r$, and remembering that

$$\sigma r^k/k = \tilde{v}(t, t')$$

for the three types of growth, we have

$$\tilde{V}(t, P) = -\frac{1}{4\pi}\int_0^{\pi}\int_0^{2\pi}\int_0^{\tilde{r}} \tilde{v}(t, t') \times\left(\frac{\partial\tilde{N}}{\partial r} + \frac{\partial\tilde{N}}{\partial t'}\frac{\partial t'}{\partial r}\right)drd\psi$$

or replacing $r$ by $t'$ as an independent variable

$$\tilde{V}(t, P) = \frac{1}{4\pi}\int_0^{\pi}\int_0^{2\pi}\int_0^{t} \tilde{v}(t, t') \times\left(\frac{\partial\tilde{N}}{\partial r}G + \frac{\partial\tilde{N}}{\partial t'}\right)dt'd\psi. \tag{4'''}$$

In the special case where $\tilde{N}$ is independent of position in the region of influence of $P$ (i.e., approximately uniform grain density), this reduces to

$$\tilde{V}(t, P) = \int_0^{t} \tilde{v}(t, t')\frac{\partial\tilde{N}}{\partial t'}dt', \tag{5}$$

which is equivalent to (6) of K.P.C. I with the mechanism of granulation assumed there.

(3) or (4) expresses $\tilde{V}$ in terms of $\tilde{N}$ (and $t'$, whose relation to $t$ depends on the law of growth $\tilde{v}(t, t')$ of the individual grain). It remains to express $\tilde{F}$ also in terms of $\tilde{N}$ and $\tilde{v}$. This may be done as follows: A grain of volume $\tilde{v}$ at time $t$ comes from a nucleus which granulated at a previous time $t'$. This time can be determined from $\tilde{v}$ and $t$ when the law of growth $\tilde{v}(t, t')$ is known. Now $\tilde{F}(\tilde{v}, t)dv$ equals the number of grains which granulated at the earlier time $t'$ in an interval $dt'$ corresponding to $d\tilde{v}$, i.e.,

$$-\tilde{F}(\tilde{v}, t)\frac{\partial\tilde{v}}{\partial t'}dt' = \frac{\partial\tilde{N}}{\partial t'}dt'.$$

From this we obtain the extended microstructure formula

$$-\tilde{F}(\tilde{v}, t)d\tilde{v} = \left(\frac{\partial\tilde{N}}{\partial t'}\Big/\frac{\partial\tilde{v}}{\partial t'}\right)d\tilde{v}. \tag{6}$$

### D. Locally Random Nuclei

We shall now see that, for very general circumstances, it is possible to express $V$ simply in terms of $\tilde{V}$. But first we must consider the possible types of grain interaction. When two grow-

ing grains of a new phase impinge, several things may happen. They may *coalesce* to form one larger grain, as frequently happens with gaseous bubbles and liquid drops. They may *adhere* to form a compound grain, ceasing growth at the common interface while continuing to grow normally elsewhere; this is usually true of crystalline grains. Again, a third mechanism may operate, especially if the surrounding phase is fluid, i.e., the interacting grains may *rebuff* each other, pushing away and continuing to grow as though there were no impingement. In this last case $\tilde{V}$ will be a good approximation to $V$ up to the last stages of transformation. In some situations, all three processes might operate to varying extents, together with motion of the grains (and nuclei) due to gravimetric or convective forces. This would complicate the transformation kinetics with considerations of mechanics. Here, however, we shall confine ourselves to stationary particles with the adhering-grain interaction alone. This assumption is usually valid for the growth of crystalline phases.

In the previous paper it was shown that, when the distribution of nuclei is uniformly random, $V$ is given by

$$V(t, P)=1-\exp(-\tilde{V}(t, P)). \tag{7}$$

We shall here show that (7) is equally true when the distribution of nuclei (and initially present grains) is only locally random, and $\tilde{V}(t, P)$ is given by (3). With this generalization most of the important nucleated reactions encountered in practice are included.

Assuming the initial nuclei to be locally random, the extended grain population at any later time is also distributed with local randomness. Now, the ratio of non-overlapped to total volume of any random region, around any point $P$, is equal to the probability of untransformed volume there, i.e., $1-V(t, P)$. As in K.P.C. II, let us choose for the random region the *increment* of transformed volume in an element of time. The non-overlapped part is $dV$, the total $d\tilde{V}$, and we have

$$dV/d\tilde{V}=1-V.$$

Integrating, we obtain Eq. (7).

An alternative derivation may be given as follows: Letting the average extended grain density around $Q$, at time $t'$, be designated as above by $\tilde{N}(t', Q)$, we may calculate the probability that the element $\Delta\omega_q$, at $q$, does not contain any grain centers. By the Bernoulli distribution this probability ($m=0$) is

$$(1-\Delta\omega_q)^{\tilde{N}(t', Q)}.$$

If we let $\Delta\omega_q$ become infinitesimally small, we get

$$\lim_{\Delta\omega_q\to 0}(1-\Delta\omega_q)^{\tilde{N}(t', Q)}=\exp(-\tilde{N}(t', Q)d\omega_q).$$

This may be used to calculate the density of untransformed volume $1-V$ around a point $P$, which is simply the probability that the volume element around $P$ is completely untransformed. This probability is the product of probabilities of zero grain center content in each of the elements $d\omega_q$ (at its associated retarded time $t'$) in the region of influence of $P$, so that we have

$$1-V(t, P)=\prod_{\text{all } Q,\ q \text{ for } t'\geq 0}\exp(-\tilde{N}(t', Q)d\omega_q)$$

$$=\exp\left(-\int\tilde{N}(t', Q)d\Omega_Q\right)=\exp(-\tilde{V}(t, P))$$

and we have justified Eq. (7).

We have now expressed $V$ in terms of $\tilde{V}$. The latter, as we have seen, can be calculated from a knowledge of $\tilde{N}$ and $\bar{v}$. Likewise, assuming local randomness, $N$, $v$, and $F$ may all be expressed ultimately in terms of $\tilde{N}$ and $\bar{v}$. Thus, taking unit volume around a given point, the ratio of actual to extended granulations in an element of time will evidently equal the fraction of untransformed volume at that time, i.e.,

$$\frac{\partial N}{\partial t}=(1-V)\frac{\partial\tilde{N}}{\partial t}=\exp(-\tilde{V})\frac{\partial\tilde{N}}{\partial t}$$

or, integrating,

$$N(t)=\int_0^t\exp(-\tilde{V}(t))\frac{\partial\tilde{N}}{\partial t}dt$$

$$=\int_0^t\exp\left(-\int\tilde{N}(t', Q)d\Omega_Q\right)\frac{\partial\tilde{N}}{\partial t}dt. \tag{8}$$

Again, as in deriving (7), the ratio of the non-overlapped increment $dv$ of an *average* grain (of size $v$) to its extended increment $d\tilde{v}$, in an element

of time $dt$, equals the untransformed fraction at that time, i.e.,

$$\frac{dv(t, t')}{d\bar{v}(t, t')} = 1 - V(t) = \exp(-\bar{V}(t)).$$

Integrating, we get

$$v(t, t') = \int_{t'}^{t} \exp(-\bar{V}(t)) \frac{\partial \bar{v}(t, t')}{\partial t} dt, \qquad (9)$$

where the values of the integrand are taken along the (space-time) route of growth of the grain around its center.

The expression for $F$ may be obtained by reasoning similar to that used for (6). An average grain of volume $v$ at time $t$ comes from a granulating center at a previous time $t'$ which can be determined as a function of $v$ and $t$ when the law of growth (9) of the actual (impinged) grains is known. $F(v, t)$ equals the number of actual grains which made their appearance at time $t'$ in the interval $dt'$ corresponding to $dv$, i.e.,*

$$-F(v, t)\frac{\partial v}{\partial t'}dt' = \frac{\partial N}{\partial t'}dt' = \exp(-\bar{V}(t'))\frac{\partial \bar{N}}{\partial t'}dt'.$$

Now, from (9)

$$\frac{\partial v}{\partial t'} = \int_{t'}^{t} \exp(-\bar{V}(t)) \frac{\partial^2 \bar{v}(t, t')}{\partial t' \partial t} dt,$$

so that the microstructure formula becomes

$$-F(v, t) = \frac{\partial \bar{N}}{\partial t'} \exp(-\bar{V}(t')) \Big/ \int_{t'}^{t} \exp(-\bar{V}(t)) \frac{\partial^2 \bar{v}}{\partial t' \partial t} dt. \qquad (10)$$

* Actually this is an approximation which is truer the more nearly $t'$ corresponds to a unique volume in the actual grain population, i.e., the narrower the size frequency distribution of grains of the same "age," a function we have not analyzed here. This approximation makes (10) less and less valid toward the end of transformation. For a more detailed analysis of this and related points see a forthcoming paper in *Philosophy of Science* (Technical Supplement), January (1941).

FEBRUARY, 1941 JOURNAL OF CHEMICAL PHYSICS VOLUME 9

# Remarks on the Fluorescence, Phosphorescence and Photochemistry of Dyestuffs

JAMES FRANCK, *University of Chicago, Chicago, Illinois*

AND

ROBERT LIVINGSTON, *University of Minnesota, Minneapolis, Minnesota*

(Received July 26, 1940)

Many of the apparently conflicting facts of the photochemistry as well as of the phosphorescence and of the fluorescence quenching of dyes can be given a rational and unified interpretation if it be assumed that an electronically excited dye molecule can go over, by a process of internal conversion, to the electronic ground state of a reactive energy-rich tautomer. The endothermic reversion of such a tautomer to the electronically excited state of the original molecule would explain the weak, temperature dependent phosphorescence observed in some systems. In the presence of a suitable reducing agent the reactive tautomer may be reduced to a semiquinone. This process and the likely subsequent reactions are sufficient to explain the majority of dye-sensitized photo-oxidations as well as the photo-bleaching of dyes by reducing agents. In the case of chlorophyll, and possibly a few other dyes, it appears to be necessary to assume that the tautomer and a normal dye molecule can undergo a process of disproportionation. The assumption of this step leads directly and simply to an explanation of the rapid reversible bleaching of chlorophyll which is consistent with the other known photochemical and optical properties of this substance. In addition to the more familiar reaction steps which have been assumed as follow reactions in setting up the various mechanisms, it is necessary to include a step in which the $HO_2$ radical reduces a partially oxidized dye molecule (i.e., radical) back to the normal state. The several reaction steps assumed in these various schemes appear to be energetically feasible.

IT is well known that many dyestuffs which are able to fluoresce in solution are efficient sensitizers for photochemical reactions, while most of those which show no sign of fluorescence in solution are extremely inefficient sensitizers.[1]

[1] Hurd and Livingston, J. Phys. Chem. **44**, 865 (1940).

The evident and commonly accepted explanation of these facts may be stated as follows. The ability of a substance to fluoresce is proof that the excitation energy of its electronic system remains intact long enough for this energy to be emitted, wholly or in part, as light. However, the oscillation energy which is associated with the electronic energy is quickly dissipated by impacts with the solvent molecules. If $\tau$ is the natural lifetime of the excited state, as calculated (to a good approximation) from the integrated absorption coefficient, and $\alpha$ is the fluorescent yield, then the product $\alpha\tau$ is the actual lifetime, which would be measured by a direct observation. A collision between an excited dye molecule and a molecule of a reactive substance may result in the utilization of the energy of excitation as energy of activation of a chemical reaction, with resultant quenching of the fluorescence. The probability of such collisions, and therefore the efficiency of utilization of the energy of excitation for chemical purposes, increases with an increase in the actual life time ($\alpha\tau$) of the excited state. In the case of those dyes which show no trace of fluorescence, even under conditions where the transfer of energy of excitation into chemical energy is extremely improbable, one must assume that the light energy is dissipated into the degrees of freedom as thermal energy directly after the absorption act. The light energy is thus lost for chemical purposes.

This interpretation, while generally correct, offers no explanation of the great difference in ability to fluoresce which the several dyes exhibit. Furthermore, it should be amplified in some respects and restricted in others. For example, the energy absorbed by some nonfluorescent dyes is not directly and completely dissipated as heat. It should also be noted that a collision between an excited dye molecule and one of the substrate is not a sufficient condition for the immediate occurrence of a chemical reaction. This point has been discussed more fully by Franck and Herzfeld,[2] who suggested the analogy between an excited dye in state of impact with a reactive molecule and an activated complicated molecule which is about to undergo a monomolecular dissociation. Just as there is in the second case a finite interval between the time when the complex molecule acquires the energy of activation and the time when it uses this energy to dissociate, so there is a lapse of time after the dye molecule absorbs the light before it can transfer the absorbed energy to a second molecule which is able to undergo a chemical reaction. It is an interesting consequence of this view that some cases are to be expected where the fluorescence will not be completely quenched either by very frequent collisions with the chemically sensitive molecule or even by the formation of a complex with this molecule. This residual or "unquenchable" fluorescence will be strongest in those cases where the time required for the attainment of that configuration which leads to the occurrence of the chemical reaction is greatest.

To arrive at any conclusion as to why the fluorescent yields of the various dissolved dyes differ so greatly it is necessary to consider the several ways in which they can lose their excitation energy. If the dye is dissolved in a pure chemically stable solvent, whose molecules are unable either to react chemically with the excited dye molecules or to take over the excitation energy into their own electronic systems, a fluorescent yield less than unity indicates that excitation energy is either converted into heat or is stored in the dye molecule, very probably by a transition into a tautomer of higher energy content. It is known, from numerous experimental studies of the quenching of the fluorescence of mono- and diatomic molecules, that energy cannot be converted,[3,4] by collisions of the second kind, from electronic energy directly into rotational or translational energy in amounts much greater than the thermal (equilibrium) energy of these degrees of freedom. Furthermore, the direct conversion of electronic energy into oscillatory energy is possible only under the special condition[5] that the potential energy curves of the acceptor molecule are greatly changed by the forces (electric or chemical) exerted by the excited molecule. If such forces existed between a dye molecule and the molecules of the solvent (which are constantly in contact with it) the

[2] Franck and Herzfeld, J. Phys. Chem. **41**, 97 (1937).

[3] Franck, Naturwiss. **14**, 211 (1926).

[4] Nordheim, Zeits. f. Physik **36**, 496 (1926).

[5] Franck and Eucken, Zeits. f. physik. Chemie **B20**, 460 (1933).

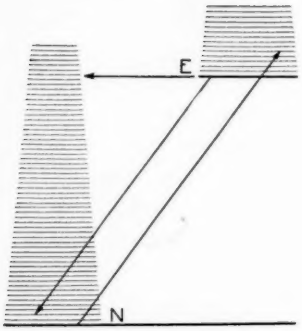


FIG. 1. Schematic representation of the energy levels and transitions corresponding to a system where internal conversion which results in the degradation of the energy of excitation is possible.

positions and intensities of its absorption bands would be greatly changed compared to those of the same dye in the gaseous state or dissolved in a solvent which does not interact with it. If the absorption bands of a dye are the same when it is dissolved in several different solvents, it may be safely assumed that no such interaction occurs, since it is very improbable that the interactions and resulting changes in the absorption spectra would be the same for the different solvents. Since many dye solutions are known which are negligibly fluorescent but which do not show such changes in their absorption bands, it is necessary to assume that electronic energy can be transferred within the dye molecule itself. This could occur by a sort of "internal impact of the second kind."

While such acts cannot occur in simple molecules, a process having these characteristics and restricted to complicated molecules has been described by E. Teller.[6] This process may be described as an internal conversion of the excitation energy of the electronic system into oscillatory energy. We shall refer to it briefly as "internal conversion." Internal conversion is possible only for those complicated molecules whose quantum states are so numerous that their spacing is comparable to their natural width. It can occur only when the molecule is in a special configuration which is common to the excited and ground states. In terms of the potential energy diagram, this transition occurs when the system is represented by a particular point lying on the line of intersection of the surfaces corresponding to the normal and excited states. The time required to reach this special constellation will differ greatly for different dyes. It seems very probable that the magnitude of this interval will be strongly effected by relatively small changes in the structure of the molecule. Since the act of fluorescence takes place during this interval, the intensity of fluorescence must also be very sensitive to small changes in molecular structure.

In condensed systems when the activated molecule is continuously in a state of multiple impact, internal conversion readily leads to the degradation of electronic energy into heat (see Fig. 1). However, it is neither necessary nor probable that internal conversion always leads to the complete dissipation of the energy of excitation as heat. Indeed, it is quite probable that the violent oscillations, which are a consequence of internal conversion, lead to the formation of a tautomer of the original dye molecule; the keto-enol transformation is a possible example of such a tautomeric change.

Both the physical and chemical properties of the molecule may be considerably altered by such a tautomeric shift in the position of a hydrogen atom. For example, if, as a consequence of this shift, the system of conjugated double bonds is interrupted, the absorption bands may be entirely changed. Of course, if the shift does not affect the resonating system (i.e., if it occurs in another part of the molecule) practically no change will occur in the absorption spectrum. The behavior of chlorophyll dissolved in an organic liquid will be discussed later as an example of the latter type. The energy relations of a molecule of this general type are illustrated by Fig. 2. In this diagram, the line $N$ represents the energy of the ground state of the dye; $E$, its first excited state; and $N'$, the ground state of the tautomer. If $N'$, as in the figure, happens to be well below $E$ but still much higher than $N$, then the molecule in the tautometric state will have optical properties which will be similar to those which it would have in a metastable electronic state, with the important difference that the tautomer may have a much longer life. This difference in half-life is likely to be especially great when the dye molecule is surrounded by solvent molecules. It is evident that a tautometric level, like $N'$, could be responsible for the phenomenon of phosphorescence. The intensity of the phosphorescence produced in this way should decay exponentially. Behavior of this type has been observed under

[6] Teller, J. Phys. Chem. **41**, 109 (1937).

certain circumstances[7–9] for several fluorescent dyes. This phosphorescence is of the ordinary type in that its wave-length distribution is the same as that of the fluorescent light, and the probability of the transitions increases rapidly with temperature. On the other hand, there is (according to the Franck-Condon principle) a small but finite probability of a transition between the states $N'$ and $N$. At low temperature, where transitions from $N'$ to $E$ (induced by collisions of the first kind) are rare events, the direct transition, $N' \rightarrow N$, becomes relatively important. The experimental counterpart to this change is the appearance at low temperatures[7,10,11] of a long-lived fluorescence whose wave-length maximum is shifted toward the red, relative to the ordinary fluorescent band.

It has been customary to explain these optical phenomena in terms of metastable states. While metastable states undoubtedly occur in dye molecules which contain many resonating groups, the observed long lives of the phosphorescence as well as some of the kinetic data make it appear very probable that tautometric rather than metastable states are responsible for these phenomena. As was mentioned before, the time, $\alpha\tau$, which elapses between the act of absorption and internal conversion is strongly affected by small changes in the internal motions of the molecule. These motions are determined only by the thermal (equilibrium) oscillations, since the excess of oscillatory energy which the molecule acquires at the moment of absorption is quickly dissipated by collisions with solvent molecules. Lowering the temperature decreases the thermal energy of oscillation, and so decreases the probability of internal conversion and therefore favors direct fluorescence. This conclusion is substantiated by the familiar experimental observation that the fluorescent yield of dye solutions increases as the temperature is lowered. While the present hypothesis leads directly to the conclusion that $\alpha\tau$, and therefore the fluorescent yield, should be strongly influenced by intermolecular forces, it is unable to predict in general the direction of this influence. However, experiments show that any circumstances, such as a viscous solvent or adsorption on a solid surface,[12] which hinders the oscillatory motion of the dye molecule acts like a low temperature in increasing the intensity of fluorescence.[13]

Internal conversion which leads to the formation of a tautomer may profoundly influence the chemical behavior. Since the tautometric shift very probably involves a shift of a hydrogen atom, it is to be expected that in some cases the tautomer will contain a very labile or loosely bound hydrogen atom. If, in this way the energy necessary to dissociate the molecule into a radical and a hydrogen atom is reduced below 50 kcal.,[14] an appropriate collision with an oxygen molecule will result in the formation of an $HO_2$ radical and a partially oxidized dye radical.

Although the most important applications of the ideas presented here are to the photochemical reactions of dyes a detailed discussion of these complicated reactions is beyond the scope of this paper. A brief outline of the established facts of dye photochemistry and of their possible interpretation is presented as an appendix. There are, however, two groups of experiments which deserve special attention.

It is particularly noteworthy that the hypothesis of tautomer formation is able to explain

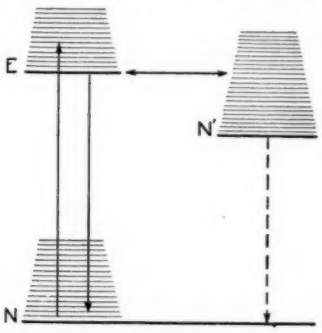


FIG. 2. Schematic representation of the energy levels and transitions corresponding to a system where internal conversion leading to tautomer formation is possible.

[7] Wavilow and Lewschin, Zeits. f. Physik **35**, 920 (1926).
[8] Lewschin and Vinokurov, Physik. Zeits. (USSR) **10**, 10 (1936).
[9] Schischlowski and Wavilow, Physik. Zeits. (USSR) **5**, 379 (1934).
[10] Kautsky and Hirsch, Ber. **65**, 401 (1932).
[11] Compare also Wick and Throop, J. Opt. Soc. Am. **25**, 318 (1935).
[12] Kautsky and Hirsch, Ber. **64**, 2677 (1931).
[13] For a discussion of this fact see Lewis and Calvin, Chem. Rev. **25**, 273 (1939). It is also possible that in some cases, particularly in solutions where the concentration of the dye is high, that viscous solvents may increase the fluorescent yield by hindering "self-quenching."
[14] There appears to be no quantitative evidence in regard to the heats of dissociation of such tautomers. However, there is evidence that the energy necessary to dissociate stable molecules into radicals and hydrogen atoms depends upon the structure of the molecule; see for example Taylor and Smith, J. Chem. Phys. **8**, 543 (1940); and Bent and Cuthbertson, J. Am. Chem. Soc. **58**, 170 (1936).

the fact that the fluorescent yield of chlorophyll in an inert organic solvent is only slightly changed[15] by the addition of oxygen and a reducing agent, at such concentrations that the quantum yield of the chlorophyll-sensitized photo-oxidation is approximately unity. Since the yield of fluorescence remains constant and is of the order of a few percent, the process which limits the lifetime of the excited dye molecule must be the same regardless of whether photo-oxidation is or is not taking place. The observed quantum yield of the photosensitized oxidation of one indicates that the greater part of the energy of excitation of the dye molecule remains available for chemical purposes (sensitization) after the molecule has (practically) lost its ability to radiate. Both of these facts are consistent with the assumption that the chlorophyll molecule undergoes internal conversion resulting in the formation of a reactive tautomer, which is capable of initiating those secondary steps which are responsible for the observed chemical changes. A brief outline of these secondary steps and their relation to the available experimental facts is given in the appendix.

A second group of experiments, performed by Kautsky,[16] deserve special treatment; not only because of their importance in the theoretical development of dye photochemistry, but also because of the controversies which have existed in regard to their interpretation. In these experiments Kautsky prepared two samples of powdered silica gel; he allowed one to adsorb the fluorescent dye trypaflavine, and the other, the easily oxidizable leuco base of a photochemically inert dye. A mixture of these two dry powders was placed in an evacuated glass vessel. When the mixture was illuminated the trypaflavine was excited to fluorescence and phosphorescence, but there was no chemical action. In the presence of 0.002 mm of $O_2$ the phosphorescence was quenched and a noticeable oxidation of the leuco base to the corresponding dye could be recognized by the change in color. Oxygen pressures greater than 0.003 mm greatly retarded this oxidation.

In an attempt to explain these results Kautsky assumed that an adsorbed dye molecule can exist in a long-lived metastable state which is capable of importing its energy to an $O_2$ molecule (by a collision of the second kind) with the formation of a metastable $^1\Sigma$ $O_2$ molecule. He also assumed that this $^1\Sigma$ $O_2$ molecule could act as a reactive oxidizing agent, the "oxygen carrier" of the reaction.

This mechanism was improved by Weiss,[17] who suggested that the excited dye molecule would split off a hydrogen atom (either spontaneously or aided by a collision of the second kind) and that this atom could react with an oxygen molecule to form an $HO_2$ radical capable of acting as an "oxygen carrier." This mechanism has the advantage that it eliminates the necessity of postulating the existence of the very improbable long-lived metastable dye molecule and of extraordinarily efficient deactivating collisions between normal and metastable oxygen molecules.[18] However, it has the disadvantage that it assumes that a dye molecule which has been excited by the absorption of a quantum of visible light is capable of spontaneously splitting off a hydrogen atom, a process which is energetically impossible.

These several difficulties may be avoided by assuming that the excited dye molecule (RH*) transforms spontaneously into a reactive tautomer (HR). This tautomer may revert either to the original dye molecule (RH) or, more rarely, to the excited molecule (RH*); the latter process accounting for the faint phosphorescence which Kautsky observed. In the presence of oxygen the following reaction is probable.

$$HR+O_2 \rightarrow R+HO_2.$$

The $HO_2$ radical, so formed, may either diffuse to and be reduced by the leuco base or be lost by the back reaction

$$HO_2+R \rightarrow RH+O_2.$$

[15] Compare Franck and Levi, Zeits. f. physik. Chemie **B27**, 409 (1934). This experimental result has been confirmed by the present authors (unpublished work) who found that the fluorescent yield of chlorophyll in a $10^{-5}$ $M$ solution saturated with air and containing allyl thiourea at a concentration of 0.5 $M$ was about 80 percent (or 85 percent) of the yield observed in a $10^{-5}$ $M$ solution in pure air-free solvent (acetone).

[16] Kautsky, de Bruijn, Neuwirth and Baumeister, Ber. **66**, 1588 (1933).

[17] J. Weiss, Naturwiss. **35**, 610 (1935).

[18] It is also very doubtful if $^1\Sigma$ $O_2$ molecules are ever of importance in photo-oxidations; Compare Gaffron, Ber. **68**, 1409 (1935); Biochem. Zeits. **264**, 251 (1933); Zeits. f. physik. Chemie **B37**, 437 (1937); Rollefson, Chem. Rev. **17**, 427 (1935).

TABLE I. *Photochemical properties of typical dyes.*

| DYE | PARARO-SANA-LINE | FLUO-RES-CEIN | METH-YLENE BLUE | CHLORO-PHYLL |
|---|---|---|---|---|
| Photosensitizes oxidations | − | + | + | + |
| Fluorescence quenched by reducing agents | no fluo-rescence | + | + | − |
| Reversibly photo-bleached by reducing agents | − | − | + | − |
| Reversibly photo-bleached by oxidizing agents | − | (−) | (−) | + |

This mechanism is also consistent with the fact that the efficiency of the oxidation of the leuco base first increases to a maximum and then falls off rapidly as the pressure of oxygen is increased. The rate of oxidation of the leuco base is directly proportional to the rate of escape of $HO_2$ radicals from the capillary spaces in which the fluorescent dye molecules are adsorbed on the "inner surfaces" of the silica gel granules. To a first approximation this rate of escape is directly proportional to the concentration of $HO_2$ radicals in the capillaries and inversely proportional to the total gas pressure. Instead of escaping from the capillaries, the $HO_2$ radicals may be lost by reacting with the partially oxidized dye molecules. High total pressure would favor this reaction relative to the escape from the capillary, if the rate of the reaction were practically independent of the pressure, as would be the case if adsorbed $HO_2$ radicals were free to migrate upon the silica gel surface. It is also possible that the $HO_2$ radicals disappear within the capillaries by a bimolecular process of decomposition. However, if this latter reaction were relatively important a noticeable photobleaching of the fluorescent dye should occur in the presence of $O_2$, a process which Kautsky did not observe.

## APPENDIX: AN OUTLINE OF THE INTERPRETATION OF THE EXPERIMENTAL FACTS OF PHOTOCHEMISTRY OF DYES IN TERMS OF THE PRECEDING DISCUSSION

The observations on the photochemistry of dyes and pigments can be interpreted in a manner which is consistent with the foregoing discussion of the optical properties of complex molecules. Published studies of the photochemistry of dye solutions include the investigation of photosensitized oxidation-reduction reactions, of photobleaching of dyes by reducing agents, and of (at least in the case of chlorophyll) rapid-reversible photo-bleaching in the absence of a substrate.

Since the various dyes differ in their behavior in respect to these reactions, it is convenient to divide them into several classes. The majority of dyes are photochemically inactive and practically nonfluorescent. Pararosanaline may be taken as representative of this group. Fluorescein and the related dyes, eosine, rose bengale, and rhodamine, constitute a second group. Methylene blue is typical of a third group which includes thianine and, presumably, other thiazine dyes. The fourth group consists of chlorophyll and possibly the porphyrines. In Table I, which summarizes some of the photochemical characteristics of these types of dyes, a minus sign (−) signifies that the indicated process either does not occur or occurs only very inefficiently, while a plus sign (+) signifies that the process occurs efficiently.

The photo-bleaching referred to in the fifth row is the reversible bleaching produced by oxidizing agents such as $Fe^{+++}$. This is, of course, quite different from the slow irreversible bleaching which solutions of all dyes undergo when they are illuminated in the presence of oxygen.

To conserve space all of the reaction steps which appear to be required for any of the photochemical reactions of the several classes of dyes are grouped together in the following list. It should be remembered, however, that the explanation of no single set of experiments requires more than a small part of this rather formidable array of reaction steps.

1 $DH + h\nu \rightarrow DH^*$
2 $DH^* \rightarrow DH + h\nu_f$ (fluorescence)
3 $DH^* \rightarrow HD$ (internal conversion accompanied by tautomerization)
4 $DH^* \rightarrow DH$ (internal conversion followed by collisions with the solvent molecules)
5 $O_2 + DH^* \rightarrow D + HO_2$
6 $AH_2 + DH^* \rightarrow DH_2 + AH$
7 $HD \rightarrow DH^*$ (reversion, responsible for phosphorescence)
8 $DH + HD \rightarrow DH_2 + D$
9 $AH_2 + HD \rightarrow DH_2 + AH$
10 $O + HD \rightarrow D + Re$
11 $2DH_2 \rightleftharpoons D + DH_3$ (reversible, semiquinone equilibrium)
12 $D + DH_2 \rightarrow 2DH$
13 $O_2 + DH_2 \rightarrow DH + HO_2$
14 $AH + DH_2 \rightleftharpoons DH_3 + A$ (reversible)
15 $AH + DH_2 \rightarrow DH + AH_2$
16 $AH_2 + D \rightarrow DH + AH$
17 $HO_2 + D \rightarrow DH + O_2$
18 $AH_2 + HO_2 \rightarrow AH + H_2O_2$
19 $AH + H_2O_2 \rightarrow$ Oxidation products
20 $AH + O_2 \rightarrow A + HO_2$.

The special symbols used in this scheme have the following significance: DH—dye, DH*—electronically excited dye, HD—tautomer of dye, $DH_2$—semiquinone, D—partially oxidized form of dye, $DH_3$—leuco base, $AH_2$—reducing agent, A and AH—oxidized or partially oxidized forms of the reducing agent, O—an oxidizing agent and Re—its reduced form.

Steps 5, 8, 10, 12, 16, and 17 appear to be required only for reactions involving chlorophyll. Since steps 8, 12, and 17

are somewhat unusual it may be worthwhile to point out that these steps are energetically feasible. Neither the heat of dissociation of the labile hydrogen of chlorophyll, nor the heat of association of normal chlorophyll with atomic hydrogen are known. We may consider, therefore, that the mechanism is a probable one if it is possible to assign plausible values to these energy terms which make steps 8, 12, 13 and 17 exothermic. It is very probable that the heat of dissociation is less than 90 cal.[19] and the heat of association less than 53 cal.,[20] which is a probable value for the hydrogen atom affinity of $O_2$. There is a fairly wide range of values which satisfy these conditions. For example, if the heat of association is taken as +45 cal. and the heat of dissociation as −80 cal. the heats of reactions 8, 12, 13, and 17 will be +3, +35, +8, and +27 cal., respectively.

**Quenching of fluorescence**

The quenching of the fluorescence of the dyes of the thiazine and fluorescein types is caused chiefly by step 6; although in some cases the added substance may, by complex formation or otherwise, increase the probabilities of steps 3 and 4 relative to 2.

In the case of the nonfluorescent dyes, the probability of the occurrence of either step 3 or step 4 must be much greater than that of step 2. The fact that these dyes are usually very poor sensitizers indicates that if (by step 3) they form the tautomer, HD, it is either energetically very close to the normal molecule or else it is very short lived. There are, however, a few "nonfluorescent" dyes which noticeably, although rather inefficiently, sensitize oxidation reduction reactions. It would not be at all surprising if further investigation were to reveal the existence of other nonfluorescent dyes which are efficient sensitizers.

**Photo-bleaching**

The bleaching of fluorescein and thiazine dyes which occurs when a solution containing a reducing agent is illuminated, is due to step 6 (or steps 3 and 9) followed by steps 11, 14, and 15. When little or no bleaching occurs, as in the case of the fluorescein dyes,[21] step 15 is much faster than step 14. The reverse is true when bleaching occurs very readily, as in solutions containing methylene blue and allyl thiourea.[22] The regeneration of the color in the dark, as with methylene blue and phenyl hydrazine,[23] probably is caused by the reverse step 14 followed by 15. Rapid reversible bleaching which is proportional to the square root of the intensity of the absorbed light, such as occurs in solutions containing thianine and KI,[24] probably involves steps 6 and 15, or 3, 9, and 15.

The irreversible photo-bleaching of chlorophyll by reducing agents is a very inefficient process. If it occurs at all it may be caused by an inefficient process similar to step 11. The reversible photo-bleaching by oxidizing agents such as $Fe^{+++}$[25] is due to steps 3, 10, and 16. The oxidized form, $D$ is yellow and photolabile, and probably differs from the oxidized form produced by step 8. When the oxidizing agent is $Fe^{+++}$, steps 10 and 16 may be rewritten as follows:

$$10' \qquad Fe(OH)^{++}+DH \rightarrow D+Fe(H_2O)^{++}$$
$$16' \qquad Fe(H_2O)^{++}+D \rightarrow DH+Fe(OH)^{++}.$$

The relatively slow bleaching of chlorophyll by $Fe^{+++}$ in the dark probably involves a slow thermal reverse of step 7 followed by 10 and 16. The rapid reversible bleaching which occurs in the absence of a substrate[26] is caused by steps 3, 8 and 12. Since the bleached chlorophyll is regenerated by a second-order process, we may conclude that the color of the reactive tautomer (HD) is practically the same as that of the normal molecule and that the actual bleaching is a consequence of a bimolecular process, probably step 8. The inhibition of this process by $O_2$ is due to 13 and 17. Since this action of $O_2$ probably does not reduce the steady state concentration of D, this substance must have about the same color as the normal molecule DH. The bleached form must be $DH_2$. The inhibition by $Fe^{++}$ is due to steps 16 and 15.

**Sensitized photo-oxidations**

Photo-oxidations sensitized by fluorescein and thiazine dyes[1,21,27,28] are the results of steps 6 (or 3 and 9), 13, 18, and 19. The sensitized oxidation of benzidine by chlorophyll[29,30] probably follows a similar course, but the chlorophyll sensitized oxidation of substrates like allyl thiourea and isoamylamine[31] is due to steps 3 and 8 (or 9), 13 and follow reactions such as 18, 19, and 20.

**Destructive oxidation of a dye**

Photo-bleaching in the presence of oxygen (i.e., destructive oxidation) of these dyes (as well as chlorophyll) is greatly accelerated by the presence of traces of oxidizable compounds.[32] This action is probably due to steps 6 (or 3 and 9) and 13, followed by a relatively inefficient reaction between the dye molecule and the $HO_2$ radical. The inefficiency of this latter process is indicated by the strong protective action of moderate concentrations of the same reducing agents which induce the bleaching when present as traces.[33]

[19] Rollefson and Burton, *Photochemistry* (Prentice-Hall, 1939), p. 422.
[20] Bray, J. Am. Chem. Soc. **60**, 82 (1937).
[21] Livingston and Hurd, J. Phys. Chem. **45** (1941), in press.
[22] Mudiovcic, Zeits. f. wiss. Phot. **26**, 171 (1928).
[23] Holst, Zeits. f. physik. Chemie **A179**, 172 (1937).
[24] Weiss, Trans. Faraday Soc. **35**, 48 (1939).
[25] Rabinowitch and Weiss, Proc. Roy. Soc. **A162**, 251 (1937).
[26] Porret and Rabinowitch, Nature **140**, 321 (1937).
[27] Schneider, Zeits. f. physik. Chemie **B28**, 311 (1935).
[28] Spealman and Blum, University of California, Pub. in Physiol. **8**, 147 (1937).
[29] Noak, Biochem. Zeits. **183**, 153 (1927).
[30] Franck and Levi, Zeits. f. physik. Chemie **B27**, 409 (1934).
[31] Gaffron, Ber. **60B**, 755, 2229 (1927).
[32] Weber, Ber. **69**, 1026 (1936).
[33] The possibility of a direct reaction between DH*, or HD, and $O_2$ cannot be excluded. Indeed, some such mechanism is probably necessary to explain the high yields of the photo-bleaching of the cyanine dyes by oxygen. Bhattacharyya and Dahr, J. Ind. Chem. Soc. **6**, 145 (1929).

# Notation for the Derivatives of the Two Types of Line Integral in Thermodynamics

G. TUNELL
*Geophysical Laboratory, Carnegie Institution of Washington, Washington, D. C.*
(Received October 19, 1940)

IN thermodynamics, quantities of two types are constantly dealt with, namely: quantities that depend only on the momentary state of the body or system (such as pressure, volume, temperature, energy, and entropy), and quantities that depend on the series of states through which the body or system passes (*viz.*, work and heat). On the one hand, energy and entropy enter the mathematical formulations of thermodynamics as line integrals that depend only on the initial and final values of the variables defining the state of the system; standard mathematical symbols altogether adequate for the purposes of thermodynamics are available for such line integrals,[1] and also for their partial derivatives. On the other hand, work and heat are defined in thermodynamics as line integrals that depend on the path (i.e., the entire series of states through which the body or system passes); standard mathematical symbols adequate for the purposes of thermodynamics are available for such line integrals, but the same is not true of their derivatives. The derivatives of the work and heat line integrals are total derivatives with respect to the variable chosen as the parameter defining the path of the integral. For example, if the path (of a homogeneous fluid system of constant mass and composition) be defined by the equation $p=f(t)$, the derivative of the work line integral is given by the following equation

$$\frac{dW}{dT}=p\left(\frac{\partial V}{\partial T}\right)_p+p\left(\frac{\partial V}{\partial p}\right)_T\frac{dp}{dT}. \qquad (1)$$

This equation for the derivative of the work line integral holds for any path in the $T$, $p$ plane (except a straight line parallel to the $p$ axis). For a path parallel to the $T$ axis in this plane the equation reduces to

$$\frac{dW}{dT}=p\left(\frac{\partial V}{\partial T}\right)_p. \qquad (2)$$

Now in thermodynamics many different planes are used (such as the $p$, $V$ plane, the $T$, $V$ plane, the $E$, $S$ plane, the $T$, $S$ plane, etc.) and a concise but unambiguous notation for the derivatives of the work and heat line integrals along paths parallel to the coordinate axes in each of these planes has been very much needed. In order to understand Eq. (2) it is necessary to have the supplementary information, not indicated in the equation itself, that the work line integral is being differentiated along a path in the $T$, $p$ plane parallel to the $T$ axis; the derivative of the work line integral along a line parallel to the $T$ axis in the $T$, $S$ plane is not equal to $p(\partial V/\partial T)_p$ but it would still be represented by the same symbol $dW/dT$ in the notation of Eq. (2). A symbol that would convey the necessary supplementary information is $(dW/dT)_p$ resp. $(dW/dT)_S$. The symbol $(dz/dx)_y$ was formerly used for the partial derivative of a function of two independent variables, and for this reason the writer previously has hesitated to suggest that it be used to fill the need in thermodynamics under discussion. However, since Legendre and Jacobi introduced the symbol $\partial z/\partial x$ for the partial derivative of a function of two or more independent variables, the symbol $(dz/dx)_y$ has fallen into disuse for this purpose, and it has seemed to the writer for some time that it might well be used in thermodynamics with the new meaning mentioned above. The reason for writing this article is that in Eucken's *Grundriss der physikalischen Chemie*[2] and in Sherwood and Reed's *Applied Mathematics in Chemical Engineering*[3] the symbol $(dQ/dT)_V$ is

[1] Cf. G. Tunell, J. Phys. Chem. **36**, 1744–1771 (1932).

[2] Eucken, *Grundriss der physikalischen Chemie* (Akademische Verlagsgesellschaft M.B.H., Leipzig, 1934). In the fourth edition (1934) Eucken writes, on page 88, the equations

$$\left(\frac{dQ}{dT}\right)_V\equiv C_V=\left(\frac{\partial U}{\partial T}\right)_V$$

and

$$\left(\frac{dQ}{dT}\right)_p\equiv C_p=\left(\frac{\partial I}{\partial T}\right)_p.$$

The same usage also occurs in earlier editions.

[3] Sherwood and Reed, *Applied Mathematics in Chemical Engineering* (McGraw-Hill, 1939), p. 163. Sherwood and Reed write the equations

$$C_v=\left(\frac{dQ}{dT}\right)_v$$

and

$$dQ=\left(\frac{dQ}{dT}\right)_v dT+\left(\frac{dQ}{dv}\right)_T dv=C_v dT+l_v dv.$$

used precisely to represent the derivative along a path parallel to the $T$ axis in the $T$, $V$ plane of the heat line integral, and it seems desirable to urge that the symbol with straight $d$'s, parentheses, and subscript be accepted generally in this sense. Eucken and Sherwood and Reed have introduced this symbol in this sense so unobtrusively that its significance may escape general notice.

The need in thermodynamics for such a symbol as $(dQ/dT)_p$ is emphasized by a comparison of certain second derivatives. In the case of a function of the state of the body there exists a well-known relation between the cross derivatives, which in the case of the energy $E$ is as follows:

$$\frac{\partial^2 E}{\partial T \partial p} = \frac{\partial^2 E}{\partial p \partial T}, \tag{3}$$

whereas, with the functions that depend on the series of states that the body passes through, one has in place of the preceding equation an inequality, which in the case of the heat $Q$ is as follows:

$$\left[\frac{\partial}{\partial T}\left(\frac{dQ}{dp}\right)_T\right]_p \neq \left[\frac{\partial}{\partial p}\left(\frac{dQ}{dT}\right)_p\right]_T. \tag{A}$$

A consideration of the preceding equation and inequality shows at once that neither the symbol $(\partial Q/\partial T)_p$ nor the symbol $dQ/dT$ is suitable for the purposes of thermodynamics. The symbol $(\partial Q/\partial T)_p$ cannot be used because according to accepted mathematical usage at the present time it would stand for the partial derivative of a function $Q$ of the two independent variables $T$ and $p$ with respect to $T$, whereas $Q$ is not a function of $T$ and $p$; moreover, one would immediately expect on seeing the symbol $(\partial Q/\partial T)_p$ that an equation could be written between

$$\frac{\partial^2 Q}{\partial T \partial p} \quad \text{and} \quad \frac{\partial^2 Q}{\partial p \partial T}$$

but the partial derivative with respect to $T$ of the total derivative of $Q$ with respect to $p$ along a line parallel to the $p$ axis is not equal to the partial derivative with respect to $p$ of the total derivative of $Q$ with respect to $T$ along a line parallel to the $T$ axis. The symbol $dQ/dT$ is also inadequate because the inequality would then be written

$$\left(\frac{\partial}{\partial T}\frac{dQ}{dp}\right)_p \neq \left(\frac{\partial}{\partial p}\frac{dQ}{dT}\right)_T,$$

which is quite ambiguous without supplementary information in the text. Actually the derivatives along paths parallel to the coordinate axes of the line integrals that depend on the path (work and heat) are themselves functions of all the independent variables that determine the state of the body or system[4] and admit partial derivatives with respect to each of these variables. This fact is well expressed by the notation

$$\left[\frac{\partial}{\partial T}\left(\frac{dQ}{dp}\right)_T\right]_p.$$

It may be suggested finally that confusion between the new usage (following Eucken and Sherwood and Reed) of the symbol with straight $d$'s, parentheses, and subscript, and the old usage, which has been discarded since the time of Jacobi, is very unlikely. In papers or books in which this symbol is used in the new sense there will also occur derivatives of functions of two or more variables, which will of course be written with rounded $\partial$'s. Thus where both types of symbol are found in one publication it will be clear that the symbol with straight $d$'s, parentheses, and subscript is used in the sense of a derivative along a line parallel to a coordinate axis of a line integral that depends on the path.

[4] A point well stated and properly emphasized by Clausius, *Abhandlungen über die mechanische Wärmetheorie*, Section 2, Part 9 (Friedrich Vieweg und Sohn, Braunschweig, 1867), p. 7.

# Letters to the Editor

*THIS section will accept reports of new work, provided these are terse and contain few figures, and especially few halftone cuts. The Editorial Board will not hold itself responsible for opinions expressed by the correspondents. Contributions to this section should not exceed 600 words in length and must reach the office of the Managing Editor not later than the 15th of the month preceding that of the issue in which the letter is to appear. No proof will be sent to the authors. The usual publication charge ($3.00 per page) will not be made and no reprints will be furnished free.*

## Influence of the Temperature of Crystallization on the Melting of Crystalline Rubber

NORMAN BEKKEDAHL AND LAWRENCE A. WOOD
*National Bureau of Standards, Washington, D. C.*
January 8, 1941

Data presented in this communication show an instance in which melting of a crystalline material is very much dependent on the temperature at which the crystals have been formed. It is well known that many substances in which crystallization is relatively slow can be crystallized at different temperatures in a range below the melting point, but no effect of the crystallization temperature on the temperature of melting seems to have been previously reported. The quantitative results for crystalline rubber, the material under investigation, are shown in Fig. 1.

The crystallization[1] of unvulcanized rubber in the unstretched state has been found to occur at temperatures between about −40°C and 13°C. The time required for crystallization is about one year at 13°C, about ten days at 0°C, and a few hours at −20°C. Below −40°C the mobility is presumably insufficient for the formation of crystals. Crystallization and fusion are accompanied by changes in volume, heat capacity, light absorption, birefringence, x-ray diffraction, and mechanical properties such as hardness. The volume decreases about 2.5 percent on crystallization, and the magnitude of the change is little influenced, if at all, by the temperature. Fusion, as measured by the volume increase, is found to be independent of the rate of heating, and to occur over a range of five or ten degrees.

In the present work, volume change as measured in a mercury-filled dilatometer was taken as the criterion of crystallization. Smoked sheet rubber was held at various fixed temperatures until no further volume change could be detected. After each crystallization the temperature was raised, and observations were taken for a graph of the volume as a function of temperature. The temperature corresponding to the beginning of melting could be located as that at which the observations began to deviate from the curve representing the normal thermal expansion of crystalline rubber. Likewise, at the end of the melting range the observations began to follow the curve representing the normal thermal expansion of amorphous rubber. These two limiting temperatures could be located within about one-half a degree and are plotted in Fig. 1. The shaded area between the curves represents the melting range.

It is to be observed from the figure that the higher the temperature of crystallization, the higher are the temperatures at which both the beginning and ending of melting occur. The range of melting itself appears to become somewhat narrower at the higher crystallization temperatures. From the fact that the broken curve does not intersect or touch the shaded area, it appears that there is no temperature at which crystalline and amorphous rubber are in equilibrium at atmospheric pressure. If the crystallization occurs between about 6° and 10°C, the melting of the crystals begins at a temperature about 4° above that at which the crystals were formed. This interval is greater than 4° for crystallization at temperatures above or below this range. In previous work in this laboratory a melting range from 6° to 16°C has been reported[1] for crystallization temperatures near 0°C. Van Rossem and Lotichius[2] found that crystals formed at −10°C melted between 2° and 14°C. Both these sets of observations are included in Fig. 1.

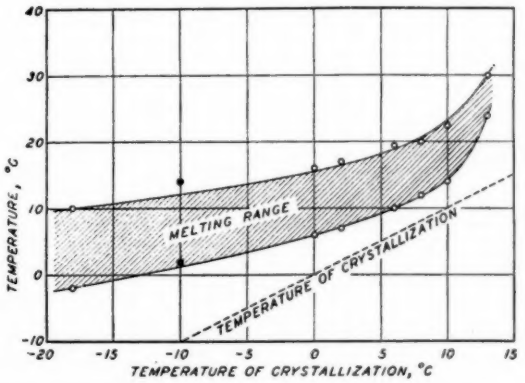


FIG. 1. Melting range of crystalline rubber as a function of the temperature of crystallization. The lower points represent the beginning of melting, the upper points the ending of melting. The broken curve shows the crystallization temperature as ordinate for easier comparison with the range of melting temperature in each case. Van Rossem and Lotichius.

The results here presented undoubtedly explain many previously reported discrepancies in the temperatures of melting of crystalline rubber. They may also be expected to furnish an explanation of certain effects with stretched rubber recently observed by Treloar,[3] who, lacking the present data, felt that he was not justified in making the assumption that "the melting point of the crystals could depend on the temperature at which they are formed."

There seems to be no reason why the effect discussed here should be limited to rubber, and, if investigations are made, this effect may be found in many other organic compounds of high molecular weight.

[1] N. Bekkedahl, J. Research Nat. Bur. Stand. 13, 411 (1934) RP717. Reprinted in Rubber Chem. Tech. 8, 5 (1935).
[2] A. Van Rossem and J. Lotichius, Kautschuk 5, 2 (1929). Reprinted in Rubber Chem. Tech. 2, 378 (1929).
[3] L. R. G. Treloar, Trans. Faraday Soc. 36, 538 (1940). Reprinted in Rubber Chem. Tech. 13, 795 (1940).

## The Reaction Between Hydrogen and Oxygen: The Upper Explosion Limit and the Reaction in Its Vicinity[1]

GUENTHER VON ELBE, *Coal Research Laboratory, Carnegie Institute of Technology, Pittsburgh, Pennsylvania*
AND
BERNARD LEWIS, *Physical Chemistry Section, Central Experiment Station, Bureau of Mines, Pittsburgh, Pennsylvania*
November 23, 1940

We have found that water vapor effects a marked lowering of the upper explosion limit of hydrogen and oxygen. This is illustrated by the following typical results for a 2 : 1 mixture at 530°C, $H_2O$ being admitted to the reaction vessel from a reservoir.

| Percent $H_2O$ | 0 | 3.35 | 6.37 | 11.03 |
|---|---|---|---|---|
| Upper limit, mm Hg | 85.6 | 54.9 | 41.8 | 29.4 |

Nine determinations with water percentages ranging from 3 to 11 gave an average value of $k_{6H_2O}/k_{6H_2}$ equal to 14.3, with a maximum error of 0.7. These results demonstrate that the water effect is no different in kind than the influence of other gases as described by the explosion condition

$$2k_2 = k_{6H_2}(H_2) + k_{6O_2}(O_2) + k_{6X}(X),$$

where X is water or any other inert gas. This equation corresponds to the reaction scheme

1. $OH + H_2 = H_2O + H$
2. $H + O_2 = OH + O$
3. $O + H_2 = OH + H$
6. $H + O_2 + (H_2, O_2, X) = HO_2 + (H_2, O_2, X)$.

The equation numbers follow those given elsewhere.[2]

The ratio $k_{6O_2}/k_{6H_2}$ was determined at 530°C as 0.35 ±0.01 by observing the upper limit for mixtures of hydrogen and oxygen containing 20, 33.3, 50, and 66.7 percent hydrogen. The value showed no dependence on mixture composition. Similarly, $k_{6X}/k_{6H_2}$ for other gases were found to be independent of the percentage present; for He, A, $N_2$ and $CO_2$ they are 0.36, 0.20, 0.43 and 1.47, respectively. The values for $O_2$, He, A and $N_2$ agree well with former determinations.[3]

On slowly approaching the upper limit from the high pressure side one may observe, very close to the limit, short bursts of reaction that die out rapidly, as is illustrated in Table I for a mixture containing 20 percent $H_2$ at 530°C.

TABLE I. *Initial pressure = 137.7 mm (upper explosion limit slightly below this).*

| Time, sec. | 0 | 15 | 23 | 30 | 37 | 100 |
|---|---|---|---|---|---|---|
| $-dO_2/dt$, mm/min. | 0.93 | 0.80 | 0.40 | 0.40 | 0.05 | |

The water thus formed pushes the limit toward lower pressures. That the water alone is responsible for this shift was shown by the precise agreement between the observed shift after allowing a known amount of water to be formed by reaction, and that calculated from the efficiency of water of 14.3.

A typical curve of the change of reaction rate with pressure above the upper explosion limit is shown in Fig. 1.

The Pyrex spherical reaction vessel, 7.2 cm in diameter, was heavily coated with KCl. The rates proved to be very well reproducible over a period of many weeks. They pass through a minimum, as expected. On the left side of the minimum the reaction inhibits itself (see above), and only initial rates are given.

We have also carried out upper-limit determinations in the same vessel from 400°C to 570°C. The values are considerably higher than those found by other investigators.[4] This and the occasional poor reproducibility found by these investigators may be explained by the water-vapor effect.

The foregoing observations furnish an explanation of most of the questions raised by Oldenberg and Sommers.[5]

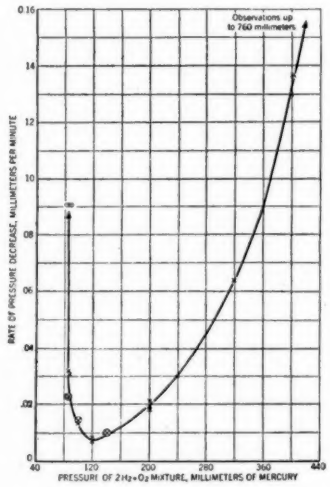


FIG. 1. Reaction rate of mixtures of $2H_2+O_2$ at 530°C in spherical KCl-coated Pyrex vessel, 7.2 cm in diameter. ⊗ indicates duplicated observations.

The latter, working at 568°C, were unable to observe a minimum rate on approaching the upper limit. However, at this temperature the rates near the minimum are some 100 times greater than at 530°C, thus tending to obscure the branch of the curve to the left of the minimum by self-inhibition. Self-heating of the mixture, even of the order of 1°, should also contribute to this because the coefficient $k_2$ increases sharply with temperature; therefore, the transition between slow and explosive reaction becomes very abrupt. Oldenberg and Sommers' observation that the limit shifted from about 180 mm to about 120 mm after 4 percent of the mixture reacted is in striking agreement with the value of 14.3 for the water-vapor efficiency, the calculated shift being identical. It is also evident that the increase of the upper limit on coating the vessel with KCl, which these authors report, is caused by the decreased rate of water formation. The same limit can be found in both vessels by operating sufficiently fast.

We are making a detailed study of the kinetics of the hydrogen-oxygen reaction and shall publish further details

later, including a discussion of the remaining points raised by Oldenberg and Sommers.

[1] Published by permission of the Director, Bureau of Mines, U. S. Department of the Interior, and the Director, Coal Research Laboratory, Carnegie Institute of Technology.
[2] Lewis and von Elbe, *Combustion, Flames and Explosions of Gases* (Cambridge Univ. Press, 1938), p. 33.
[3] G. H. Grant and C. N. Hinshelwood, Proc. Roy. Soc. (London) **A141**, 29 (1933); A. A. Frost and H. N. Alyea. J. Am. Chem. Soc. **55**, 3227 (1933).
[4] H. W. Thompson and C. N. Hinshelwood, Proc. Roy. Soc. (London) **A122**, 610 (1929); A. A. Frost and H. N. Alyea, reference 3; G. H. Grant and C. N. Hinshelwood, *ibid.*
[5] O. Oldenberg and H. S. Sommers, J. Chem. Phys. **8**, 468 (1940).

## Coriolis Perturbations and Molecular Dimensions in Germane $GeH_4$

TA-YOU WU
*Department of Physics, National South-West Ass. University, Kun-ming, China*
November 25, 1940

In a recent paper Murphy[1] has calculated the structure of the $\nu_4$ fundamental in $SiH_4$ and in $GeH_4$ by evaluating the matrix elements of the coriolis perturbations between $\nu_4$ and the doubly degenerate $\nu_2$. It was found that these perturbations satisfactorily explain the observed complexities in these bands and in particular the unsymmetrical shapes of the $Q$ branches. While the agreement between the observed and the calculated structure is good in the case of $SiH_4$, it is less so in the case of $GeH_4$. The purpose of this note is to suggest that the poorer agreement is probably due to the use of a vlaue for the moment of inertia of $GeH_4$ which is highly questionable.

Steward and Nielsen estimated $I$ at $7.0\times10^{-40}$ g cm² for $GeH_4$ from the spacings $\Delta\nu_3=5.56$, $\Delta\nu_4\sim6$ cm$^{-1}$ according to the theory of Teller and of Johnston and Dennison. This value of $I$ yields the value 1.27A for the Ge-H distance which has been pointed out by the writer to be unreasonable on comparison with the Si-H distance in $SiH_4$.[2] On account of the complexities in the structure of $\nu_4$ due to the perturbation by $\nu_2$, the $\Delta\nu_4$ has no strict meaning and must hence not be used in determining $I$. On the other hand, the assumption of pure valence and deformation forces in such molecules as $CH_4$, $SiH_4$, $GeH_4$ is probably a good approximation. On this assumption and from the observed value of $\Delta\nu_3$ in the $\nu_3$ band which is not perturbed by $\nu_2$, we obtain the following dimensions (Table I). These values of $I$ are also only approximate since the internal angular momenta $\xi$'s obtained on the assumption of pure valence force system are approximate, as can be seen in the case of $CH_4$ in which the C−H distance is known to be 1.09A. Their relative values are, however, more reasonable than those obtained by employing $\Delta\nu_3$ and $\Delta\nu_4$ since one would expect the Ge-H distance to be greater than Si-H. It is hoped that the use of $I\simeq9.8\times10^{-40}$ g cm for $GeH_4$ in the perturbation calculations will improve the agreement between the calculated and the observed structure of $\nu_4$.

TABLE I.

| | $\Delta\nu_3$ | $\xi_3$ | $\xi_4$ | $I=\frac{(1-\xi_3)h}{4\pi^2\Delta\nu_3}$ | X−H | From $\Delta\nu_3$ and $\Delta\nu_4$ $I$ | X−H |
|---|---|---|---|---|---|---|---|
| $CH_4$ | 9.77 | 0.100 | 0.400 | $5.09\times10^{-40}$ | 1.07A | $5.47\times10^{-40}$ | 1.11A |
| $SiH_4$ | 5.65 | 0.046 | 0.454 | $9.34\times10^{-40}$ | 1.45 | $8.9\times10^{-40}$ | 1.41 |
| $GeH_4$ | 5.56 | 0.018 | 0.482 | $9.77\times10^{-40}$ | 1.49 | $7.0\times10^{-40}$ | 1.27 |

[1] G. M. Murphy, J. Chem. Phys. **8**, 71 (1940).
[2] T.-Y. Wu, *Vibrational Spectra and Structure of Polyatomic Molecules* (National University of Peking), pp. 230–231.

## Conductivity of Calcium Salts

ARTHUR S. JENSEN, *Physics Department, University of Pennsylvania, Philadelphia, Pennsylvania*
AND
M. RUTH UNANGST, *Pharmacology Department, Hahnemann Medical College, Philadelphia, Pennsylvania*
December 16, 1940

It is of interest to the medical world to prevent convulsive effects that usually follow the administration of certain anesthetics. Drs. R. Beutner and G. P. Miley,[1, 2] Department of Pharmacology, Hahnemann Medical College, observed that the simultaneous injection of certain calcium salts with these anesthetics inhibited convulsions. Dr. Beutner[3] suggested that the action of the salt could be correlated with its calcium ion content, that a measurement of the salt's electrical conductivity would be of interest to the formulation of a theory of the salt's physiological action.

Since there were found in the literature almost no data on the electrical conductivities of the salts used in the animal experiments,[4] we measured them, using the standard Kohlrausch bridge method with 60-cycle current and a conductivity cell with Pt electrodes, at 18°C, and the following results (Table I) were obtained:

TABLE I.

| Salt | $\sigma$ in mho/cm 0.1 $N$ | 0.01 $N$ | 0.001 $N$ |
|---|---|---|---|
| Ca Gluconate | $2.52\times10^{-3}$ | $4.97\times10^{-4}$ | $6.92\times10^{-5}$ |
| Ca Benzoate | 2.68 | 7.25 | 8.46 |
| Ca Lactate | 3.79 | 6.40 | 9.50 |
| Ca Levulinate | 4.75 | 6.55 | 8.13 |
| Ca Salicylate | 5.35 | 7.50 | 9.49 |
| Ca Chloride | 8.62 | 10.1 | 12.5 |
| Ca Bromide | 9.10 | 10.7 | 10.1 |

Calcium gluconate held special interest to the pharmacologist, so further detailed measurements were made on it (Table II).

TABLE II.

| | Concentration | Average Conductivity |
|---|---|---|
| 18°C | 0.1 $N$ | $2.52\times10^{-3}$ mho/cm |
| | 0.05 $N$ | $1.62\times10^{-3}$ " |
| | 0.01 $N$ | $4.97\times10^{-4}$ " |
| | 0.005 $N$ | $2.75\times10^{-4}$ " |
| | 0.001 $N$ | $6.92\times10^{-5}$ " |
| 25°C | 0.1 $N$ | $3.24\times10^{-3}$ mho/cm |
| | 0.01 $N$ | $6.50\times10^{-4}$ " |

Deviation for these readings was within ±3 percent.

These measurements were made in the Pharmacology Department of the Hahnemann Medical College.

[1] R. Beutner and G. P. Miley, Proc. Soc. Exp. Biol. Med. **38**, 279 (1938).
[2] R. Beutner and G. P. Miley, Proc. Soc. Exp. Biol. Med. **42**, 547 (1939).
[3] R. Beutner, Am. J. Physiol. **129**, 489 (1940).
[4] Curr. Researches in Anes. and Analgesia **19**, 132 (1940).